A Thesis for the Degree of Doctor of Philosophy

Application of near-infrared heating as an antimicrobial intervention for food safety

식품 안전성 확보를 위한 근적외선 가열의 활용

August, 2015

Jaewon Ha

Department of Agricultural Biotechnology
College of Agriculture and Life Sciences
Seoul National University

Application of near-infrared heating as an antimicrobial intervention for food safety

식품 안전성 확보를 위한 근적외선 가열의 활용

지도교수 강 동 현

이 논문을 농학박사학위논문으로 제출함
2015 년 4 월

서울대학교 대학원
농생명공학부
하 재 원

하재원의 박사학위논문을 인준함
2015 년 6 월

위 원 장 _____ (인)

부위원장 _____ (인)

위 원 _____ (인)

위 원 _____ (인)

위 원 _____ (인)

Abstract

Ha, Jaewon

Department of Agricultural Biotechnology

The Graduate School

Seoul National University

The application of infrared (IR) radiation heating to food processing has gained momentum due to its inherent advantages over the conventional heating systems. Certain characteristics of IR heating such as emissivity and transmissivity set it apart from and make it more effective for industrial applications than others. IR radiation transfers thermal energy in the form of an electromagnetic wave and can be classified into 3 regions, near IR (NIR; 0.76 to 2 μm), medium IR (MIR; 2 to 4 μm), and far IR (FIR; 4 to 1,000 μm). Among them, NIR heating has been gaining wider acceptance because of its higher heat transfer capacity and high energy efficiency compared with MIR and FIR heating. This thesis explored the potential and utilization of NIR heating as an alternative antimicrobial intervention for food safety.

The specific objectives of this study were, (ⅰ) to investigate the efficacy of NIR heating to reduce major foodborne pathogens, such as *Salmonella enterica* serovar Typhimurium, *Escherichia coli* O157:H7, and *Listeria monocytogenes* in

ready-to-eat (RTE) food (focused on deli meat product) compared to conventional convective heating as well as its effect on product quality, (ii) develop and validate the inactivation kinetic models of the three major pathogens on RTE sliced ham by NIR heating, as a function of the processing parameter, radiation intensity, (iii) investigate the effect of the simultaneous application of NIR heating and ultraviolet (UV) irradiation on inactivation of these pathogens in RTE sliced ham, (iv) elucidate the underlying mechanisms of the synergistic bactericidal action of NIR heating and UV irradiation, (v) extensively apply the combined treatment to other food systems (dry powdered foods) with a mild NIR heat, and (vi) evaluate the efficacy of organic acid spray along with NIR heating for inactivating *Salmonella* Enteritidis on dry nut kernel products.

A cocktail of three pathogens was inoculated on the exposed or protected surfaces of ham slices, followed by NIR or conventional convective heating at identical conditions (1.8 kW). NIR heating for 50 s achieved 4.1-, 4.19-, and 3.38-log reductions in surface-inoculated *S.* Typhimurium, *E. coli* O157: H7, and *L. monocytogenes*, respectively, without affecting product quality whereas convective heating needed 180 s to attain comparable reductions for each pathogen. There were no statistically significant ($P > 0.05$) differences in reduction between surface- and internally inoculated pathogens at the end of NIR treatment (50 s). However, when treated with conventional heating,

significant ($P < 0.05$) differences were observed at the final stages of the treatment (150 and 180 s). Thus, NIR heating can be applied to control internalized pathogens as well as surface-adhering pathogens in RTE sliced meats as an alternative to conventional heat treatment. For investigation of the inactivation kinetics as a function of radiation intensity, precooked ham slices inoculated with the three pathogens were treated at different NIR intensities (ca. 100, 150, and 200 μW/cm^2/nm). The survival curves of the three pathogens exhibited both shoulder and tailing behavior at all light intensities. Among nonlinear models, the relationship between the scale & shape parameters (α & β values) of the Weibull model and applied radiation intensity was almost a straight line, and single linear equations for the three pathogens were obtained. The final predictive models (tertiary models) for the three pathogens were developed by substituting the secondary linear models into the Weibull primary model and allowed us to predict survival curves at NIR intensities different from those used in this study. The tertiary models were validated with data obtained from further experiments within the range of the experimental domain. The R^2, *RMSE*, B_f, and A_f values were within the acceptable range indicating the suitability of the model for predictive purposes. These results would be beneficial to the deli meat industry in selecting the optimum processing conditions of NIR heating to meet the desired target level of pathogen inactivation.

Simultaneous application of NIR heating and UV irradiation at ca. 0.9 kW (half of NIR treatment alone) for 70 s achieved 4.17, 3.62, and 3.43 log CFU reductions of *S.* Typhimurium, *E. coli* O157:H7, and *L. monocytogenes,* respectively. For all three pathogens, the simultaneous application of both technologies resulted in an additional log unit reduction as a result of their synergism compared to the sum of the reductions obtained after the individual treatments. To investigate the mechanisms of NIR-UV synergistic injury for a particular microorganism in a food base, I evaluated the effect of four types of metabolic inhibitors using the overlay method and confirmed that damage to cellular membranes and the inability of cells to repair these structures due to ribosomal damage were the primary factors related to the synergistic lethal effect. The NIR-UV combined treatment for a maximum of 70 s did not alter the color values or texture parameters of ham slices significantly ($P > 0.05$). Additionally, simultaneous NIR-UV combined processing was employed for decontaminating red pepper powder (target pathogens: *S.* Typhimurium and *E. coli* O157:H7) and powdered infant formula (target pathogen: *Cronobacter sakazakii*). Many pathogens have been known to be more resistant in low-water-activity environments. Due to its ability to survive in dry food matrices, controlling pathogens in the final dehydrated product is of great concern to the food industry. NIR-UV combined treatment for 5 min achieved 3.34- and 2.78-log CFU reductions in *S.* Typhimurium and *E. coli* O157:H7 in powdered red pepper,

respectively, and for 7 min achieved a 2.79-log CFU reduction of *C. sakazakii* in powdered infant formula without causing any deterioration in product quality due to the lower intensity of NIR. The sum of NIR and UV inactivation was lower than that obtained by the simultaneous application of both technologies due to their synergism. Through qualitative (transmission electron microscopy) and quantitative (propidium iodide uptake) analyses, disruption of the bacterial cell membrane was identified again as the main factor contributing to the synergistic lethal effect of NIR-UV combined treatment. The results of these extensive studies suggest that a NIR-UV decontaminating system can be applied as an alternative to other interventions in various kinds of powdered/granulated foods.

As an another available hurdle combination, the efficacy of NIR heating combined with 2% lactic acid (LA) sprays for decontaminating dry nut kernels (almonds and pine nuts) was investigated. Although surface temperatures of nuts treated with NIR were higher than those subjected to NIR-distilled water spray (DW) or NIR-LA treatment, more *S.* Enteritidis survived after NIR treatment alone. The effectiveness of NIR-DW and NIR-LA was similar, but significantly more sublethally injured cells were recovered from NIR-DW treated samples. I confirmed that the enhanced bactericidal effect of the NIR-LA combination may not be attributed to cell membrane damage per se. NIR heat treatment might allow *S.* Enteritidis cells to become permeable to applied LA solution. Due to the

lower levels of NIR and applied LA, combined NIR-LA treatments did not change quality attributes of nut kernels significantly ($P > 0.05$). Thus, the NIR-LA treatment may be a potential intervention for controlling food-borne pathogens on nut kernel products.

The simultaneous NIR-UV or NIR-LA combinations have some advantages not only regarding the germicidal effect but also in terms of simplified handling, environmental preservation, and reduced costs through lower inputs of energy. Furthermore, the NIR or combined processing techniques can easily be expanded to practical industrial scale on a continuous basis. In conclusion, application of NIR heating in the food industry is expected to represent a novel and innovative antimicrobial process for the production of high-quality & safe foods at low cost.

Keywords: near-infrared heating, ultraviolet irradiation, organic acid, lactic acid, spray, inactivation, foodborne pathogen, radiation intensity, kinetics model, deli meat, dry powdered food, nut kernel

Student Number: 2011-21325

Contents

List of Figures

List of Tables

Chapter I.

Evaluation of Near-Infrared Pasteurization in Controlling Food-Borne Pathogens in Ready-To-Eat Deli Meat

This chapter was published in *Applied and Environmental Microbiology* (2012) 78(18):6458-6465.

I-1. Introduction

Salmonella enterica serovar Typhimurium, *Escherichia coli* O157:H7 and *Listeria monocytogenes* are the main foodborne pathogens involved in numerous outbreaks related to delicatessen meats (Belongia et al., 1991; CDC, 2005-2006). *S.* Typhimurium is the most prevalent pathogen among *Salmonella* serotypes. The most common symptoms caused by *S.* Typhimurium are diarrhea, abdominal pain, mild fever, and chills (Baird-Parker, 1990; Rhee et al., 2003). In 2006, an outbreak of *S.* Typhimurium infection occurred in the United States, which was traced back to contaminated deli meats (CDC, 2006). By January 2012, a reported 199 persons had become ill due to the outbreak (CDC, 2006). *Salmonella* spp. can proliferate in fresh meats at temperature as low as 2.0 °C within 6 to 10 days (D'Aoust, 1991). Thus, refrigeration does not guarantee the inhibition of *Salmonella* spp. in vacuum-packaged ham products. *E. coli* O157:H7 has emerged as an important foodborne pathogen, causing hemorrhagic colitis, which is occasionally complicated by hemolytic uremic syndrome (Doyle, 1991; Wang et al., 1996), and it requires a very low dose (fewer than 700 organisms) to cause infection (Tuttle et al., 1999). Most reported infections with Shiga toxin producing *E. coli* (STEC) are linked to insufficiently cooked ground meats (Rangel et al., 2005). *Listeria monocytogenes* can cause severe illness or even fatalities among the elderly, pregnant women, persons

with weakened immune systems, neonates and fetuses. Listeriosis has a high rate of mortality (>20%) in this group (Mead et al., 1999). Vacuum-packaged, refrigerated ham products may also provide a potential growth environment for a psychrotrophic, facultatively anaerobic foodborne pathogen such as *Listeria monocytogenes* (Schwartz et al., 1988; Zhu et al., 2005). Sporadic foodborne illness outbreaks have been traced to contaminated deli meats in the United States in recent years (CDC, 2005-2006). Outbreaks of foodborne listeriosis have resulted in large-scale recalls of ready-to-eat deli meat products (USDA, 2011).

Delicatessen meat, especially precooked sliced ham, is a perishable RTE product. Precooked sliced ham has been used widely in delicatessens and home kitchens due to the convenience it provides. Vacuum packaged ham should have an extended shelf life, because mild cooking decreases the initial microbial populations and vacuum packaging inhibits the growth of undesirable aerobic microorganisms (Jones et al., 1987; Kotzekidou and Bloukas, 1996; Stites et al., 1989). However, insufficient cooking may happen or postcooking contamination may occur during chilling and before packaging. Furthermore, rehandling at consumer outlets permits the introduction of pathogenic bacteria (Mol et al., 1971; Steele and Stiles, 1981), and this is a major cause of foodborne outbreaks associated with RTE meats (Ryser and Marth, 1991).

Therefore, a post-lethality intervention step, which is a process designed to destroy the post-processing contaminating organisms immediately before the products are packaged or after unwrapping the vacuum-packaged sliced ham products at delicatessens or other retail outlets, may become necessary to ensure the final microbial safety of the products. Inactivation of bacteria by heat is still one of the most effective methods for food preservation, particularly for RTE meats. As contamination occurs primarily on product surfaces, an additional superficial heat treatment may be needed to inactivate pathogenic bacteria on the products.

Infrared (IR) is an invisible form of electromagnetic energy emitted from objects at extremely high temperature. By exposing an object to infrared radiation, the heat energy generated can be absorbed by a food product. The intense thermal energy from infrared-emitting sources has been widely applied to various thermal processing operations in the food industry, such as dehydration and pasteurization of a variety of materials and products (Sakai et al., 1993). Infrared heating is also gaining popularity because of its higher thermal efficiency and fast heating rate/response time in comparison to conventional heating (Krishnamurthy et al., 2008). Huang and Sites (2009) reported near-infrared (NIR) treatment of cooked chicken breast meat at 1kW for 156 s reduced surface-inoculated *Listeria monocytogenes* by 3.4 log CFU/g, and hot water immersion heating at a set temperature (75 °C) for 5 min reduced

Listeria monocytogenes by 3.15 log CFU/g. However, these relatively long treatment times are not practical for use by industry and could adversely affect the organoleptic qualities of the products by increasing denaturation of meat surfaces. Comparing the efficiency of NIR heating to the hot water immersion method also is not reasonable due to the differences in electric power consumed and interference of plastic film packaging (0.4 mm thick) with the conduction of thermal energy from heated water to chicken breast meat. Furthermore, a comparison between the sterilization efficacy of NIR and conventional convective heating (electric resistive heater) has not been reported. Accordingly, inactivation rates between NIR heating and conventional convective heating need to be assessed and statistically evaluated under identical conditions. Also, the investigation and optimization of a NIR treatment system which can quickly reduce pathogens by at least 2 to 3 logs on deli meat products while maintaining product quality is required.

In this study, the efficacy of NIR treatment and conventional convective heating for reducing the populations of foodborne pathogens, including *S.* Typhimurium, *E. coli* O157:H7, and *L. monocytogenes* on RTE sliced ham were compared under identical conditions. Also, the inactivation of internalized pathogens was investigated through additional experiments utilizing the same treatments.

I-2. Materials and Methods

Bacterial strains. Three strains each of *S.* Typhimurium (ATCC 19585, ATCC 43971, and DT 104), *E. coli* O157:H7 (ATCC 35150, ATCC 43889, and ATCC 43890), and *L. monocytogenes* (ATCC 7644, ATCC 19114, and ATCC 19115) were obtained from the School of Food Science bacterial culture collection of Seoul National University (Seoul, South Korea) for this study and were used for all experiments. Stock cultures were stored at -80 ℃ in 0.7 ml of tryptic soy broth (TSB; Difco, Becton, Dickinson, Sparks, MD, USA) and 0.3 ml of 50 % glycerol. Working cultures were streaked onto tryptic soy agar (TSA; Difco), incubated at 37 ℃ for 24 h, and stored at 4 ℃.

Preparation of pathogen inocula. Each strain of *S.* Typhimurium, *E. coli* O157:H7, and *L. monocytogenes* was cultured in 5 ml of TSB at 37 ℃ for 24 h, followed by centrifugation (4,000 × g for 20 min at 4℃) and washing three times with buffered peptone water (BPW; Difco). The final pellets were resuspended in BPW, corresponding to approximately 10^7 to 10^8 CFU/ml. Subsequently, suspended pellets of each strain of the three pathogenic species were combined to produce mixed culture cocktails (nine strains). These cocktails at a final concentration of approximately 10^8 CFU/ml were used in this study.

Sample preparation and inoculation. Precooked and vacuum-packaged sliced ham (approximately 90 by 90 by 2 mm) was purchased from a local grocery store (Seoul, South Korea). The samples were maintained in a refrigerator (4 °C) and were used for experiments within 2 days. For surface inoculation (on the exposed surfaces), 8 ml of prepared mixed culture cocktail (*S.* Typhimurium, *E. coli* O157:H7, and *L. monocytogenes*) was diluted in 0.8 liters of distilled water. Each ham slice was immersed into the combined pathogen suspension for 10 min at room temperature (22 ± 2 °C), drained on a sterilized rack, and dried in a laminar-flow biosafety hood for 20 min with the fan running. Two ham slices (ca. 25 g, inoculum level of 10^5 to 10^6 CFU/sample) were used in each experimental batch.

Internal inoculation (on the protected surfaces) with pathogens was performed as follows. One hour prior to inoculation, sliced ham products were removed from the refrigerator until the temperature of the sample reached that of surface-inoculated samples. Pairs of ham slices were selected, and single slices were placed on a sterilized rack in a biosafety hood with the fan running, and then 0.1 ml of culture cocktail (10^6 to 10^7 CFU/ml) was spread onto one of the paired ham slices, resulting in an inoculum level of 10^5 to 10^6 CFU/sample. Before being overlapped with the other slice, the spread-inoculated ham slice was dried for 10 min.

Near-infrared heating and conventional convective heating. A model aluminum chamber (41 by 34 by 29 cm) was used in this study for both NIR and convective heating (Fig. I-1). Four quartz halogen infrared heating lamps (NS-104; 350 mm; NSTECH, Gyunggido, South Korea), each with a maximum power of 500 W for a 230-V input, were used as the near-infrared emitting source. The four infrared emitters were arranged horizontally in parallel with the four emitting surfaces facing each other, and four aluminum reflectors were installed behind the emitters to redirect the infrared waves and enhance the efficiency of infrared radiation (Fig. I-1). Total power consumption of the four emitters was approximately 1.8 kW as measured by a digital power meter (WT-230; Yokogawa, Japan) at standard voltage (220 V). The vertical distance between emitters and sample was 13.5 cm (or 5.3 in) at each side.

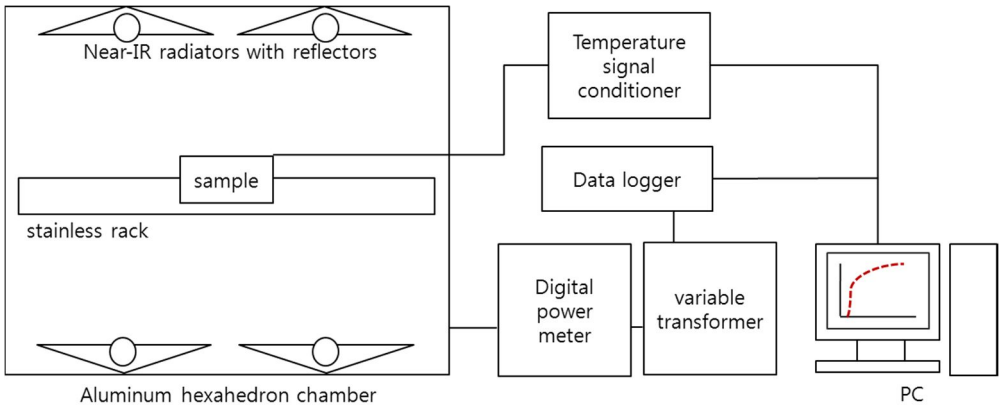

FIG. I-1. Schematic diagram of the NIR heating system used in this study.

For conventional convective heating studies, the four NIR emitters were replaced with four electric resistive emitters (NC420RC; 350 mm; LK, South Korea). The total power of the four resistive heaters was adjusted to match the 1.8 kW used by the NIR system using a variable transformer and data logger (34790A; Agilent Technologies, Palo Alto, CA, USA). The matching wattage was simultaneously verified by means of a digital power meter. The positions and vertical distances of emitters, as well as chamber sizes, were identical to those of the NIR heating system, and the total wattage used was the same.

Surface-inoculated ham slices were placed side by side in the center of a sterilized stainless rack with the long axis parallel to the infrared lamps, whereas the overlapping slices and internally inoculated samples were placed in the center of the treatment rack for the subsequent pasteurization experiment.

Temperature measurement. A fiber optic temperature sensor (FOT-L; FISO Technologies Inc., Quebec, Canada) connected to a signal conditioner (TMI-4; FISO Technologies Inc., Quebec, Canada) was used to measure real-time temperatures in samples during NIR and convective heating. The sensor was placed directly on the surface of the treated ham slices or inserted between two ham slices, and the temperature was manually recorded every 5 s. In the case of convective heating, the temperature was recorded every 10 s after 50 s of treatment. Since the fiber optic sensors were coated with electrical insulating

material, they did not interfere with the temperature profile of the treated sample (Wang et al., 2003). All experiments were repeated three times, and averages and standard deviations of sample temperatures for NIR and convective heating were compared to determine the heating rate of samples.

Bacterial enumeration. For enumeration of pathogens, each of two treated ham slices (ca. 25 g) was placed at room temperature for 30 s and then immediately transferred into a sterile stomacher bag (Labplas Inc., Sainte-Julie, Quebec, Canada) containing 225 ml of BPW (detection limit, 10 CFU/g) and homogenized for 2 min with a stomacher (620 rpm, Easy mix; AES Chemunex, Rennes, France). After homogenization, 1-ml aliquots of sample were 10-fold serially diluted in 9-ml blanks of BPW, and 0.1 ml of sample or diluent was spread plated onto each selective medium. Xylose lysine desoxycholate agar (XLD; Difco), sorbitol MacConkey agar (SMAC; Difco), and Oxford agar base with Bacto Oxford antimicrobial supplement (MOX; Difco) were used as selective media for the enumeration of *S.* Typhimurium, *E. coli* O157:H7, and *L. monocytogenes*, respectively. Where low numbers of surviving cells were anticipated, 1 ml of undiluted stomacher bag contents was divided between four plates to lower the detection limit. All agar media were incubated at 37 °C for 24 to 48 h before counting. To confirm the identity of the pathogens, random colonies were selected from the enumeration plates and subjected to biochemical

and serological tests. These tests consisted of the *Salmonella* latex agglutination assay (Oxoid, Ogdensberg, NY, USA), *E. coli* O157:H7 latex agglutination assay (RIM; Remel, Lenexa, KS, USA), and API Listeria (bio-Mérieux, Hazelwood, MO, USA) for *S.* Typhimurium, *E. coli* O157:H7, and *L. monocytogenes*, respectively.

Enumeration of heat-injured cells. Phenol red agar base with 1% sorbitol (SPRAB; Difco) was used to enumerate heat-injured cells of *E. coli* O157:H7 (Rhee et al., 2003). After incubation at 37 °C for 24 h, typical white colonies characteristic of *E. coli* O157:H7 were enumerated. Randomly selected isolates from SPRAB plates were subjected to serological confirmation as *E. coli* O157:H7 (RIM *E. coli* O157:H7 latex agglutination test; Remel), because SPRAB is not typically used as a selective agar for enumerating *E. coli* O157:H7. The overlay (OV) method was used to enumerate injured cells of *S.* Typhimurium and *L. monocytogenes* (Lee and Kang, 2001). TSA was used as a nonselective medium to repair and resuscitate heat-injured cells. One hundred microliters of appropriate dilutions were spread onto TSA medium, and plates were incubated at 37 °C for 2 h to allow injured microorganisms to repair and resuscitate (Kang and Siragusa, 1999). The plates were then overlaid with 7 to 8 ml of selective medium (XLD or OAB agar). After solidification, plates were

further incubated for an additional 24 to 48 h at 37 °C. Following incubation, typical black colonies were enumerated.

Color and texture measurement. To evaluate the effect of NIR heating on the color of ham slices, a Minolta colorimeter (model CR300; Minolta Co., Osaka, Japan) was used to measure the color changes of NIR-treated surfaces. The color attributes were quantified by the value of L*, a*, and b* and measured at random locations on ham slices. L*, a*, and b* values indicate color lightness, redness, and yellowness of the sample, respectively. All measurements were taken in triplicate.

Changes in texture of NIR-treated ham slices were evaluated with a TA-XT2i texture analyzer (Texture Technology Corp., Scarsdale, NY, USA) with a blade set probe. After cooling the treated samples, six stacked slices (45 by 45 mm) were placed onto the press holder, and a blade was moved down at 2 mm/s. Maximum force was recorded using Texture Expert software (version 1.22; Texture Technology Corp.). These experiments were replicated three times.

Statistical analysis. All experiments were repeated three times with duplicate samples. Data were analyzed by analysis of variance (ANOVA) using the ANOVA procedure of SAS (SAS Institute, Cary, NC, USA), and mean values

were separated using Duncan's multiple-range test. $P < 0.05$ was used to indicate significant difference.

I-3. Results

Average temperature-time histories of ham slices. Average surface temperatures of ham slices during conventional convective and NIR heating, both performed at 1.8 kW, are shown in Fig. I-2. The rate of NIR heating was much higher than that of conventional convective heating, especially the initial rate of increase. The surface temperature rose immediately in response to infrared waves when the ham slice samples were exposed to NIR radiation, while the surface temperature of ham slices began to increase approximately 30 s after convective heating was initiated (Fig. I-2). After 50 s of NIR heating, the surface temperature of ham slices reached ca. 87 °C. To raise the surface temperature from room temperature to 87 °C, convective heating for a maximum of ca. 200 s was required. Figure I-3 shows temperature histories of the insides of two contiguous ham slices during conventional convective and NIR heating. The patterns of temperature growth were similar to those for surface treatment. During 50 s of NIR treatment, the internal temperature reached ca. 74 °C. For convective heating, the maximum time required for the inside to increase from room temperature to 74 °C was ca. 230 s; furthermore, ca. 50 s was needed for the initiation of temperature increase (Fig. I-3).

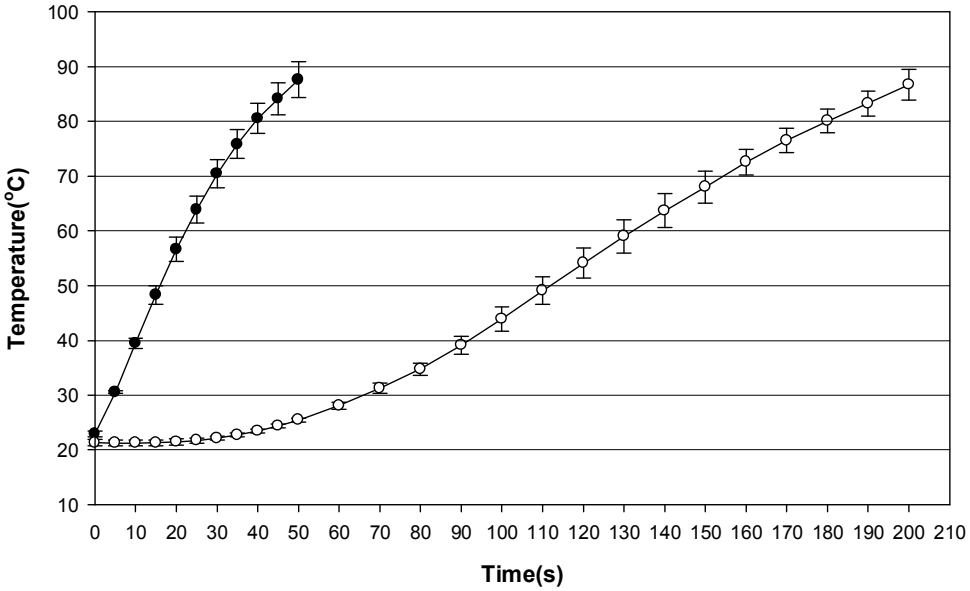

FIG. I-2. Average temperature-time histories of ham slice surfaces during conventional convective and NIR heating. The error bars indicate standard deviations calculated from triplicates. ○, Convective heating at 1.8 kW; ●, NIR heating at 1.8 kW.

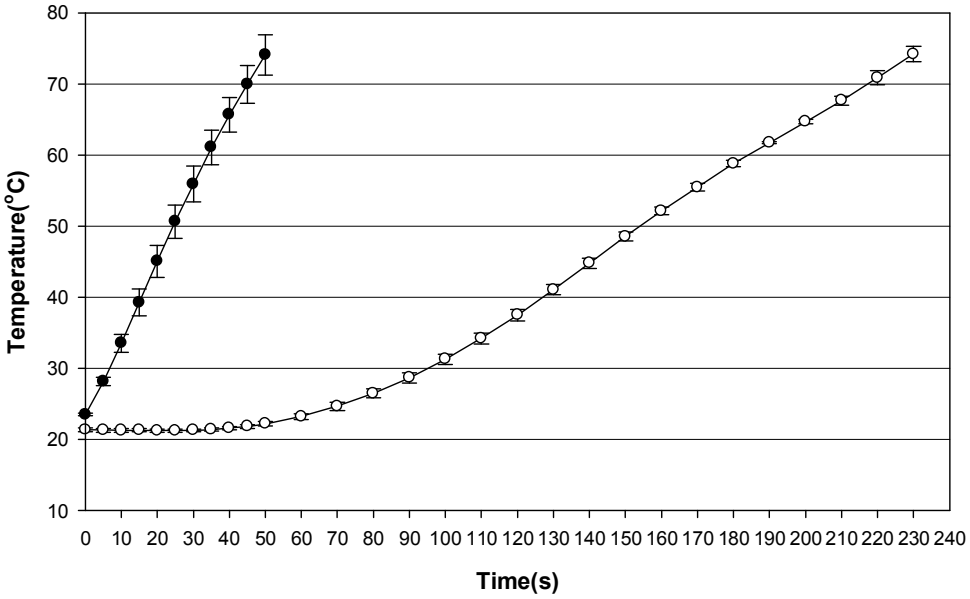

FIG. I-3. Average temperature-time histories of insides of two contiguous ham slices during conventional convective and NIR heating. The error bars indicate standard deviations calculated from triplicates. ○, Convective heating at 1.8 kW; ●, NIR heating at 1.8 kW.

Survival curves of food-borne pathogens. Populations (log CFU/g) of *S.* Typhimurium, *E. coli* O157:H7, and *L. monocytogenes* on ham slice surfaces during NIR and convective heating are shown in Fig. I-4. Significant ($P < 0.05$) log reductions of the three pathogens were observed after 30 s of NIR heating and 150 s of convective heating. NIR heating for 50 s achieved 4.1-, 4.19-, and 3.38-log reductions in *S.* Typhimurium, *E. coli* O157:H7, and *L. monocytogenes*, respectively, whereas convective heating required 180 s to attain comparable reductions for each pathogen (Fig. I-4).

Figure I-5 shows the different effects of NIR and convective heating on inactivation of internally inoculated pathogens. Log reductions of 4.69, 4.56, and 4.16, respectively, were observed in *S.* Typhimurium, *E. coli* O157:H7, and *L. monocytogenes* after NIR heating for 50 s. The overall reduction patterns of *S.* Typhimurium, *E. coli* O157:H7, and *L. monocytogenes* were similar to those of the surface-inoculated test group; however, the initiation time of significant ($P < 0.05$) reduction was delayed about 10 and 30 s for NIR and convective heating, respectively. Especially for convective heating, 190 s of treatment time was required to reduce each pathogen by ca. 4 log CFU/g (Fig. I-5).

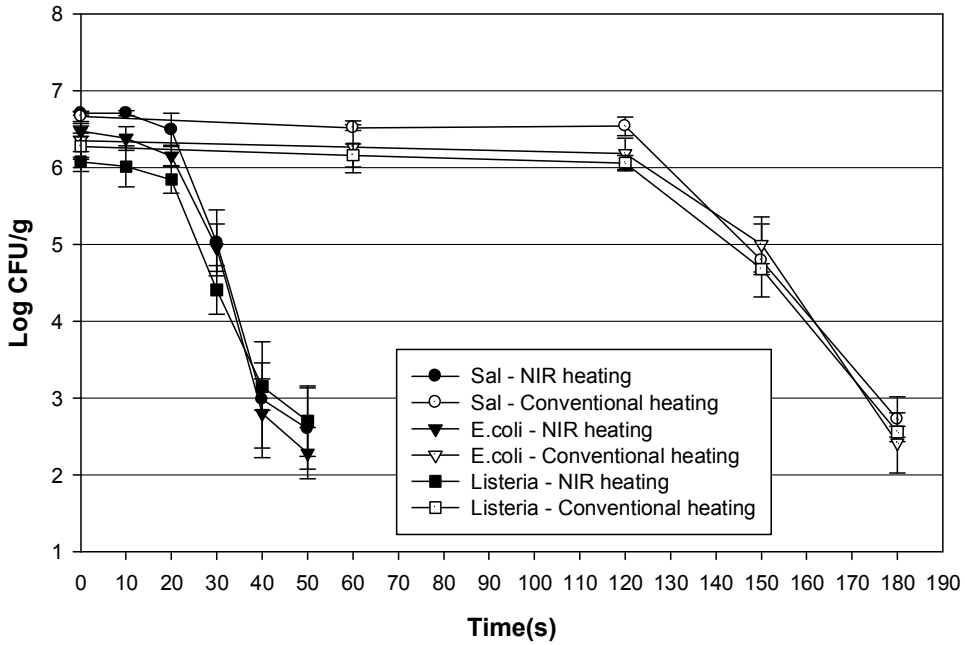

FIG. I-4. Survival curves of *Salmonella* Typhimurium, *Escherichia coli* O157:H7, and *Listeria monocytogenes* on ham slice surfaces treated with NIR or conventional convective heating. The error bars indicate standard deviations calculated from triplicates.

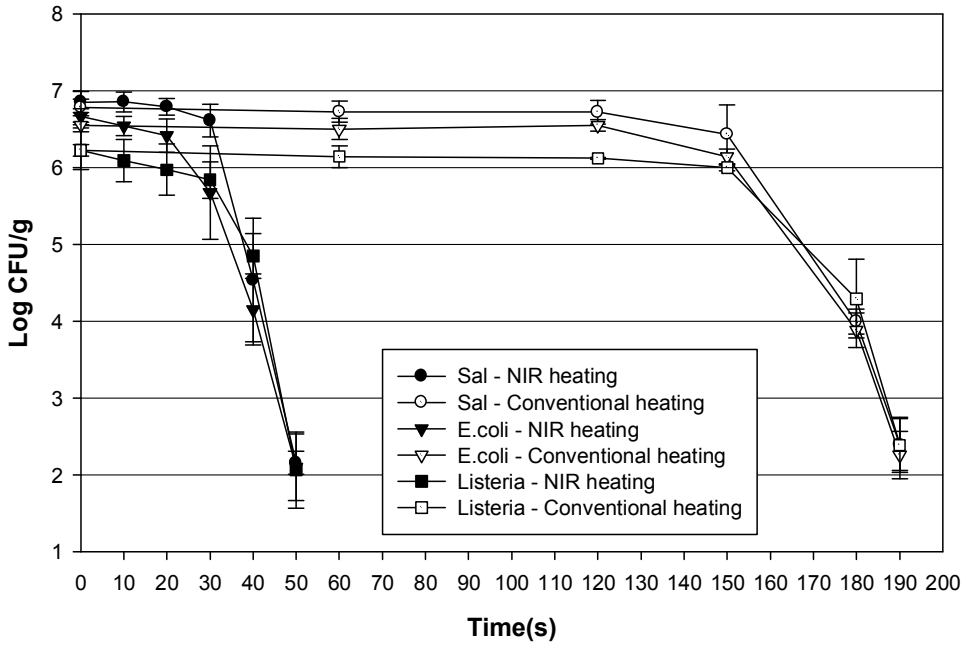

FIG. I-5. Survival curves of *Salmonella* Typhimurium, *Escherichia coli* O157:H7, and *Listeria monocytogenes* inside two contiguous ham slices treated with NIR or conventional convective heating. The error bars indicate standard deviations calculated from triplicates.

Comparison of pathogen populations between surface- and internally inoculated ham slices. The results of the surface and internal inoculation methods following NIR and convective heating were arranged for comparison of penetration efficiency (Table I-1). Table I-1 shows surviving bacterial cells from exposed or protected surfaces of ham slices treated with NIR. There were no statistically significant ($P > 0.05$) differences between surface or internal populations of *S.* Typhimurium, *E. coli* O157:H7, and *L. monocytogenes* at the end of NIR treatment (50 s). However, when conventional convective heating was applied, significant ($P < 0.05$) differences between levels of surface- or internally inoculated cells of the three pathogens were observed during the final part of the treatment (150 and 180 s).

The recovery of heat-injured cells. Table I-2 shows surviving cells, including heat-injured *S.* Typhimurium, *E. coli* O157:H7, and *L. monocytogenes*, on the surfaces of ham slices following NIR or conventional convective heating. When surface-inoculated ham slices were treated with NIR heating (Table I-2), slightly higher numbers of the three pathogens were detected by the agar OV method (SPRAB in the case of *E. coli* O157:H7) than on selective agar. However, there were no significant ($P > 0.05$) differences between the levels of cells enumerated on the appropriate selective agar (XLD, SMAC, and OAB)

Table I-1. Comparison of pathogen populations between surface- and internally inoculated ham slices following NIR (A) or conventional convective heating (B)[a].

(A) Treatment time (s)	Population (log_{10} CFU/g) by organism and inoculation site											
	S. Typhimurium				*E. coli* O157:H7				*L. monocytogenes*			
	Surface		Internally		Surface		Internally		Surface		Internally	
0s	6.70±0.02	Aa	6.85±0.14	Aa	6.47±0.06	Aa	6.66±0.10	Aa	6.08±0.13	Aa	6.22±0.25	Aa
10s	6.71±0.04	Aa	6.85±0.13	Aa	6.38±0.15	Aa	6.54±0.12	Aa	6.01±0.27	Aa	6.09±0.27	Aa
20s	6.49±0.22	Aa	6.79±0.11	Aa	6.15±0.13	Aa	6.41±0.22	Aa	5.84±0.18	Aa	5.97±0.33	Aa
30s	5.02±0.43	Ba	6.61±0.21	Ab	4.96±0.31	Ba	5.67±0.61	Ba	4.41±0.32	Ba	5.84±0.24	Ab
40s	2.98±0.75	Ca	4.53±0.80	Ba	2.80±0.45	Ca	4.15±0.46	Cb	3.15±0.31	Ca	4.85±0.29	Bb
50s	2.60±0.53	Ca	2.16±0.15	Ca	2.29±0.33	Da	2.10±0.43	Da	2.70±0.46	Ca	2.06±0.50	Ca
(B) Treatment time (s)	Population (log_{10} CFU/g) by organism and inoculation site											
	S. Typhimurium				*E. coli* O157:H7				*L. monocytogenes*			
	Surface		Internally		Surface		Internally		Surface		Internally	
0s	6.66±0.06	Aa	6.78±0.11	Aa	6.35±0.22	Aa	6.55±0.04	Aa	6.28±0.17	Aa	6.22±0.07	Aa
60s	6.52±0.04	Aa	6.73±0.14	Aa	6.27±0.34	Aa	6.50±0.14	Aa	6.16±0.15	Aa	6.14±0.14	Aa
120s	6.54±1.12	Aa	6.72±0.16	Aa	6.18±0.20	Aa	6.55±0.07	Ab	6.06±0.10	Aa	6.12±0.01	Aa
150s	4.79±0.48	Ba	6.43±0.39	Ab	5.00±0.36	Ba	6.14±0.10	Bb	4.68±0.07	Ba	6.00±0.04	Ab
180s	2.73±0.29	Ca	3.99±0.16	Bb	2.42±0.39	Ca	3.88±0.22	Cb	2.56±0.07	Ca	4.29±0.51	Bb

[a] Means ± standard deviations from three replications. Means with the same capital letter in the same column are not significantly different ($P > 0.05$). Means with the same lowercase letter in the same row are not significantly different ($P > 0.05$).

Table I-2. Levels of surviving cells and cells including heat-injured *Salmonella* Typhimurium, *Escherichia coli* O157:H7, and *Listeria monocytogenes* on the ham slices following NIR (A) or conventional convective heating (B)[a].

(A)	Population (log_{10} CFU/g) by organism and selection medium											
Treatment	*S.* Typhimurium				*E. coli* O157:H7				*L. monocytogenes*			
time (s)	XLD[b]		OV-XLD		SMAC		SPRAB		OAB		OV-OAB	
0s	6.70±0.02	Aa	6.99±0.21	Aa	6.47±0.06	Aa	6.69±0.21	Aa	6.08±0.13	Aa	6.22±0.07	Aa
10s	6.71±0.04	Aa	6.83±0.12	Aa	6.38±0.15	Aa	6.28±0.25	ABa	6.01±0.27	Aa	6.04±0.15	Aa
20s	6.49±0.22	Aa	6.60±0.18	Aa	6.15±0.13	Aa	6.14±0.15	Ba	5.84±0.18	Aa	5.91±0.17	Aa
30s	5.02±0.43	Ba	5.54±0.15	Ba	4.96±0.31	Ba	5.37±0.08	Ca	4.41±0.32	Ba	4.66±0.47	Ba
40s	2.98±0.75	Ca	4.06±0.66	Ca	2.80±0.45	Ca	3.50±0.45	Da	3.15±0.31	Ca	3.54±0.20	Ca
50s	2.60±0.53	Ca	3.18±0.61	Da	2.29±0.33	Da	2.83±0.16	Ea	2.70±0.46	Ca	3.00±0.36	Da
(B)	Population (log_{10} CFU/g) by organism and selection medium											
Treatment	*S.* Typhimurium				*E. coli* O157:H7				*L. monocytogenes*			
time (s)	XLD		OV-XLD		SMAC		SPRAB		OAB		OV-OAB	
0s	6.60±0.18	Aa	6.69±0.18	Aa	6.06±0.06	Aa	5.98±0.16	Aa	6.23±0.07	Aa	6.49±0.16	Aa
60s	6.53±0.16	Aa	6.75±0.06	Aa	5.91±0.23	Aa	5.99±0.16	Aa	6.33±0.24	Aa	6.43±0.20	Aa
120s	6.36±0.11	Aa	6.60±0.12	Aa	5.79±0.10	Aa	5.94±0.08	Aa	6.13±0.11	Aa	6.41±0.18	Aa
150s	4.34±0.56	Ba	5.78±0.24	Bb	4.34±0.36	Ba	5.44±0.12	Bb	4.01±0.28	Ba	4.97±0.45	Bb
180s	2.71±0.12	Ca	4.15±0.25	Cb	2.24±0.41	Ca	3.47±0.47	Cb	2.73±0.25	Ca	3.01±0.56	Ca

[a] Means ± standard deviations from three replications. Means with the same capital letter in the same column are not significantly different ($P > 0.05$). Means with the same lowercase letter in the same row are not significantly different ($P > 0.05$).
[b] XLD, xylose lysine desoxycholate; OV-XLD, overlay XLD agar on TSA; SMAC, sorbitol MacConkey agar; SPRAB, phenol red agar base with 1 % sorbitol; OAB, Oxford agar base; and OV-OAB, overlay OAB agar on TSA.

versus the agar for resuscitation (OV-XLD, SPRAB, and OV-OAB) during the entire treatment time. In conventional convective heating (Table I-2), however, statistically significant ($P < 0.05$) differences between levels of surviving cells, including sublethally injured *S.* Typhimurium, *E. coli* O157:H7, and *L. monocytogenes* cells, were observed after 150 and 180 s of treatment.

The effect of near-infrared heating on product quality. Color values of ham slices after NIR treatment are summarized in Table I-3. L*, a*, and b* values of NIR-treated (50 s) ham slices were not significantly ($P > 0.05$) different from those of nontreated samples. Although the L values (lightness) slightly decreased in accordance with prolonged treatment time, statistically significant differences were not detected during the entire heating interval (Table I-3). Table I-4 shows the texture parameters of ham slices following NIR treatment. There were no significant ($P > 0.05$) differences in maximum load values of texture measurements among all tested samples, indicating treatment with NIR for 50 s did not significantly ($P > 0.05$) change the quality of ham slices.

Table I-3. Surface color values of NIR-treated ham slices[a].

Treatment time(s)	Parameter[b]		
	L*	a*	b*
0	68.10±0.56 a	11.69±0.24 a	11.38±0.39 a
10	68.45±0.95 a	11.35±0.99 a	11.41±0.30 a
20	68.04±0.47 a	11.32±0.30 a	12.03±0.37 a
30	67.55±1.10 a	11.36±1.04 a	11.95±0.53 a
40	66.63±0.80 a	11.41±0.54 a	12.55±0.80 a
50	66.64±0.75 a	11.04±0.47 a	12.74±0.80 a

[a] Means ± standard deviations from three replications. Values followed by the same letters within the column per parameter are not significantly different ($P > 0.05$).

[b] Color parameters are lightness (L*), redness (a*), and yellowness (b*).

Table I-4. Maximum load values for quantifying texture of ham slices following treatment with NIR[a].

Treatment time (s)	Maximum load (g)	
0s	1171.47±51.21	a
10s	1158.90±13.24	a
20s	1135.27±24.45	a
30s	1175.87±58.02	a
40s	1110.57±8.80	a
50s	1141.70±59.58	a

[a] Means ± standard deviations from three replications. Values followed by the same letters within the column per parameter are not significantly different ($P > 0.05$).

I-4. Discussion

In recent years, large-scale outbreaks related to consumption of RTE meats have occurred, in addition to the recall and destruction of massive quantities of products. Because of the high risk potential to the general public, the U.S. Department of Agriculture Food Safety and Inspection Service (USDA-FSIS) recommends that food manufacturers adopt postlethality intervention treatments to control the growth of pathogens in these products (Zhu et al., 2005).

Infrared heating has been explored as a means for pasteurizing meat products to kill pathogens or other spoilage microorganisms. Infrared surface pasteurization has been investigated by several researchers for inactivation of *L. monocytogenes* on RTE meats. Gande and Muriana (2003) reported on the use of a radiant heat oven for surface pasteurization of various meat products. The heating time varied from 60 to 120 s, and *L. monocytogenes* levels were reduced by about 1.25 to 3.5 logs after treatment. Huang and Sites (2004) conducted surface pasteurization processing of turkey frankfurters using a ceramic infrared heater. The temperature reached the set point (70, 75, or 80 °C) during 82, 92, and 103 s of treatment, respectively, and 3.5- to 4.5-log reductions in *L. monocytogenes* were achieved. However, far- or medium-infrared (F/MIR) heating, which is generated by a quartz tube or ceramic heater, has much lower thermal energy and penetrating capability than NIR. Therefore, the long heating

time was shortened by using an NIR lamp-type emitter in a previous study (Huang and Sites, 2009).

NIR radiation, with its short wavelength, has a relatively higher energy level than F/MIR radiation, which has a longer wavelength, because total energy decreases as the peak wavelength increases (Krishnamurthy et al., 2008). The response of the NIR lamps to electric power was very fast; high-intensity, bright, visible light was emitted from the lamps almost as soon as the power was switched on. The maximum wavelength (λ_m) generated from the infrared heater used in this study was about 1,210 nm and was measured by the Choice spectral light measurement system (LMS 7600; Labsphere, NH). This wavelength was located in the near-infrared wave range (Dagerskog and Osterstrom, 1979). According to Wien's displacement law (Knudsen et al., 1984), the absolute temperature of the emitting source can be calculated from the peak wavelength emitted from the infrared heater [$\lambda_m = (2.898 \times 10^{-3}) / T_k$]. At 1,210 nm, the theoretical maximum temperature attainable by the emitter was 2,122 °C (3,852 °F).

A study by Bolshakov et al. (1976) suggested that a maximum transmission of IR radiation was affected by spectral wavelength. The penetration depths into cooked pork were 2.3, 1.0, and 0.7 mm at a λ_m of 1.07, 2.4, and 4.2 μm, respectively. Since the wavelength used in this study was 1,210 nm, the

penetration depth at this wavelength could be almost 2 mm below the surface of ham slices.

Bacterial cells are very small and are never completely located on ham slice surfaces due to the uneven microscopic topography of meat products. Some bacteria may survive during heat treatment if they harbor in the crevices and cracks under the surface (Huang and Sites, 2008) and potentially present a risk to the consumer. As conduction of heat from the surface to the interior by F/MIR or conventional convective heating is a very slow process, these heating types could contribute to greater deterioration in product quality. Actually, browning was visually observed on meat products which were treated with F/MIR for a slightly excessive time (Huang and Sites, 2004; 2008). In contrast, with NIR heating, thermal energy transfers through both direct penetration and conduction at the same time (Fig. I-3). Furthermore, similar bactericidal effects were observed between pathogens located on the surface and located internally between two contiguous ham slices following NIR heating (Table I-1). These results imply that NIR radiation used in this study sufficiently penetrated the thickness (1.82 ± 0.05 mm, measured by a digital micrometer) of ham slices and delivered thermal energy to the inoculated interface between the slices. NIR heating was more efficient in inactivating pathogens which were internalized or hidden under the surface of ham slices than was convective heating (Table I-1).

The average bacterial concentrations of *S.* Typhimurium, *E. coli* O157:H7, and *L. monocytogenes* inoculated on the exposed or the protected surfaces of ham slices were 6 to 7 log CFU/g. A high-inoculum concentration was used to make enumeration of surviving bacteria easier. These inoculation levels were extremely high for precooked meat product, far higher than would be encountered in commerce, since the USDA-FSIS has established a zero-tolerance level for *L. monocytogenes* in RTE foods (USDA, 1989). Even in noncooked meats, usually less than 3 logs of pathogens are detected (Zaika et al., 1990). Therefore, bearing in mind the low numbers of pathogens present on vacuum-packaged precooked ham products, the application of a treatment capable of achieving a 2- to 3-log reduction in pathogen numbers would be more than sufficient to render the treated product pathogen free. These 2- to 3-log reductions were achieved with just 40 s of NIR treatments both on surface- and internally inoculated samples (Table I-1). Also, this treatment time is much shorter (40 to 50 s) than that of an experiment conducted by Huang and Sites (156 s) (Huang and Sites, 2009) for reducing *Listeria monocytogenes* on the surface of chicken meat using NIR heating.

Following heating treatment, sublethally injured food-borne pathogens could assume added significance, because they are potentially as dangerous as their uninjured counterparts (Lee and Kang, 2001; McCleery and Rowe, 1995). Under favorable environmental conditions, heat-injured cells usually undergo repair

and become functionally normal. Therefore, the cell numbers enumerated on selective media probably are not representative of the total surviving populations in the samples. In this study, the occurrence of sublethally injured pathogens on ham slices was assessed by plating on selective agars with and without a resuscitation step. More sublethally injured cells were produced in conventional convective heating than in NIR heating (Table I-2). This suggests that NIR heating effectively inactivated *S.* Typhimurium, *E. coli* O157:H7, and *L. monocytogenes* on ham slices without generating many heat-injured cells which could recover and grow.

It is essential and advantageous to investigate the quality changes occurring during NIR heat treatment for commercial practical application of this intervention. In a previous NIR study, the statistical measurements of quality changes were insufficient and limited to visual examination (Huang and Sites, 2009). Therefore, in my study, the experimental conditions for investigating the quality change of ham products were focused on treatment with the NIR rather than conventional heating. After the maximum treatment of 50 s, color values (L*, a*, and b*) and cutting maximum load values of samples were not significantly ($P > 0.05$) different from those of the control (Tables I-3 and I-4). These results suggest that NIR heating can be applied to control pathogens in RTE sliced meats without affecting product quality.

NIR heating on an industrial scale for controlling postprocessing contamination can be performed on a continuous basis. Sliced deli meats moving on a stainless steel conveyor belt could be exposed to banks of NIR heaters oriented horizontally on both sides of the belt. Treatment times could be adjusted by altering the speed of the belt. This step is essential in order to evaluate the efficacy and capital costs of NIR processing compared to conventional heat treatment. In addition, further studies to shorten the NIR treatment time for minimization of quality changes or enhancing the effect of inactivation are required.

Chapter II.

Modeling Inactivation of Food-Borne Pathogens in Ready-To-Eat Deli Meat by NIR Heating at Different Radiation Intensities

This chapter was published in *Journal of Food Protection* (2014) 77(7):1224-1228.

II-1. Introduction

The consumption of ready-to-eat (RTE) meats, especially precooked sliced ham, has increased because of their convenience (Sommers et al., 2006). However, foodborne illness outbreaks linked to RTE delicatessen meats have increased worldwide. *Salmonella enterica* serovar Typhimurium, *Escherichia coli* O157:H7, and *Listeria monocytogenes* are the primary foodborne pathogens involved in numerous outbreaks related to delicatessen meats (Belongia et al., 1991, CDC, 2013). The surface of RTE sliced ham products is the primary site of contamination during postprocessing handling (e.g., conveying, cutting, and slicing). Therefore, an additional decontamination step may be needed as a postlethality intervention to inactivate pathogenic bacteria on sliced ham products before final packaging or after the meats are unwrapped at the delicatessen or other retail outlet. Thermal inactivation is still one of the most effective bacterial control methods for RTE meats (Huang and Sites, 2009).

Infrared radiation is a form of electromagnetic energy and is categorized as near infrared (NIR; 0.76 to 2 μm), medium infrared (2 to 4 μm), and far infrared (4 to 1,000 μm). Infrared heating has been gaining wider acceptance because of its higher thermal efficiency and fast heating rate and response time compared with conventional heating (Krishnamurthy et al., 2008). Various infrared surface pasteurization technologies have been developed for surface treatment of

precooked deli meats (Ha et al., 2012; Huang and Sites, 2004; 2009). In my previous study (Ha et al., 2012), the effectiveness of infrared heat processing for surface pasteurization of RTE sliced ham could have been improved and the long heating time shortened by use of NIR radiation as a heat source.

Several primary mathematical models have been used to describe the kinetics of microbial inactivation by various processing methods in RTE meats (Benedito et al., 2011; Bover-Cid et al., 2011; Chun et al., 2009); however, kinetics models describing the inactivation of major foodborne pathogens on deli meats by NIR heating have not been developed. Predicting the effectiveness of NIR heating against foodborne pathogens based on accurate inactivation kinetics is essential to permit establishment of safe processing conditions and is critical for the effective application of this processing technology in industrial pasteurization.

When survival curves are nonlinear, the *D*-value is usually determined by considering the linear portion of the survival curve. However, this approach is definitely not desirable and would result in over- or underestimation, depending on the shape of the survival curve (Pele et al., 1998). Significant and systematic deviations from linearity have been frequently observed in many thermal treatments (Cole et al., 1993; Pagan et al., 1997; Peleg et al., 1998; van Boekel, 2002). The survival curves of *S.* Typhimurium, *E. coli* O157:H7, and *L. monocytogenes* on sliced ham during NIR treatment were not log linear and were clearly concave in my previous study (Ha et al., 2012).

The objective of this study were to find a suitable inactivation kinetics model for *S.* Typhimurium, *E. coli* O157:H7, and *L. monocytogenes* on RTE sliced ham by NIR heating as a function of the processing parameter of radiation intensity, to determine the effect of radiation intensity on the parameters of the kinetics model for practical application by industry, and to validate whether the developed tertiary models could be used to predict survival curves at radiation intensities other than the experimental intensity levels.

II-2. Materials and Methods

Bacterial strains and inoculum preparation. Strains of *S.* Typhimurium (DT 104), *E. coli* O157:H7 (ATCC 35150), and *L. monocytogenes* (ATCC 19115) were obtained from the School of Food Science bacterial culture collection of Seoul National University (Seoul, Korea). Stock cultures were kept frozen at -80 °C in 0.7 ml of tryptic soy broth (TSB; Difco, BD, Sparks, MD, USA) and 0.3 ml of 50 % glycerol. Working cultures were streaked onto tryptic soy agar (TSA; Difco, BD), incubated at 37 °C for 24 h, and stored at 4 °C.

Each strain of *S.* Typhimurium, *E. coli* O157:H7, and *L. monocytogenes* was cultured in 5 ml of TSB at 37 °C for 24 h, centrifugation (4000 × g for 20 min at 4 °C), and washing three times with buffered peptone water (BPW; Difco, BD). The final pellets were resuspended in BPW, corresponding to approximately 10^7 to 10^8 CFU/ml. Suspended pellets of each strain of the three pathogenic species were combined to produce mixed culture cocktails. These culture cocktails with a final level of approximately 10^8 CFU/ml were used in this study.

Sample preparation and inoculation. Precooked, vacuum-packaged sliced ham (approximately 90 by 90 by 2 mm) was purchased from a local grocery store (Seoul, Korea). For surface inoculation, 8 ml of the prepared mixed culture cocktail was diluted in 0.8 liter of sterile peptone water. Each ham slice was

immersed in the mixed pathogen suspension for 1 min at room temperature (22 ± 2 °C), drained on a sterilized rack, and dried in a laminar flow biosafety hood for 20 min with the fan running. Two ham slices (ca. 25 g, inoculum level of 10^6 to 10^7 CFU per sample) were used with each experimental batch.

NIR heating and radiation intensity measurement. A model aluminum chamber (41 by 34 by 29 cm) was used in this study for NIR heating (Fig. II-1). Four quartz halogen infrared heating lamps (350 mm; NS-104, NS-TECH Co., Ltd., Gyunggido, Korea), each with a maximum power of 500 W for 230 V input, were used as an NIR radiation emitting source. The maximum wavelength (λm) of the infrared heater used in this study was about 1,300 nm, which is in the NIR wave range. The four NIR radiation emitters were arranged horizontally in parallel with the four emitting surfaces facing each other, and four aluminum reflectors were installed behind the emitters to redirect the infrared waves and enhance the efficiency of infrared radiation (Fig. II-1). The vertical distance between emitters and sample was 13.5 cm (5.3 in.) at each side. Surface-inoculated ham slices were placed side-by-side in the center of a sterilized stainless rack with the long axis parallel to the NIR lamps. The radiation intensity was selected as the control parameter to provide applicability to other NIR operating conditions. The radiation intensity generated from the NIR heater was measured and recorded by an NIR fiber optic spectrometer (AvaSpec-

NIR256-1.7, Avantes, Eerbeek, The Netherlands). At the sample location, the radiation intensity of the four NIR emitters was adjusted to 99.74 μW/cm^2/nm (1.0 kW), 150.03 μW/cm^2/nm (1.4 kW), and 200.36 μW/cm^2/nm (1.8 kW, standard line voltage) using a variable transformer and a data logger (34790A, Agilent Technologies, Palo Alto, CA, USA). The adjusted electric power was simultaneously verified with a digital power meter (WT-230, Yokogawa, Tokyo, Japan).

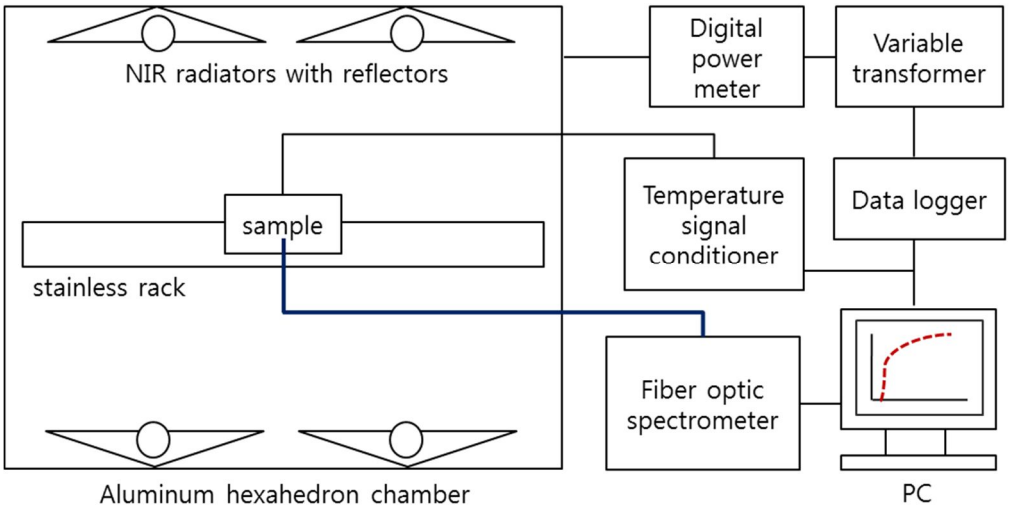

FIG. II-1. Schematic view of the NIR heating system used in this study.

Temperature measurement. A fiber optic temperature sensor (FOT-L, FISO Technologies Inc., Quebec, Quebec, Canada) connected to a signal conditioner (TMI-4, FISO Technologies) was used to measure real-time temperatures in samples during NIR heating at different radiation intensities. The sensor was placed directly on the surface of the treated ham slices, and the temperature was manually recorded every 5 s. All experiments were replicated three times, and means and standard deviations of sample temperatures for selected radiation intensities were compared to determine the heating rate of samples.

Bacterial enumeration. For enumeration of pathogens, each of two treated ham slices (ca. 25 g) were removed, immediately transferred into sterile stomacher bags (Labplas Inc., Sainte-Julie, Quebec, Canada) containing 225 ml of BPW (detection limit of 10 CFU/g), and homogenized for 2 min with a stomacher (620 rpm, EASY MIX, AES Chemunex, Rennes, France). After homogenization, 1 ml of sample was serially diluted in 9 ml of BPW, and 0.1 ml of sample or diluent was spread plated onto each selective medium. Xylose lysine desoxycholate agar (Difco, BD), sorbitol MacConkey agar (Difco, BD), and Oxford agar base with Bacto Oxford antimicrobic supplement (Difco, BD) were used as selective media for the enumeration of *S.* Typhimurium, *E. coli* O157:H7, and *L. monocytogenes*, respectively. When low numbers of surviving cells were anticipated, 1 ml of undiluted stomacher bag contents was equally

distributed onto four plates to lower the detection limit. All agar media were incubated at 37 °C for 24 to 48 h before colonies were counted. To confirm the identity of the pathogens, random colonies were selected from the enumeration plates and subjected to biochemical and serological tests: the *Salmonella* latex agglutination assay (Oxoid, Ogdensberg, NY, USA), the *E. coli* O157:H7 latex agglutination assay (Remel, Lenexa, KS, USA), and the API *Listeria* test (bioMe´rieux, Hazelwood, MO, USA).

Modeling of survival curves. All microbial experiments were conducted three times with duplicate samples, and survival curves obtained under nonisothermal conditions were fitted with the Weibull distribution (equation 1), and log-logistic model (equation 3).

The Weibull model (Bialka et al., 2008) is given by:

$$\log\frac{N}{N_0} = -\left(\frac{1}{2.303}\right)\left(\frac{t}{\alpha}\right)^{\beta} \qquad (1)$$

where α and β are the scale and shape parameters, respectively. The α value represents the time necessary to inactivate the first 0.434 log cycles of the population. The β value accounts for upward concavity of a survival curve (β <1), downward concavity of a survival curve (β >1), and a linear survival curve (β =1). The α and β factors can be applied to calculate d_R using equation 2 (Bialka et al., 2008).

$$d_R = \alpha \times (2.303)^{\frac{1}{\beta}} \quad (2)$$

d_R is defined as NIR treatment time required for 90 % reduction of the population of pathogens, similar to the conventional D-value in thermal processing.

The log-logistic model (Chen and Hoover, 2003a) is described as:

$$\log \frac{N}{N_0} = \frac{A}{1+e^{4\sigma(\tau-\log t)/A}} - \frac{A}{1+e^{4\sigma(\tau+6)/A}} \quad (3)$$

where σ is the maximum rate of inactivation (log CFU per milliliter), τ is the log time to the maximum rate of inactivation (log minutes), t is the thermal treatment time (seconds), and A is the lower asymptote minus the upper asymptote (log CFU per milliliter). Model parameter values and their confidence intervals were obtained by fitting the experimental data to the primary models using GraphPad PRISM (GraphPad Software, Inc., San Diego, CA, USA). The regression coefficient (R^2) and mean square error (*MSE*) were used to evaluate the goodness of fit of the two models.

Tertiary model and validation. It is necessary to follow several steps to develop a predictive model (McMeekin and Ross, 2002). First, microbial inactivation as a function of time was described (primary model). Secondary models characterized parameters appearing in primary models approaches as a function of radiation intensity level. Lastly, primary and secondary models were

combined to predict the pathogen inactivation as a function of treatment time and intensity level (tertiary model).

To determine whether developed tertiary models could predict survival data at radiation intensities other than the experimental intensity levels; two intensities, 125.08 μW/cm^2/nm (1.2 kW) and 175.44 μW/cm^2/nm (1.6 kW), were used in this validation study. These intensities were within the wattage range used previously to develop the model. NIR heating of inoculated ham samples were done at ca. 125 or 175 μW/cm^2/nm under the same conditions. Enumeration of the three pathogens in the samples was performed and compared with values obtained by the predictive models. The regression coefficient (R^2), root mean square error (*RMSE*), bias factor (B_f), and accuracy factor (A_f) were used as quantitative ways to measure the performance of the tertiary models. The B_f and A_f values were calculated with the following equations (Ross, 1996):

$$B_f = 10^{\frac{\sum \log(predicted / observed)}{n}} \quad (4)$$

$$A_f = 10^{\frac{\sum |\log(predicted / observed)|}{n}} \quad (5)$$

Where n is the number of observations. B_f indicates by how much, on average, a model over-predicts or under-predicts the observed data. A_f represents how absolutely close, on average, the predictions are to the observations.

II-3. Results and Discussion

Average temperature-time histories of ham slices at different radiation intensities. Average surface temperatures of ham slices during NIR heating at various radiation intensities are shown in Fig. II-2. The surface temperature rose immediately in response to infrared waves when the ham slice samples were exposed to NIR radiation, and the heating rate of ham slices was dependent on the radiation intensity. The temperature increase at 200 μW/cm^2/nm (1.29 °C/s) was higher than that at 150 μW/cm^2/nm (1.09 °C/s) and 100 μW/cm^2/nm (0.93 °C/s). After 50 s of NIR heating, the surface temperature of ham slices reached ca. 87, 77, and 69 °C at 200, 150, and 100 μW/cm^2/nm, respectively. For the 150- and 100-μW/cm^2/nm treatments, the maximum heating times to reach 87 °C from room temperature were ca. 75 and 95 s, respectively.

In my previous NIR heating study (Ha et al., 2012), treatment at 200 μW/cm^2/nm (1.8 kW) for 50 s did not significantly change ($P > 0.05$) the quality (color and texture) of ham slices. Significant color and texture changes also were not observed at any other intensity levels used in this study (100 and 150 μW/cm^2/nm, data not shown), indicating that NIR treatment at various intensities is acceptable for use in deli meat industry.

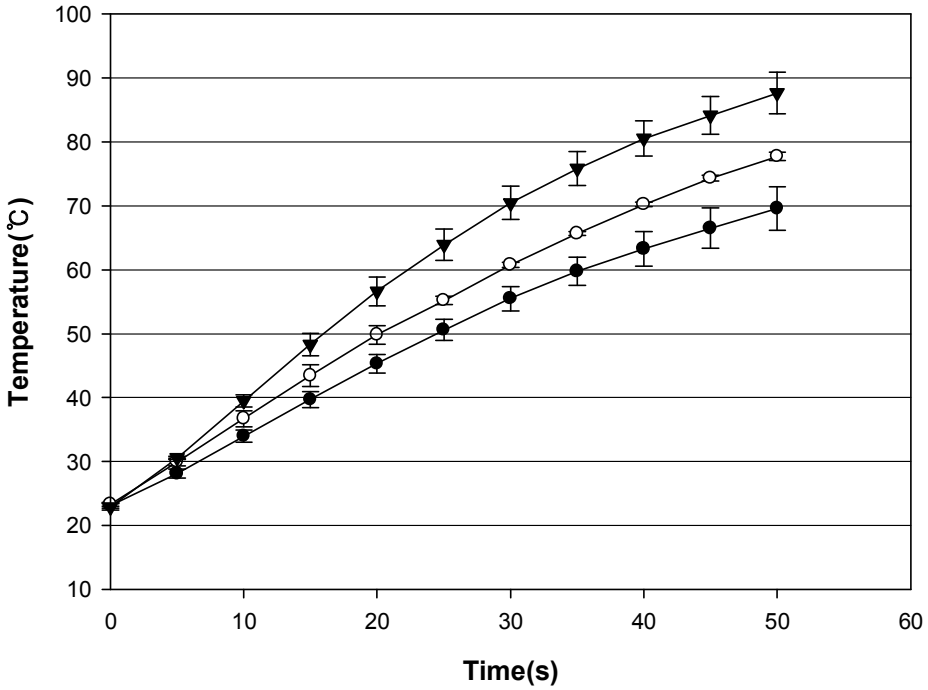

FIG. II-2. Average temperature-time histories of ham slice surfaces during NIR heating at different radiation intensities. Error bars indicate standard deviations calculated from triplicate results. ●, NIR treatment at 100 μW/cm^2/nm; ○, NIR treatment at 150 μW/cm^2/nm; ▼, NIR treatment at 200 μW/cm^2/nm.

Inactivation of pathogenic bacteria by NIR heating at various radiation intensities. The survival curves corresponding to the inactivation of *S.* Typhimurium, *E. coli* O157:H7, and *L. monocytogenes* by NIR heating at different radiation intensities on ham slices are shown in Fig. II-3. An increase in the applied radiation intensity resulted in a faster heating rate and therefore a gradual increase in inactivation of all pathogens. Treatment at 100 $\mu W/cm^2/nm$ for 50 s inactivated populations of *S.* Typhimurium, *E. coli* O157:H7, and *L. monocytogenes* by about 0.87, 0.77, and 0.67 log CFU/g, respectively. The 200 $\mu W/cm^2/nm$ treatment for 50 s reduced the three pathogens by an additional 3.22, 3.41, and 2.72 log CFU/g, respectively, more than did the 100 $\mu W/cm^2/nm$ treatment. Especially for *L. monocytogenes*, the 100 $\mu W/cm^2/nm$ treatment required more than 90 s to attain a ca. 3-log reduction. In the first moments of treatment at all intensities, the change in the level of the three pathogens was very small (shoulder of the survival curve) and then the microbial populations declined following a concave downwards curve (when the temperature increased into the > 60°C range). The downwardly concaved survival curves exhibited characteristic tailing at 40 to 50 s for the 200 $\mu W/cm^2/nm$ treatment, 60 to 70 s for the 150 $\mu W/cm^2/nm$ treatment, and 80 to 90 s for the 100 $\mu W/cm^2/nm$ treatment.

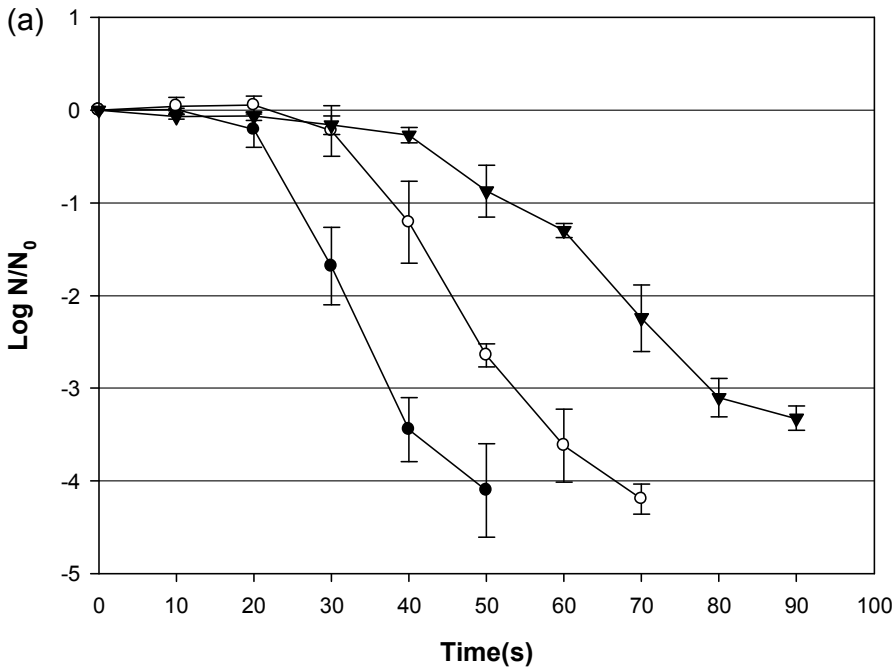
(a)
1
0
-1
-2
-3
-4
-5
Log N/N0
0
10
20
30
40
50
60
70
80
90
100
Time(s)

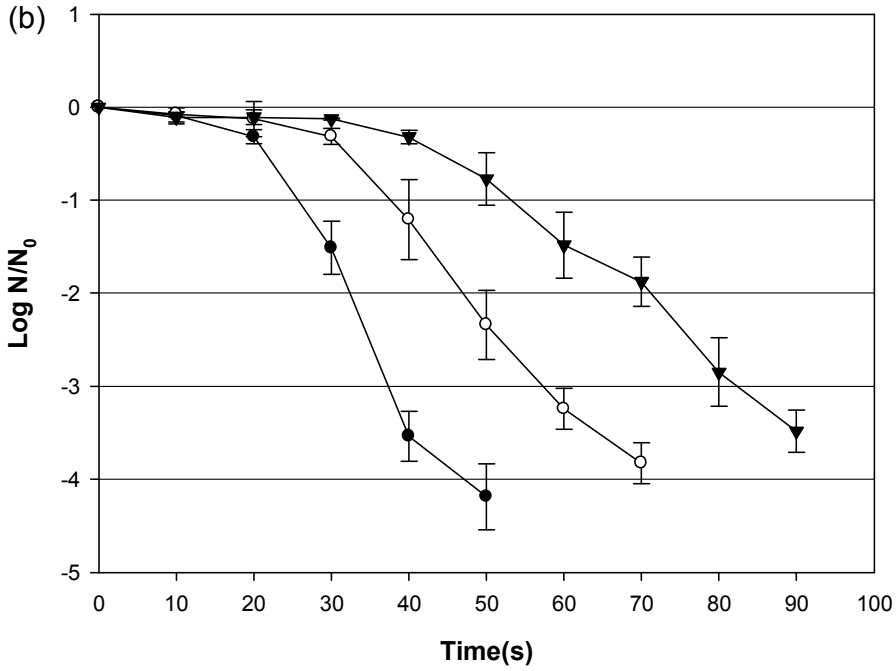
(b)
1
0
-1
-2
-3
-4
-5
Log N/N0
0
10
20
30
40
50
60
70
80
90
100
Time(s)

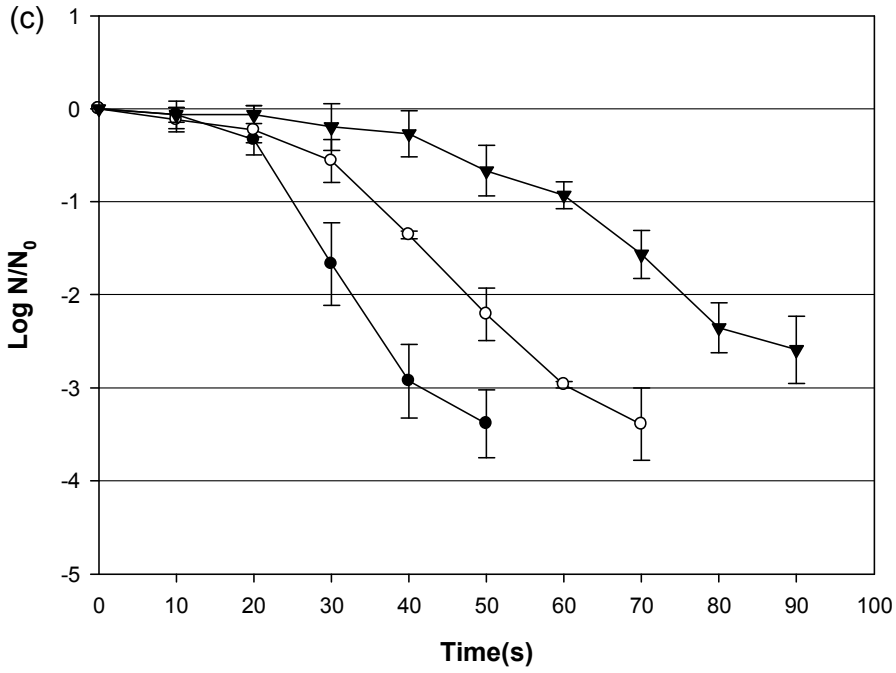

FIG. II-3. Survival curves for *Salmonella enterica* serovar Typhimurium (a), *Escherichia coli* O157:H7 (b), and *Listeria monocytogenes* (c) on ham slice surfaces treated at different NIR intensities. Error bars indicate standard deviations calculated from triplicate results. ●, NIR treatment at 200 μW/cm^2/nm; ○, NIR treatment at 150 μW/cm^2/nm; ▼, NIR treatment at 100 μW/cm^2/nm.

Suitable model of survival curves. Various models have been proposed to describe non-log-linear survival curves (Baranyi and Roberts, 1994; Bhaduri et al., 1991; Cole et al., 1993). Non-log-linear models assume that bacterial cells in a population do not have identical heat resistances, and a survival curve is the cumulative form of a distribution of lethal agents (Chen and Hoover, 2004). In the present study, among the non-log-linear inactivation models the Weibull distribution (equation 1) and the log-logistic model (equation 3) were selected to describe the experimental data obtained under nonisothermal conditions, and the fitness of the models was compared. These two models performed better statistically than did other non-log-linear models in my preliminary studies. Table II-1 shows the computed *MSE* and R^2 values to compare the goodness of fit of the Weibull and log-logistic models. The *MSE* is a measure of the variability remaining in the predictive models, and a lower *MSE* indicates that the model describes the data adequately (Adair et al., 1989). The R^2 value ($0 < R^2 < 1$) is often used as an overall measure of predictive models, and a higher R^2 value indicates a better prediction attained by a particular model (Grau and Vanderlinde, 1993). For *S.* Typhimurium, *E. coli* O157:H7, and *L. monocytogenes*, mean *MSE* values with the Weibull model were 0.15, 0.11, and 0.1, respectively, and those with the log-logistic model were 0.05, 0.04, and 0.05, respectively. Mean R^2 values of the log-logistic model were 0.98, 0.98, and 0.97, respectively, which were better than the values of 0.95, 0.96, and 0.95,

respectively, of the Weibull model. Therefore, for deli meat pasteurization by NIR heating, the log-logistic model more accurately described the survival curves for the three pathogens than did the Weibull distribution at various radiation intensities.

Table II-1. Comparison of goodness of fit of the Weibull model and log-logistic model for the survival curves of *S.* Typhimurium, *E. coli* O157:H7, and *L. monocytogenes* on ready-to-eat sliced ham treated with near-infrared heating at different radiation intensities[a].

Microorganism	Radiation intensity ($\mu W/cm^2/nm$)	Weibull model		log-logistic model	
		MSE	R^2	*MSE*	R^2
Salmonella Typhimurium	100	0.06	0.96	0.03	0.98
	150	0.16	0.95	0.05	0.98
	200	0.22	0.93	0.08	0.98
E. coli O157:H7	100	0.05	0.97	0.04	0.97
	150	0.10	0.96	0.05	0.98
	200	0.17	0.95	0.04	0.99
Listeria monocytogenes	100	0.05	0.95	0.04	0.96
	150	0.07	0.96	0.04	0.98
	200	0.16	0.93	0.07	0.97

[a] *MSE*, mean square error; R^2, regression coefficient.

In general, many non-loglinear models are capable of describing survival curves of a unique shape by using three or more parameters for an adequate description of the data (Virto et al., 2006). Although a model with more parameters can be expected to show a better fit to data, models should be as simple as possible. The reduction of the number of parameters would result in more reliable predictions. A mathematical model based on the Weibull distribution is often used because of its convenience. The Weibull model uses only two parameters (α and β) to describe the extent of inactivation and degree of curvilinearity, respectively (Peleg and Cole, 1998). Since the Weibull model consistently produced a reasonably good fit to all the survival curves (Table II-1), it was further analyzed to determine the effect of radiation intensity on the α and β values of the Weibull distribution. These parameters provide better understanding to the shapes of the survival curves (Table II-2). For the three pathogens, the shape parameters (β value) are greater than 1, which demonstrate the downward concavity of survival curves. These results likely indicate that under NIR treatment the thermal sensitivity of the cells increased as a result of damage accumulation. Additionally, analysis of the β values indicates that the level of treatment intensity significantly affects the shapes of the survival curves. The β values decreased as intensity increased from 100 to 200 $\mu W/cm^2/nm$ for all pathogens and the curves in which tailing occured at the final part of the treatment had lower β values. The scale parameters (α value) of three pathogens

also decreased with increased applied intensity. A lower α value corresponds to a steeper slope of the log survival curve, which indicates that pathogen inactivation occurred at a faster rate. This α value is known to be dependent on the intrinsic heat resistance and the heating rate (Hassani et al., 2007). The d_R value reflects the sensitivity of the pathogen to NIR heating, similar to the conventional *D*-value. Based on the Weibull distribution, significant differences in the estimated d_R values of the three pathogens were not detected.

Table II-2. Kinetic parameters of the Weibull model for *S.* Typhimurium, *E. coli* O157:H7, and *L. monocytogenes* on ready-to-eat sliced ham treated with near-infrared heating at different radiation intensities.

Microorganism	Radiation intensity ($\mu W/cm^2/nm$)	α (CL 95%)	β (CL 95%)	d_R
Salmonella Typhimurium	100	44.13 (41.94-46.31)	5.28 (2.91-7.64)	51.69
	150	30.42 (27.27-33.58)	3.74 (2.87-4.61)	38.01
	200	15.06 (10.88-19.23)	1.95 (1.46-2.45)	23.09
E. coli O157:H7	100	43.23 (40.89-45.57)	3.66 (2.10-5.23)	54.29
	150	28.82 (24.82-32.81)	3.16 (2.27-4.06)	37.52
	200	15.13 (11.49-18.76)	1.98 (1.54-2.41)	23.07
Listeria monocytogenes	100	43.98 (41.04-46.91)	4.45 (1.83-7.06)	53.06
	150	25.54 (21.85-29.24)	2.45 (1.85-3.05)	35.90
	200	14.38 (10.37-18.40)	1.72 (1.29-2.14)	23.37

CL 95%, confidence limit; d_R, decimal reduction time.

Secondary and tertiary models. In many studies, the β value randomly changed with changing external treatment factors or remained within a certain range of conditions. Chen and Hoover (2003b; 2004) reported the simplified Weibull models which set the shape parameters at fixed values for these reasons. Fernández et al. (2002) also observed that the shape factor of the Weibull model was independent of heating temperature. However, in this study, it is obvious that the two parameters, α and β, were radiation intensity level-dependent (Table II-2). Equations describing how these parameters of the primary model change with changes in applied intensity levels correspond to the secondary level of modeling. Since the α and β values of the Weibull distribution were almost in a straight line, single linear equations for all pathogens investigated were developed to describe the effect of radiation intensity level on the two parameters. Table II-3 shows the equations obtained and the corresponding mean R^2 value was 0.98. The linear relationship between α value and temperature has also been observed in thermal inactivation of *C. botulinum* (Peleg and Cole, 2000).

Table II-3. Secondary models developed for α and β values of Weibull distribution.

Microorganism	Equation	R^2
Salmonella Typhimurium	$\alpha = 73.475 - 0.2907*I$	0.9989
	$\beta = 8.6415 - 0.0332*I$	0.9979
E. coli O157:H7	$\alpha = 71.21 - 0.281*I$	0.9998
	$\beta = 5.4622 - 0.0169*I$	0.9478
Listeria monocytogenes	$\alpha = 72.367 - 0.296*I$	0.9802
	$\beta = 6.9637 - 0.0273*I$	0.9334

I, applied radiation intensity; R^2, regression coefficient.

Substituting equations of Table II-3 into equation 1 allowed us to predict the survival curves at NIR intensity levels different from those used in this study. The corresponding tertiary models obtained for three pathogens are as follows:

For *Salmonella enterica* serovar Typhimurium:

$$\log\frac{N}{N_0} = -\left(\frac{1}{2.303}\right)\left(\frac{t}{73.475 - 0.2907 * I}\right)^{8.6415 - 0.0332 * I} \quad (6)$$

For *Escherichia coli* O157:H7:

$$\log\frac{N}{N_0} = -\left(\frac{1}{2.303}\right)\left(\frac{t}{71.21 - 0.281 * I}\right)^{5.4622 - 0.0169 * I} \quad (7)$$

For *Listeria monocytogenes*:

$$\log\frac{N}{N_0} = -\left(\frac{1}{2.303}\right)\left(\frac{t}{72.367 - 0.296 * I}\right)^{6.9637 - 0.0273 * I} \quad (8)$$

Where I is the applied radiation intensity. It should be pointed out that equations 6, 7, and 8 were developed based on survival data that covered a range of approximately 4 log reductions that did not significantly change the quality of ham slices as shown in my previous study (Ha et al., 2012). Therefore, the developed predictive models should only be used within this range and estimation for over 4 log reductions would be inappropriate.

Model validation. After the preliminary steps of model building, it is essential to assess whether developed tertiary models could provide accurate

predictions at other radiation intensity levels. The validation step of the model supports its suitability for predictive purposes and thus it has been performed to show a possible application of the model in food safety management.

Several mathematical and statistical indices of R^2, *RMSE*, B_f, and A_f are employed to validate the performance of developed models in this study. The validation results obtained in 125.08 μW/cm^2/nm (1.2 kW) and 175.44 μW/cm^2/nm (1.6 kW) for the tertiary models are summarized in Table II-4. B_f and A_f have been widely used as worthy tools for the evaluation of the performance of predictive models (Gómez et al., 2005; Hassani et al., 2007). B_f is a measurement of the extent of under ($B_f < 1$) or over ($B_f > 1$) prediction by the model giving the structural deviations (Te-Griffel and Zwietering, 1999). If the B_f value is in the range of 0.9-1.05, the results are considered to be accurate, while 0.7-0.9 or 1.06-1.15 is regarded acceptable and less than 0.7 or greater than 1.15 is regarded unacceptable (Ross, 1999). According to this standard, the B_f values obtained in this validation study were all within the accurate or acceptable range (Table II-4). Whereas, A_f disregards whether the difference between the predicted and observed value is positive or negative and indicates the average distance between each point and the line of equivalence as a measure of how close the estimates are to observations (Ross, 1996). It will always be equal to (which corresponds to the best fit) or greater than 1. The mean R^2, *RMSE*, B_f, and A_f values of *S.* Typhimurium, *E. coli* O157:H7, and *L.*

monocytogenes were (0.97, 0.24, 0.96, 1.31), (0.97, 0.20, 0.86, 1.20), and (0.99, 0.13, 0.99, 1.14), respectively, indicating that the tertiary models produced reasonably good fit for all pathogens in the range of 100 μW/cm^2/nm (1.0 kW) to 200 μW/cm^2/nm (1.8 kW). In addition, Fig. II-4 shows the scatter plot of the observed survival fraction data versus the estimated data obtained from tertiary models. The difference between a point of the graph and the line of equivalence is a measure of the inaccuracy of the corresponding estimation. An overall R^2 value of whole plotted points (125 and 175 μW/cm^2/nm) was 0.96, indicating that the predictive capability of developed tertiary models is comparable.

In conclusion, the present work provided the mathematical models describing the inactivation of *S.* Typhimurium, *E. coli* O157:H7, and *L. monocytogenes* as a function of the significant technical parameters of NIR heating: radiation intensity and treatment time. Both the obtained statistical performances and validation indices demonstrate the suitability of the model for prediction. The results of this study can be used to define the optimum operational conditions for NIR heating to achieve adequate microbial population reductions on RTE sliced ham. Furthermore, in a timely and cost-effective manner, derived models in this study can be utilized in the engineering design of a NIR heating process as an alternative technique for controlling post-processing contamination by deli meat industry.

Table II-4. The validation of developed tertiary models with the data measured at other radiation intensities for determining the goodness of prediction.

Microorganism	Radiation intensity ($\mu W/cm^2/nm$)	R^2	*RMSE*	B_f	A_f
Salmonella Typhimurium	125	0.998	0.103	0.866	1.155
	175	0.942	0.381	1.056	1.457
E.coli O157:H7	125	0.993	0.129	0.897	1.115
	175	0.955	0.266	0.817	1.286
Listeria monocytogenes	125	0.994	0.095	0.932	1.073
	175	0.984	0.174	1.043	1.205

R^2, regression coefficient; *RMSE*, root mean square error; B_f, bias factor; A_f, accuracy factor.

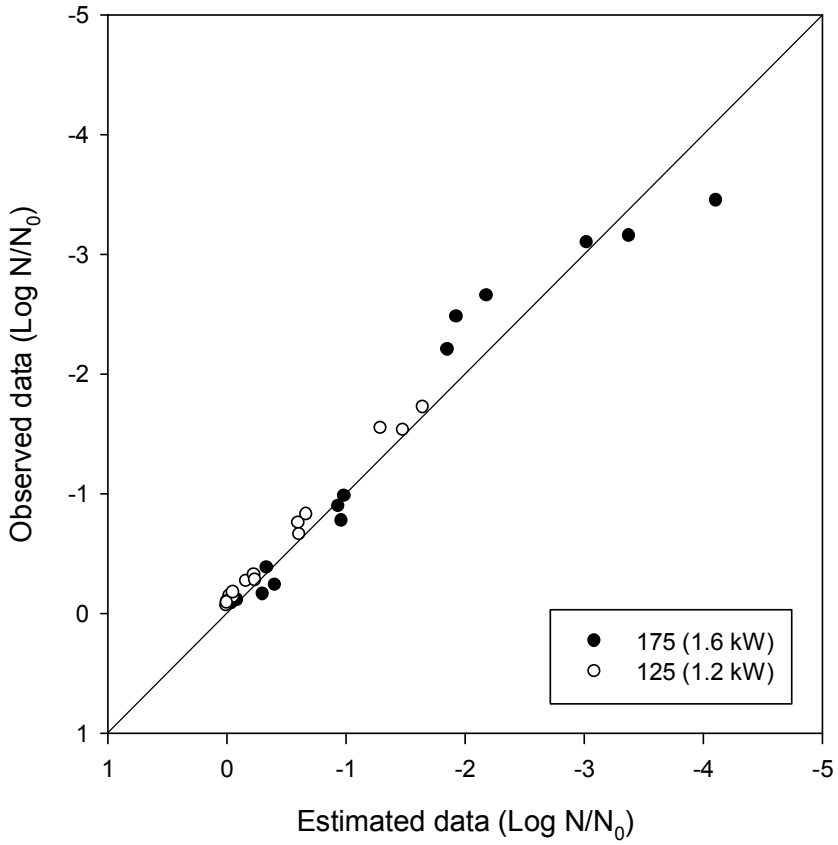

FIG. II-4. Plot of the observed and estimated data obtained with the models developed for *Salmonella enterica* serovar Typhimurium, *Escherichia coli* O157:H7, and *Listeria monocytogenes* on ham slices.

Chapter III.

Enhanced Inactivation of Food-Borne Pathogens in Ready-To-Eat Deli Meat by NIR Heating Combined with UV-C Irradiation and Mechanism of the Synergistic Bactericidal Action

This chapter was published in *Applied and Environmental Microbiology* (2015) 81(1):2-8.

III-1. Introduction

Ready-to-eat (RTE) meat products, especially precooked sliced ham, are widely sold in delicatessens and consumed in homes due to their convenience. However, deli meats have been identified to be high-risk products, as they are highly perishable and easily contaminated (USDA, 2010). *Salmonella enterica* serovar Typhimurium, *Escherichia coli* O157:H7, and *Listeria monocytogenes* are the major causes of outbreaks and product recalls associated with contaminated delicatessen meats (CDC, 2014; Chen et al., 2014; Bravo et al., 2014; USDA, 2014). Recent outbreaks of *S.* Typhimurium and *E. coli* O157:H7 infections in the United States resulted in a total of 311 cases, which were traced to precooked salami (Chen et al., 2014). *L. monocytogenes* is the most relevant pathogen in RTE meat products (Zhang et al., 2012). A significant trend toward an increase in the incidence of listeriosis has been observed in many European countries, with deli meat products having the highest frequency of positive samples (EFSA, 2007). *L. monocytogenes* has been listed in the top 5 highest-ranking pathogens regarding the total cost of foodborne illness in the United States (Ruckman et al., 2004), and deli meats have been reported to be the leading vehicle of foodborne listeriosis (Zhang et al., 2012).

In many recent studies, cross contamination during slicing has been suspected to be the mode of transmission of these three pathogens (Lin et al., 2006; Berzins

et al., 2010; Chaitiemwong et al., 2014; Chen et al., 2014). In other words, the most important route of sliced deli meat contamination is probably via contact with surfaces. Therefore, an additional superficial decontamination step may become necessary to control pathogenic bacteria on sliced ham products immediately before final packaging or after the products are unwrapped at the delicatessen or other retail outlet.

Infrared (IR) radiation transfers thermal energy in the form of an electromagnetic wave and can be classified into 3 regions, near IR (NIR; 0.76 to 2 μm), medium IR (MIR; 2 to 4 μm), and far IR (FIR; 4 to 1,000 μm). IR radiant heating provides significant advantages over convection and conduction heating, including a higher heat transfer capacity and high energy efficiency, as it heats the product directly without being influenced by the air surrounding the food (Krishnamurthy et al., 2008). Several studies have employed infrared heating for surface pasteurization of precooked deli meats (Huang and Sites, 2004; 2009; Ha et al, 2012). In my previous study, NIR radiation was investigated as a heat source and showed improved heating and pasteurization efficacy on RTE sliced ham compared to the heating and pasteurization efficacy of conventional convective heating (Ha et al, 2012).

UV radiation covers part of the electromagnetic spectrum from 100 to 400 nm and is distinguished as UV-A (320 to 400 nm), UV-B (280 to 320 nm), and UV-C (200 to 280 nm) (Gayán et al., 2012). Among them, surface disinfection by

253.7-nm UV irradiation (UV-C) has been widely utilized as an antimicrobial treatment of food surfaces. However, industrial application is still limited because of the low penetration capacity of UV photons into foods. For this reason, UV-C radiation has been used in combination with other antimicrobial processing techniques to produce a hurdle effect on pathogen contaminants (Walkling-Ribeiro et al., 2008; Char et al., 2010; Ukuku and Geveke, 2010). Thus, the combination of NIR heating with UV-C irradiation could be especially efficient in decontaminating the surfaces of sliced deli meats. In addition, despite being a topic of great interest and importance, the mechanism of bactericidal improvement by simultaneous NIR-UV treatment is not well-known.

The aims of the present study were, first, to investigate the efficacy of the simultaneous use of the combination of NIR heating and UV-C irradiation for inactivating foodborne pathogens, including *S.* Typhimurium, *E. coli* O157:H7, and *L. monocytogenes*, on RTE sliced ham and to determine the effect of the combination treatment on factors related to the quality of the sliced ham product. Second, I tried to elucidate the mechanism of synergistic bacterial inactivation by the simultaneous application of NIR and UV-C radiation.

III-2. Materials and Methods

Bacterial strains. Three strains each of *S.* Typhimurium (ATCC 19585, ATCC 43971, and DT 104), *E. coli* O157:H7 (ATCC 35150, ATCC 43889, and ATCC 43890), and *L. monocytogenes* (ATCC 15313, ATCC 19111, and ATCC 19115), obtained from the bacterial culture collection of Seoul National University (Seoul, South Korea), were used in this experiment. Stock cultures were kept frozen at -80 °C in 0.7 ml of tryptic soy broth (TSB; Difco, Becton, Dickinson, Sparks, MD, USA) and 0.3 ml of 50 % glycerol. Working cultures were streaked onto tryptic soy agar (TSA; Difco), incubated at 37 °C for 24 h, and stored at 4 °C.

Preparation of pathogen inocula. All strains of *S.* Typhimurium, *E. coli* O157:H7, and *L. monocytogenes* were cultured individually in 5 ml of TSB at 37 °C for 24 h, followed by centrifugation (4000 × g for 20 min at 4 °C) and washing three times with buffered peptone water (BPW; Difco). The final pellets were resuspended in BPW, corresponding to ca. 10^7 to 10^8 CFU/ml. Subsequently, suspended pellets of each strain of the three pathogenic species (nine strains total) were combined to construct mixed culture cocktails. These cocktails were used in this inactivation study at a final concentration of approximately 10^8 CFU/ml. To analyze the mechanism of inactivation, *S.*

Typhimurium strain DT 104 was selected as a model microorganism, and the cell suspension was grown and prepared in the same way.

Sample preparation and inoculation. Precooked, vacuum-packaged sliced ham (approximately 90 by 90 by 2 mm) was purchased from a local grocery store (Seoul, South Korea), maintained in a refrigerator (4 °C), and used within 2 days. For surface inoculation, 8 ml of the prepared mixed culture cocktail was diluted in 0.8 liter of sterile 0.2 % peptone water. Each ham slice was immersed in the mixed pathogen suspension for 3 min at room temperature (22 ± 2 °C), drained on a sterilized rack, and dried for 20 min inside a biosafety hood with the fan running. Two ham slices (ca. 25 g; inoculum level, 10^5 to 10^6 CFU per sample) were used in each experimental trial.

Near-infrared heating and UV-C irradiation. A model aluminum chamber (41 by 34 by 29 cm) was used in this study for NIR heating (NIR), UV-C irradiation (UV), and NIR-UV combined treatment (Fig. III-1). A quartz halogen infrared heating lamp (350 mm; NS-104; NSTECH, Gyunggido, South Korea) with a maximum power of 500 W (radiation intensity at the sample location, 200.36 μW/cm^2/nm) at a 230-V input was used as a NIR emitting source. The maximum wavelength (λm) generated from the infrared heater used in this study was about 1,300 nm, which is within the NIR wave range. A UV germicidal

lamp (357 mm; G10T5/4P; Sankyo, Japan) with a nominal output power of 16 W (radiation intensity at the sample location, 2.62 mW/cm^2) was used as a UV-C-emitting source. The radiation intensities generated from the NIR and UV lamps were measured and recorded by a NIR fiber optic spectrometer (AvaSpec-NIR256-1.7; Avantes, Eerbeek, Netherlands) and a UV fiber optic spectrometer (AvaSpec-ULS2048; Avantes). Two NIR emitters and two UV-C emitters were arranged horizontally in parallel with the four emitting surfaces facing each other, and four aluminum reflectors were installed behind the emitters to focus as much of the radiation as possible uniformly onto the process line and enhance the efficiency of NIR and UV irradiation (Fig. III-1). The total power consumption of the four emitters was approximately 0.9 kW, as measured by a digital power meter (WT-230; Yokogawa, Japan) at the standard voltage (220 V). The vertical distance between the emitters and the sample was 13.5 cm (5.3 in.) on each side. For the subsequent pasteurization experiments (NIR radiant heating, UV-C irradiation, and the simultaneous application of both technologies), the surface-inoculated ham slices were placed side-by-side in the center of a sterilized stainless rack with the long axis parallel to the NIR and UV lamps.

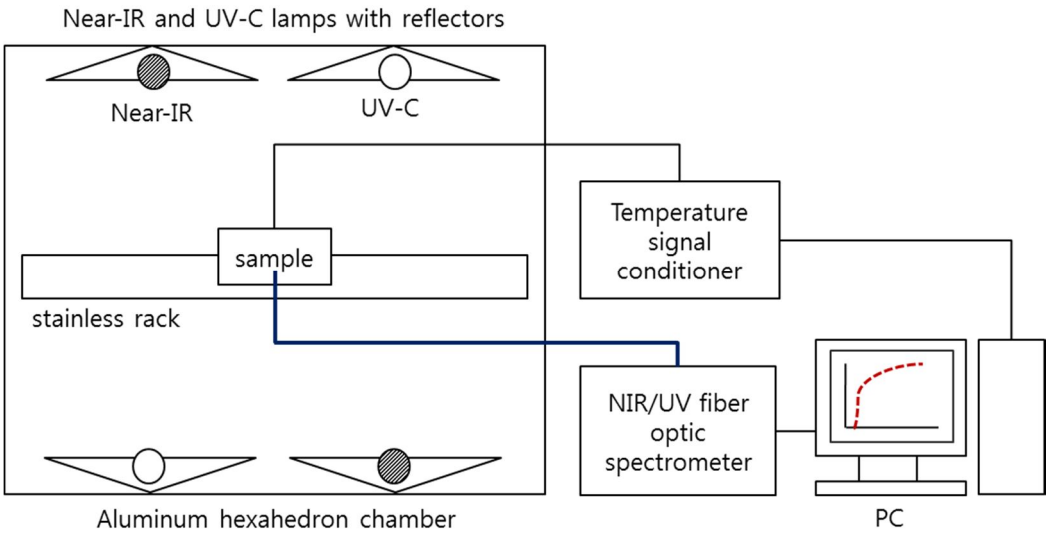

FIG. III-1. Schematic diagram of the NIR-UV combined treatment system used in this study.

Temperature measurement. A fiber optic temperature sensor (FOT-L; FISO Technologies Inc., Quebec, Canada) connected to a signal conditioner (TMI-4; FISO Technologies Inc.) was used to measure the temperatures in the samples in real time during NIR heating and simultaneous NIR-UV treatment. The sensor was placed directly on the surface of the treated ham slices, and the temperature was manually recorded every 5 s. The fiber optic sensors were coated with electrical insulating material. All experiments were replicated three times, and means and standard deviations of sample temperatures for the NIR and NIR-UV combined treatment were compared to determine the rate of heating of the samples.

Bacterial enumeration. At selected time intervals, each of two treated ham slices (ca. 25 g) was removed, immediately transferred into a sterile stomacher bag (Labplas Inc., Sainte-Julie, Quebec, Canada) containing 225 ml of BPW (detection limit, 10 CFU/g), and homogenized for 2 min with a stomacher (620 rpm, Easy mix; AES Chemunex, Rennes, France). After homogenization, 1-ml aliquots of the sample were 10-fold serially diluted in 9 ml of BPW, and 0.1 ml of sample or diluent was spread plated onto each selective medium. Xylose lysine desoxycholate agar (XLD; Difco), Sorbitol MacConkey agar (SMAC; Difco), and Oxford agar base (OAB) with Bacto Oxford antimicrobial supplement (MOX; Difco) were used as selective media for the enumeration of *S.*

Typhimurium, *E. coli* O157:H7, and *L. monocytogenes*, respectively. Where low numbers of surviving cells were anticipated, 1 ml of undiluted sample was equally distributed onto four plates to lower the detection limit. All agar media were incubated at 37 °C for 24 to 48 h before colonies were counted. To confirm the identity of the pathogens, random colonies were selected from the enumeration plates and subjected to biochemical and serological tests. These tests consisted of the *Salmonella* latex agglutination assay (Oxoid, Ogdensburg, NY, USA), the *E. coli* O157:H7 latex agglutination assay (RIM; Remel, Lenexa, KS, USA), and the API *Listeria* test (bioMérieux, Hazelwood, MO, USA).

Enumeration of injured cells. The overlay (OV) method was used to enumerate injured cells of *S.* Typhimurium and *L. monocytogenes* (Lee and Kang, 2001). TSA was used as a nonselective medium to repair injured cells. One hundred microliters of the appropriate dilutions was spread plated onto TSA medium, and the plates were incubated at 37 °C for 2 h to allow injured cells to resuscitate (Kang and Siragusa, 1999). The plates were then overlaid with 7 to 8 ml of selective medium (XLD or OAB). After solidification, the plates were further incubated for an additional 22 to 46 h at 37 °C. Following incubation, typical black colonies were counted. In the case of *E. coli* O157:H7, it is not appropriate to overlay with SMAC medium. Instead, phenol red agar base with 1% sorbitol (SPRAB; Difco) was used to enumerate injured cells of this pathogen

(24). After incubation at 37 °C for 24 h, presumptive colonies of *E. coli* O157:H7 with typical white colonies were enumerated. Isolates randomly selected from SPRAB plates were subjected to serological confirmation as *E. coli* O157:H7 (*E. coli* O157:H7 latex agglutination assay; RIM; Remel), because SPRAB is not typically used as a selective agar for enumerating *E. coli* O157:H7.

Investigation of the bactericidal mechanism. To investigate sites of cellular damage in *S.* Typhimurium DT 104 (the strain selected as a model microorganism) caused by NIR, UV, and simultaneous NIR-UV treatments, four kinds of metabolic inhibitors, chloramphenicol (28.0 μg/ml; Sigma-Aldrich, St. Louis, MO, USA), nalidixic acid (1.2 μg/ml; Sigma-Aldrich), penicillin G (350.0 μg/ml; Sigma-Aldrich), and rifampin (5.0 μg/ml; Sigma-Aldrich), were utilized. The concentrations of the metabolic inhibitors applied were chosen after preliminary experiments were performed, and the synthesis inhibition targets of these antibiotics are presented in Table III-1.

Table III-1. Concentrations of metabolic inhibitors incorporated into TSA medium and targets of synthesis inhibition.

Metabolic inhibitors	Concn (μg/ml)[a]	Target of synthesis inhibition
Chloramphenicol	28.0	Protein (ribosome)
Nalidixic acid	1.2	DNA
Penicillin G	350.0	Cell wall
Rifampicin	5.0	RNA (RNA polymerase)

[a] The maximum concentration at which selective antibiotics had no effect on colony formation of intact *Salmonella* Typhimurium DT 104 cells

Two ham slices (ca. 25 g) inoculated with *S.* Typhimurium DT 104 were treated with NIR, UV, and NIR-UV for 70 s and homogenized in BPW as described above. One hundred microliters of the appropriate dilutions was spread plated onto TSA medium (with or without metabolic inhibitors incorporated at the concentrations listed above), and the plates were incubated at 37 °C for 2 h to allow injured cells to resuscitate. The plates were then overlaid with 7 to 8 ml of selective medium (XLD). After solidification, the plates were further incubated for an additional 22 h at 37 °C. Following incubation, typical black colonies were enumerated. The quantitative levels of recovery inhibition were calculated by subtracting the population numbers on medium containing each antibiotic from the population numbers obtained on nonselective controls that did not contain a selective reagent in the TSA medium and were thus used to probe the site of injury corresponding to the particular metabolic inhibitor.

Color and texture measurement. In order to determine the effect of NIR-UV treatment on the color of the ham slices, a Minolta colorimeter (model CR400; Minolta Co., Osaka, Japan) was used to measure changes to the color of the treated samples. The color attributes were quantified from the values of L*, a*, and b*, which indicate the color lightness, redness, and yellowness of the sample, respectively, and which were measured at random locations on the ham slices. All measurements were taken in triplicate.

Changes in the texture of the NIR-UV-treated ham slices were evaluated with a Brookfield texture analyzer (CT3-10k; Brookfield Engineering Laboratories, Inc., MA, USA) with a blade set probe (TA7; knife edge, 60 mm wide). After the treated samples were cooled, four stacked slices (45 by 90 mm) were placed onto the press holder, and a blade was moved down at 2 mm/s. The maximum force required to cut the sample was recorded using TexturePro CT software (version 1.2; Brookfield Engineering Laboratories, Inc.). The peak force required to shear the samples was utilized as an indicator of hardness. All experiments were replicated three times.

Statistical analysis. All experiments were repeated three times with duplicate samples. Triplicate data were analyzed by analysis of variance (ANOVA) and Duncan's multiple-range test of a statistical analysis system (SAS Institute, Cary, NC, USA). A P value of < 0.05 was used to indicate significant differences.

III-3. Results

Inactivation of pathogenic cells by simultaneous NIR-UV treatment. Reductions in the viable counts of *S.* Typhimurium, *E. coli* O157:H7, and *L. monocytogenes* cells on ham slice surfaces during NIR radiant heating (NIR), UV-C irradiation (UV), and the simultaneous application of both technologies (NIR-UV) are summarized in Table III-2, 3, and 4, respectively. Significant ($P < 0.05$) log reductions of the three pathogens were observed after 10 s of UV irradiation alone and the NIR-UV combined treatment, whereas for NIR radiant heating, the time to initiation of a significant ($P < 0.05$) reduction was delayed about 30 to 40 s (Table III-2 to 4). In addition, the UV sensitivities (irradiation dose based) of the treated pathogens were consistent with those presented in another report describing *S.* Typhimurium and *L. monocytogenes* inactivation by UV-C light in RTE sliced ham (Chun et al., 2009). The simultaneous NIR-UV combined treatment for 70 s led to mean reductions of 4.17, 3.62, and 3.43 log CFU/g in *S.* Typhimurium, *E. coli* O157:H7, and *L. monocytogenes*, respectively. For all three pathogens, the sums of the reductions for NIR and UV inactivation were lower than the values reached by the simultaneous application of both technologies. In other words, the existence of a synergistic effect against all pathogens was confirmed for all treatment times. However, statistically significant ($P < 0.05$) differences between the sums of NIR and UV inactivation

and the inactivation obtained with the combination treatment were observed for the three pathogens only after treatment times of 70 s (Table III-2 to 4). The reductions in the *S.* Typhimurium, *E. coli* O157:H7, and *L. monocytogenes* counts resulting from the synergistic effect occurring after 70 s of treatment, calculated by subtracting the sums of the NIR and UV reductions from those achieved during simultaneous NIR-UV treatment, were 0.76, 0.64, and 0.43 log units, respectively.

Table III-2. Reductions in numbers of viable *Salmonella* Typhimurium cells on ham slice surfaces treated with UV, NIR, and NIR-UV.

Treatment time (sec)	Log reduction [$\log_{10}(N_0/N)$] by treatment type and selective medium[a]							
					NIR-UV			
	UV (XLD)		NIR (XLD)		XLD		OV-XLD	
0	0.00±0.00	A	0.00±0.00	A	0.00±0.00	Aa	0.00±0.00	Aa
10	1.16±0.17	B	0.03±0.03	A	1.55±0.23	Ba	1.38±0.16	Ba
20	1.22±0.16	B	0.06±0.00	A	1.68±0.37	Ba	1.46±0.19	Ba
30	1.48±0.22	C	0.06±0.04	A	1.71±0.34	Ba	1.55±0.23	Ba
40	1.56±0.14	C	0.11±0.12	A	1.96±0.35	BCa	1.83±0.39	BCa
50	1.57±0.15	C	0.43±0.30	B	2.31±0.30	Ca	2.25±0.24	Ca
60	1.63±0.12	C	1.19±0.20	C	3.05±0.32	Da	2.78±0.27	Da
70*	1.73±0.03	C	1.68±0.03	D	4.17±0.11	Ea	3.66±0.34	Ea

[a] The values are means ± standard deviations from three replications. Means with the same uppercase letter in the same column are not significantly different ($P > 0.05$). Within the NIR-UV columns, values in the same row followed by the same lowercase letter are not significantly different ($P > 0.05$). XLD, xylose lysine desoxycholate; OV-XLD, overlay XLD agar on TSA.

* Statistically significant ($P < 0.05$) difference between the sum of NIR and UV inactivation and inactivation achieved with combination treatment was observed.

Table III-3. Reductions in numbers of viable *Escherichia coli* O157:H7 cells on ham slice surfaces treated with UV, NIR, and NIR-UV.

Treatment time (sec)	Log reduction [$\log_{10}$ (N_0/N)] by treatment type and selective medium[a]							
					NIR-UV			
	UV (SMAC)		NIR (SMAC)		SMAC		SPRAB	
0	0.00±0.00	A	0.00±0.00	A	0.00±0.00	Aa	0.00±0.00	Aa
10	1.22±0.27	B	0.06±0.07	A	1.57±0.33	Ba	1.49±0.01	Ba
20	1.24±0.26	B	0.11±0.07	A	1.88±0.24	BCa	1.54±0.02	Ba
30	1.29±0.22	B	0.21±0.11	A	2.00±0.38	BCDa	1.62±0.08	BCa
40	1.43±0.23	B	0.25±0.11	A	2.14±0.30	CDa	1.81±0.34	BCa
50	1.46±0.21	B	0.69±0.27	B	2.46±0.19	DEa	1.96±0.25	Ca
60	1.50±0.24	B	1.05±0.23	C	2.68±0.16	Ea	2.46±0.30	Da
70*	1.52±0.15	B	1.46±0.09	D	3.62±0.26	Fa	3.23±0.23	Ea

[a] The values are means ± standard deviations from three replications. Means with the same uppercase letter in the same column are not significantly different ($P > 0.05$). Within the NIR-UV columns, values in the same row followed by the same lowercase letter are not significantly different ($P > 0.05$). SMAC, sorbitol MacConkey agar; SPRAB, phenol red agar base with 1% sorbitol. * Statistically significant ($P < 0.05$) difference between the sum of NIR and UV inactivation and inactivation achieved with combination treatment was observed.

Table III-4. Reductions in numbers of viable *Listeria monocytogenes* cells on ham slice surfaces treated with UV, NIR, and NIR-UV.

Treatment time (sec)	Log reduction [$\log_{10}(N_0/N)$] by treatment type and selective medium[a]							
					NIR-UV			
	UV (OAB)		NIR (OAB)		OAB		OV-OAB	
0	0.00±0.00	A	0.00±0.00	A	0.00±0.00	Aa	0.00±0.00	Aa
10	1.00±0.21	B	0.06±0.10	A	1.37±0.42	Ba	1.26±0.03	Ba
20	1.08±0.28	B	0.11±0.14	A	1.66±0.26	BCa	1.36±0.15	Ba
30	1.11±0.28	BC	0.23±0.26	AB	1.73±0.20	BCa	1.52±0.21	BCa
40	1.18±0.18	BC	0.48±0.31	BC	1.96±0.05	Ca	1.83±0.34	Ca
50	1.27±0.16	BCD	0.67±0.21	CD	2.45±0.25	Da	2.26±0.20	Da
60	1.46±0.16	CD	0.87±0.20	D	2.73±0.36	Da	2.62±0.32	Da
70*	1.55±0.17	D	1.45±0.21	E	3.43±0.10	Ea	3.16±0.18	Ea

[a] The values are means ± standard deviations from three replications. Means with the same uppercase letter in the same column are not significantly different ($P > 0.05$). Within the NIR-UV columns, values in the same row followed by the same lowercase letter are not significantly different ($P > 0.05$). OAB, Oxford agar base; OV-OAB, overlay OAB agar on TSA.

* Statistically significant ($P < 0.05$) difference between the sum of NIR and UV inactivation and inactivation achieved with combination treatment was observed.

Resuscitation of NIR-UV-injured cells. The levels of sublethally injured *S.* Typhimurium, *E. coli* O157:H7, and *L. monocytogenes* cells on ham slice surfaces following simultaneous NIR-UV treatment are presented in Table III-2, 3, and 4, respectively. At the maximum treatment time of 70 s, injured cell levels of 0.51, 0.39, and 0.27 log CFU/g were detected for *S.* Typhimurium, *E. coli* O157:H7, and *L. monocytogenes*, respectively. Overall, the reductions in the numbers of the three pathogens observed at whole treatment time intervals using the agar OV method (SPRAB in the case of *E. coli* O157:H7) were slightly less than the reductions observed by direct plating on selective agar. However, statistically significant ($P > 0.05$) differences between the inactivation levels enumerated on the appropriate selective agar (XLD, SMAC, and OAB) versus the agar used for recovery (OV-XLD, SPRAB, and OV-OAB) were not observed for any treatment time interval (Table III-2 to 4).

Average temperature-time histories of ham slices. The average surface temperatures of the ham slices during NIR heating and simultaneous NIR-UV treatment are shown in Fig. III-2. The surface temperature rose immediately in response to infrared waves when the ham slice samples were exposed to NIR radiation, and the heating rate of the simultaneous NIR-UV treatment was not significantly ($P > 0.05$) different from that of the NIR treatment alone (Fig. III-2). The surface temperature of the ham slices increased from room temperature

(22 ± 2 °C) and reached ca. 74 °C after 70 s of NIR-UV treatment. The difference in temperature between treatment with NIR alone and NIR-UV treatment at 70 s was under 1 °C.

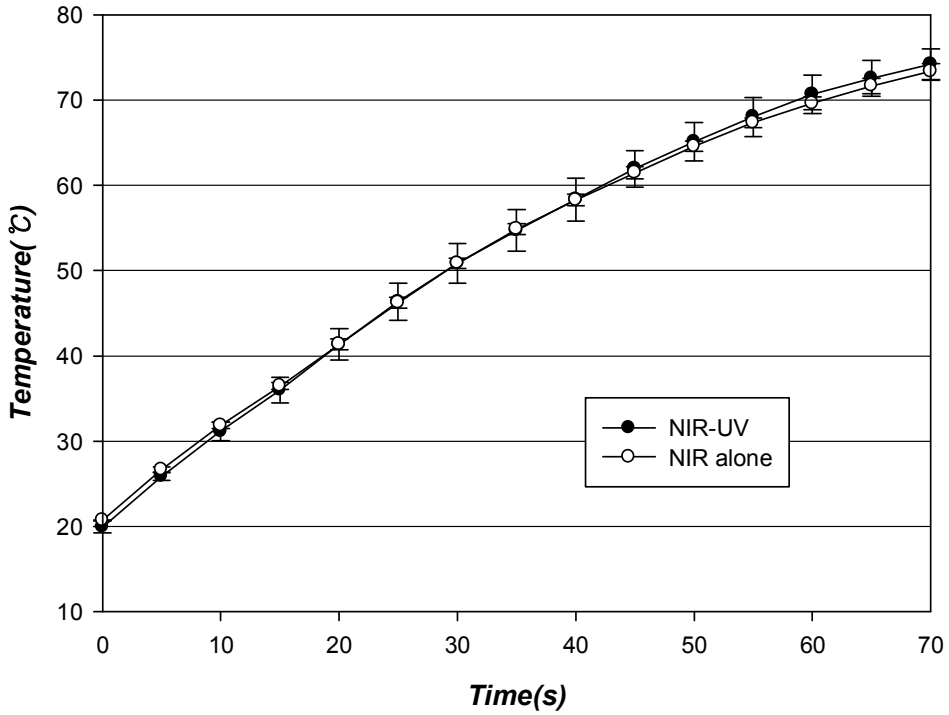

FIG. III-2. Average temperature-time histories of ham slice surfaces during NIR heating and simultaneous NIR-UV treatment. The error bars indicate standard deviations calculated from triplicates.

Determination of injury sites in NIR-UV-treated cells. To gain further insight into the basis of NIR-UV injury, the effect of metabolic inhibitors on repair of *S.* Typhimurium DT 104 cells injured by UV, NIR, and NIR-UV was examined. Table III-5 shows the quantitative levels of recovery inhibition of *S.* Typhimurium DT 104 after each treatment. The degree of recovery inhibition of intact *S.* Typhimurium DT 104 cells (untreated control) was close to zero; namely, the resuscitated populations of untreated *S.* Typhimurium DT 104 cells were not significantly different in the presence or absence of the selective antibiotics (chloramphenicol, nalidixic acid, penicillin G, and rifampin). Penicillin G did not inhibit the recovery of UV- or NIR-treated cells at all. However, significant ($P < 0.05$) inhibition of repair (ca. 0.27 log unit) was detected following the NIR-UV combined treatment. In the presence of chloramphenicol, the degree of recovery inhibition of NIR-UV-treated cells (ca. 0.58 log unit) was significantly ($P < 0.05$) higher than the degree of recovery inhibition of UV- or NIR-treated cells (ca. 0.02 or 0.29 log unit, respectively). Nalidixic acid only slightly inhibited the repair of injuries induced by UV or NIR-UV and did not affect the viability of NIR-treated cells, whereas in the presence of rifampin, equal ca. 0.65 log unit of resuscitation of NIR- or NIR-UV-treated cells, respectively, was inhibited.

Table III-5. Effect of metabolic inhibitors on resuscitation of UV-, NIR-, and NIR-UV-injured *Salmonella* Typhimurium DT 104 cells.

Treatment type	Level of recovery inhibition (Log_{10} CFU/g) by selective antibiotics[a]			
	Chloramphenicol	Nalidixic acid	Penicillin G	Rifampicin
Untreated control	0.09±0.01 A	-0.01±0.07 AB	0.01±0.09 A	0.02±0.05 A
UV	0.02±0.04 A	0.07±0.06 B	-0.01±0.06 A	0.23±0.04 B
NIR	0.29±0.17 A	-0.04±0.01 A	-0.01±0.07 A	0.65±0.11 C
NIR-UV	0.58±0.23 B	0.06±0.04 B	0.27±0.03 B	0.65±0.08 C

[a] Values are means of three replications ± standard deviations. Values followed by the same letters within the column for each metabolic inhibitor are not significantly different ($P > 0.05$). The quantitative levels of recovery inhibition were calculated by subtracting the populations on medium containing each antibiotic from the populations obtained on nonselective medium that did not contain a selective reagent (control).

Therefore, *S.* Typhimurium DT 104 cells subjected to simultaneous NIR-UV treatment showed significantly ($P < 0.05$) greater values of recovery inhibition than cells subjected to the other treatments in the presence of chloramphenicol or penicillin G.

Effect of simultaneous NIR-UV treatment on product quality. The color and texture parameters of the ham slices after simultaneous NIR-UV treatment are shown in Table III-6. The color (L*, a*, and b*) values for NIR-UV-treated (70 s) ham slices were not significantly ($P > 0.05$) different from those for nontreated samples. Although the values of a* and b* (redness and yellowness, respectively) slightly increased and the values of L* (lightness) slightly decreased, in accordance with the prolonged treatment time, statistically significant differences were not observed during the entire treatment interval (Table III-6). Also, the NIR-UV combined treatment for 70 s did not significantly ($P > 0.05$) change the maximum load values of the texture measurements. Thus, the simultaneous application of NIR and UV treatment for 70 s did not significantly alter the quality of the ham slice products.

Table III-6. Surface color values and maximum load values for quantifying texture of ham slices simultaneously treated with NIR-UV[a].

Treatment time(s)	Color value for parameter			Maximum load (g)
	L*	a*	b*	
0	63.54±0.57 A	15.69±0.10 A	9.60±0.55 A	1015.67±43.66 A
10	63.43±0.55 A	15.91±0.18 A	9.59±1.02 A	1001.00±72.33 A
30	63.54±0.96 A	15.81±0.27 A	9.88±0.98 A	1012.67±52.00 A
50	62.82±0.56 A	16.00±0.53 A	10.21±0.40 A	1007.33±73.93 A
70	62.31±0.29 A	16.19±0.41 A	10.79±0.67 A	1022.33±71.63 A

[a] Values are means from three replications ± standard deviations. Values followed by the same letters within each column are not significantly different ($P > 0.05$). L*, lightness; a*, redness; b*, yellowness.

III-4. Discussion

Recently, to meet the needs of food industries, new designs of combined antimicrobial processes that are applied at lower intensities but that exhibit degrees of microbial inactivation equivalent to or even higher than that of either treatment used alone are in demand. Therefore, in order to prevent excessive heating of sliced ham without compromising decontamination ability, I explored the effect of decreasing the input energy of NIR heating while combining it with UV-C irradiation. As a result, the simultaneous NIR-UV treatment resulted in a level of inactivation of *S.* Typhimurium, *E. coli* O157:H7, and *L. monocytogenes* significantly greater than that achieved with either treatment used alone as a result of synergism (Table III-2 to 4) without causing any deterioration in product quality due to the lower intensity of NIR (Table III-6). Many researchers have emphasized the importance of the presence of sublethally injured cells after bactericidal treatments, since they are able to repair themselves and resume growth under favorable conditions (Wu, 2008). In the present study, the extent to which sublethally injured pathogens survived after NIR-UV treatment was evaluated by plating on selective agars with and without a resuscitation step, yet there were no significant ($P > 0.05$) differences at any of the treatment time intervals (Table III-2 to 4).

One of the purposes of the current study was to examine the mechanism of the synergistic lethal effect induced by simultaneous NIR and UV treatment. On the basis of the extent of synergistic inactivation of the three pathogens detected and the treatment interval at which statistically significant ($P < 0.05$) synergism was observed, *S*. Typhimurium strain DT 104 and a 70-s treatment time were chosen as model factors for investigation of the mechanism (Table III-2 to 4). I postulated that UV-, NIR-, and NIR-UV-injured cells have different sensitivities to antibiotics which promote specific inhibitory actions on bacteria, and four types of metabolic inhibitors (antibiotics), of which primary synthesis inhibitions are well-known, were employed in order to specify the character of the injury in the target microorganism. Antibiotic-induced cell death has been well studied and predominantly falls into four classes: inhibition of DNA synthesis, inhibition of protein synthesis, inhibition of cell wall synthesis, and inhibition of RNA synthesis (Kohanski et al., 2010). Antibiotics can be also classified on the basis of whether they induce cell death with an efficiency of > 99.9% (bactericidal) or merely inhibit cell growth (bacteriostatic) (Kohanski et al., 2007). In this study, I employed chloramphenicol, nalidixic acid, penicillin G, and rifampin as the protein, DNA, cell wall, and RNAspecific synthesis inhibitors, respectively, since each is bacteriostatic. The bacteriostatic antibiotics block a particular cellular process and do not produce highly deleterious hydroxyl radicals, whereas in Gram-negative and Gram-positive bacteria, all classes of bactericidal

antibiotics stimulate the production of hydroxyl radicals, which ultimately contribute to cell death (Kohanski et al., 2007), and in those instances it may be difficult to determine the specific site of injury in cells.

Several research studies have used these metabolic inhibitors to investigate the cellular metabolic activities and the site of damage in treated cells (Flowers and Adams, 1976; Gomez et al., 1976; Restaino et al., 1980; LeChevallier et al., 1987; Sawai et al., 1995; 2000). In all previous studies, however, liquid suspensions of bacterial cells were treated and then subjected to analysis of the mechanism. It is well-known that the physicochemical state and composition of the treatment medium may affect the bactericidal efficacy of most food preservation technologies, and more specifically, sites of cellular damage or the extent of damage at a particular cellular site could be different (Restaino et al., 1980). Therefore, to accurately study the mechanism of NIR-UV-induced injury for a particular microorganism on ham slices, the studies should be performed in the same food system. For this purpose, I combined the metabolic inhibitors with the overlay method (TSA-XLD). TSA medium containing the antibiotics was used as the selective medium. *S*. Typhimurium DT 104 cells treated on ham slices were spread plated onto selective medium and nonselective medium that did not contain an antibiotic. Colonies of target *Salmonella* cells could be readily enumerated on the overlaid XLD medium. The difference in colony counts obtained with and without the addition of selective reagents can thus be taken as

a measure of injury resulting from each treatment. This proposed method could be utilized in a food base as a simple and effective means of detecting and classifying sites of cellular damage to bacterial cells induced by physical or chemical antimicrobial technologies.

Since the number of colonies of noninjured cells on selective medium (TSA-antibiotic) has to be same as that on nonselective medium, I investigated the effects of various concentrations of metabolic inhibitors in TSA medium on inactivation of intact *S*. Typhimurium DT 104 cells to find the maximum concentrations at which selective antibiotics had no quantitative effect on the formation of colonies. The applied maximum concentrations, especially those of chloramphenicol and penicillin G, were relatively high due to the multidrug resistance of *S*. Typhimurium strain DT 104 (Threlfall et al., 1996). As a result, exposure of intact *S*. Typhimurium DT 104 cells to the selective antibiotic agents at the concentrations listed in Table III-1 caused no substantial effects on colony formation (Table III-5). These concentrations are adequate to allow detection of any slight damage to bacterial cells (resulting in a reduction in colony numbers). In the present study, there were no significant ($P > 0.05$) differences in the level of recovery inhibition between NIR- and NIR-UV-treated cells in the presence of rifampin or between UV- and NIR-UV-treated cells in the presence of nalidixic acid. Rifampin acts on RNA polymerase to arrest DNA-dependent RNA synthesis, and nalidixic acid targets DNA replication and repair by binding

DNA gyrase complexed with DNA (Kohanski et al., 2010). These results indicate that RNA or DNA damage did not affect the synergistic effect of the NIR-UV combined treatment. On the other hand, simultaneous NIR-UV treatment markedly enhanced the level of recovery inhibition in the presence of penicillin G or chloramphenicol. Moreover, the extent of recovery inhibition induced by the simultaneous application of NIR and UV was significantly higher than the sum of the recovery inhibition levels obtained by separate NIR and UV treatments (Table III-5). From this synergistic tendency, the main cellular damage contributing to the synergistic lethal effect of the NIR-UV combined treatment could be inferred. The mode of inhibition for penicillin G is interference with cell wall synthesis by blocking transpeptidation on peptidoglycan strands, and that for chloramphenicol is disruption of protein synthesizing systems (blockage of protein translation) depending on the reaction with the 50S subunit of ribosomes (Kohanski et al., 2010). Typically, structural proteins are necessary for the normal development of the cell membrane or cell wall. Especially, during restoration of injured cell envelopes, ribosomal damage can significantly affect membrane integrity owing to the inhibition of membrane protein synthesis (Tsuchido et al., 1989). Therefore, the mechanism of synergistic bacterial inactivation by simultaneous NIR-UV treatment might be related to damage to cellular envelopes and the inability of cells to repair these

structures due to ribosomal damage. Thus, more than one type of damage may be related to the synergistic lethal effect.

The outputs involving NIR radiant heating do not contradict the findings of other research studies which dealt with the metabolic requirements involved in the thermal injury and repair of bacteria (Gomez et al., 1976; Restaino et al., 1980; Tomlins and Ordal; 1971). Tomlins and Ordal (1971) reported that rifamycin, an inhibitor of RNA synthesis, blocked the repair of heat-injured *S.* Typhimurium. Thus, in *S.* Typhimurium, RNA is degraded during heat treatment and resynthesized during repair. The function of RNA polymerase in cells is very sensitive to temperature change since it plays an important role in induction of heat shock proteins (Yura et al., 1993). Therefore, in NIR and NIR-UV combined treatment, there were equal levels of recovery inhibition by rifampin (Table III-5), which demonstrated that similar degrees of thermal damage occurred in both NIR- and NIR-UV-treated cells due to the same patterns of temperature growth (Fig. III-2).

In conclusion, the simultaneous application of NIR and UV-C radiation was especially effective in inactivating three major pathogenic bacteria (*S.* Typhimurium, *E. coli* O157:H7, and *L. monocytogenes*) on RTE sliced ham owing to their aforementioned synergistic mechanisms without affecting product quality. Furthermore, the NIR-UV processing technique can easily be utilized in industrial applications on a continuous basis, and the effectiveness of this

decontaminating system can be further improved by refining the procedure, such as rearranging the radiation intensities of NIR and UV-C emitters and adjusting the treatment intervals.

Chapter IV.

Simultaneous NIR Radiant Heating and UV Radiation for Inactivating Food-Borne Pathogens in Powdered Red Pepper

This chapter was published in *Applied and Environmental Microbiology* (2013) 79(21): 6568-6575.

IV-1. Introduction

Dried powdered spices are widely used in processed food products and many other convenience foods. Among them, red pepper (*Capsicum annuum* L.) is one of the most important spices used as a natural flavoring and coloring agent worldwide. However, since red peppers are of agricultural origin, they may be burdened with high levels of mesophilic bacteria (Schweiggert et al., 2007; Rico et al., 2010). Pathogenic bacteria such as *Salmonella* spp., *Bacillus cereus*, and *Escherichia coli* have been identified in spices (Little et al., 2003; Nicorescu et al., 2013). Such contaminated spices can result in serious food-borne illnesses when added to foods that undergo no further processing or are eaten raw (Rico et al., 2010; Kim et al., 2012). In 2009, a multistate outbreak of *Salmonella* infections in the United States was traced to ground pepper products (CDC, 2009). As a consequence, ground spices should be decontaminated to prevent further food spoilage and food-borne diseases.

Different physical and chemical treatments have been used to reduce the microbial loads of powdered spices. The most frequently used decontamination techniques are irradiation, fumigation with ethylene oxide, and thermal processing (superheated steam) (Schweiggert et al., 2007; Tainter and Grenis, 2001). However, irradiation at high doses adversely affects the aroma of red pepper powder (Lee et al., 2004). Furthermore, in certain cases where spices

were irradiated in prepackaged form to prevent postpackaging contamination, undesirable compounds (e.g., 1,3-ditert-butylbenzene) from packaging materials migrated into the spice products (Krzymien et al., 2001). The use of ethylene oxide is prohibited in many countries due to possible toxic residues remaining after the process (Fowles et al., 2001). The application of high-temperature steam is associated with a decrease in volatile oil content, color degradation, and an increase in moisture content of the dried spices, which leads to a decreased shelf life (Lilie et al., 2007).

As none of these methods has proved to be completely satisfactory, searches for safe and efficient control methods, including investigations into the use of infrared (IR) heating and UV irradiation, for decontamination of dried spices are being undertaken (Staack et al., 2008a; 2008b; Erdogdu and Ekiz, 2011). IR radiation is part of the electromagnetic spectrum, with wavelengths between those of UV and microwave radiation, and is distinguished as near IR (0.76 to 2 μm), medium IR (2 to 4 μm), and far IR (4 to 1,000 μm). IR heating has advantages over convection and conduction heating, as it heats the product directly without being influenced by air around the powdered spices, and is a fast and effective thermal process (Ranjan et al., 2002). This rapid surface heating can be used to improve the sealing of moisture, flavor, and aroma compounds, leading to products with better sensory characteristics (Sakai and Hanzawa, 1994). In my previous study, the effectiveness of near-infrared heating

processing for surface pasteurization of solid foods was compared to conventional convective heating (Ha et al., 2012). Staack et al. (2008b) examined the effect of infrared radiation at near and medium wavelengths on the microbial decontamination of paprika powder, and 1- to 2-log reductions of microbial flora were obtained at an a_w of 0.8. On the other hand, UV-C irradiation at a 253.7-nm wavelength is a nonthermal method approved for use as an antimicrobial treatment of food surfaces (Rhim et al., 1999). UV-C radiation has been recommended for use in combination with other preservation techniques, since the cumulative damage based on microbial DNA appears to be effective in decreasing the overall number of bacterial cells (Rame et al., 1997). Recently, some studies demonstrated that the killing effect of UV-C irradiation was accelerated by combining treatments with other antimicrobial techniques (Hadjok et al., 2008; Jung et al., 2008; Murphy et al., 2008).

Hamanaka et al. (2011) reported that the combination of IR heating and UV-C irradiation was found to be effective in inactivation of *Rhodotorula mucilaginosa* cells on fig fruits. Erdogdu and Ekiz (2011) also reported that combined IR and UV-C treatments reduced total mesophilic aerobic bacteria on cumin seeds to acceptable levels. However, since these combination studies were limited to sequential treatments, it may be difficult to determine their efficiency on a practical industrial scale and demonstrate their synergistic effect as an innovative antimicrobial intervention. In addition, no report has elucidated the

effects of simultaneous application of both technologies on the efficiency of microbial decontamination of powdered foods.

The aims of this study were to investigate the efficacy of simultaneous combination of near-infrared heating and UV irradiation for reducing populations of food-borne pathogens, including *Salmonella enterica* serovar Typhimurium and *E. coli* O157:H7, in powdered red pepper and to determine the effect of the combination treatment on quality factors of red pepper powder. Also, I explored the mechanisms of inactivation.

IV-2. Materials and Methods

Bacterial strains. Three strains each of *S.* Typhimurium (ATCC 19585, ATCC 43971, and DT 104) and *E. coli* O157:H7 (ATCC 35150, ATCC 43889, and ATCC 43890) were obtained from the School of Food Science bacterial culture collection of Seoul National University (Seoul, South Korea) for this study. Stock cultures were kept frozen at -80 ℃ in 0.7 ml of tryptic soy broth (TSB; Difco, Becton, Dickinson, Sparks, MD, USA) and 0.3 ml of 50 % glycerol. Working cultures were streaked onto tryptic soy agar (TSA; Difco), incubated at 37 ℃ for 24 h, and stored at 4 ℃.

Preparation of pathogen inocula. All strains of *S.* Typhimurium and *E. coli* O157:H7 were cultured individually in 5 ml of TSB at 37 ℃ for 24 h, followed by centrifugation (4,000 × g for 20 min at 4 ℃) and washing three times with buffered peptone water (BPW; Difco). The final pellets were resuspended in BPW, corresponding to ca. 10^7 to 10^8 CFU/ml. Subsequently, suspended pellets of each strain of the two pathogenic species were combined to construct mixed culture cocktails (six strains total). These cell suspensions, consisting of a final concentration of approximately 10^8 CFU/ml, were used in this inactivation study. To analyze the mechanism of inactivation, each final pellet of *S.* Typhimurium and *E. coli* O157:H7 was resuspended in 5 ml of phosphate-buffered saline (PBS;

0.1 M) and inoculated into a sterile glass petri dish (16mm [height] by 90mm [inside diameter]).

Sample preparation and inoculation. Commercially processed dried red pepper powder was purchased at a local grocery store (Seoul, South Korea). For inoculation, 6 ml of culture cocktail was applied to 250-g samples inside sterile high-density polyethylene (HDPE) bags (300 mm by 450 mm). The inoculated samples were thoroughly mixed by hand massaging for 10 min to ensure even distribution of the pathogens and dried for 1 h inside a biosafety hood (22 ± 2 °C) with the fan running until the a_w of the sample equaled that of a noninoculated sample (ca. 0.68). The final cell concentration was 10^6 to 10^7 CFU/25g. Inoculated red pepper powder samples were then immediately used in each experimental batch.

Near-infrared heating and UV irradiation. A stainless chamber (concave upwards base, 380 by 205 by 158 mm) with a rotational mixer was used in this study for combined near-infrared (NIR) and UV-C treatment (Fig. IV-1). A quartz halogen infrared heating lamp (NS-104, 350 mm; NSTECH, Gyunggido, South Korea), with a maximum power of 500 W (light intensity of 141.75 $\mu W/cm^2/nm$ at the sample location) at a 230-V input, was used as a NIR-emitting source. A UV germicidal lamp (G10T5/4P, 357 mm; Sankyo, Japan)

with a nominal output power of 16 W (light intensity of 1.85 mW/cm^2 at the sample location) was used as a UV-C-emitting source. Since both lamps radiate in all directions, they were placed within aluminum reflectors to focus as much of the radiation as possible uniformly onto the process line and to prevent energy from leaking out of the chamber (Fig. IV-1). After the outputs of the NIR and UV lamps had been stabilized (following 2 min of run time), inoculated samples (250 g) were placed in the treatment chamber for the subsequent inactivation experiments (NIR radiant heating, UV-C irradiation, and simultaneous application of both technologies). All treatments were accompanied by stirring (23 rpm) by means of a rotational mixer in the chamber (Fig. IV-1). For the inactivation mechanism study, 5 ml of cell suspensions kept in glass petri dishes were treated with NIR, UV, and NIR-UV for 3 min under identical conditions. The volume of the cell suspension (5 ml) and the treatment time (3 min) were selected on the basis of the temperatures of red pepper powder during NIR treatment.

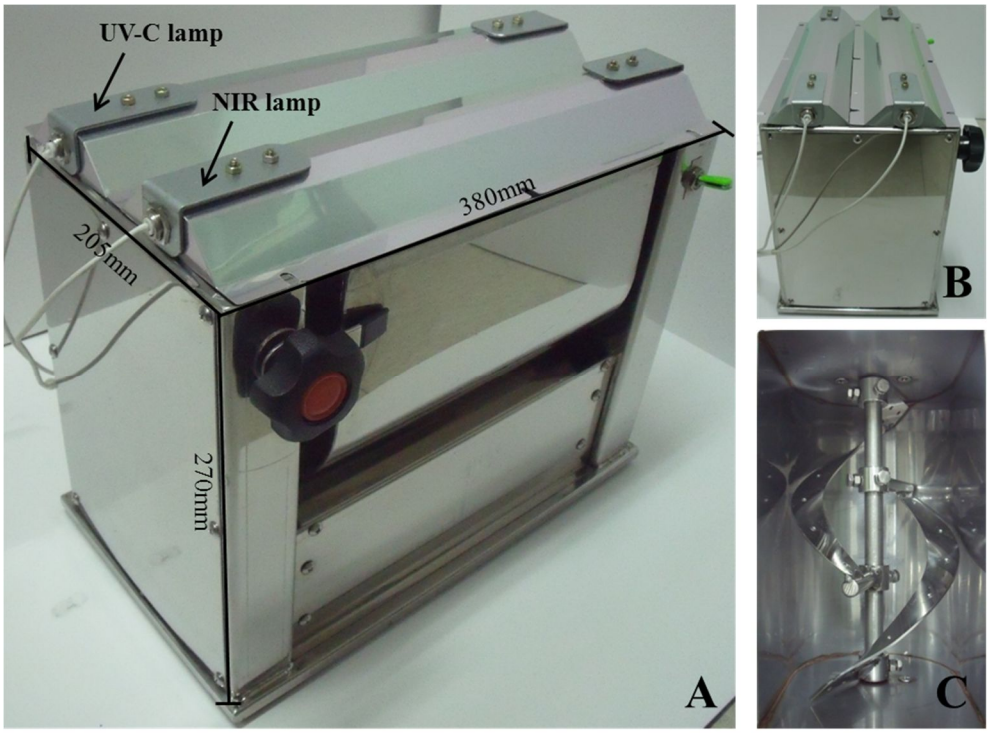

FIG. IV-1. Combined NIR-UV treatment system used in this study. (A) overall view of the experimental device; (B) side view; (C) the rotational mixer (23 rpm) in treatment chamber.

Bacterial enumeration. At selected intervals, 25-g treated samples were removed and immediately transferred into sterile stomacher bags (Labplas Inc., Sainte-Julie, Quebec, Canada) containing 225 ml of BPW (detection limit = 10 CFU/g) and homogenized for 2 min with a stomacher (620 rpm, Easy Mix; AES Chemunex, Rennes, France). After homogenization, 1-ml aliquots of sample were 10-fold serially diluted in 9-ml blanks of BPW, and 0.1 ml of sample or diluent was spread-plated onto each selective medium. Xylose lysine desoxycholate agar (XLD; Difco) and sorbitol MacConkey agar (SMAC; Difco) were used as selective media for the enumeration of *S.* Typhimurium and *E. coli* O157:H7, respectively. Where low numbers of surviving cells were anticipated, 250 µl of sample was spread-plated onto each of four plates to lower the detection limit. All agar media were incubated at 37 °C for 24 h before counting. To confirm the identity of the pathogens, random colonies were selected from the enumeration plates and subjected to biochemical and serological tests. These tests consisted of the *Salmonella* latex agglutination assay (Oxoid, Ogdensberg, NY, USA) and *E. coli* O157:H7 latex agglutination assay (RIM; Remel, Lenexa, KS, USA) for *S.* Typhimurium and *E. coli* O157:H7, respectively.

Enumeration of injured cells. The overlay (OV) method was used to enumerate injured cells of *S.* Typhimurium (Lee and Kang, 2001). TSA was used as a nonselective medium to repair injured cells. One hundred microliters

of appropriate dilutions was spread-plated onto TSA medium in duplicate, and plates were incubated at 37 °C for 2 h to allow injured microorganisms to resuscitate (Kang and Siragusa. 1999). Plates were then overlaid with 7 to 8 ml of the selective medium XLD agar. After solidification, plates were further incubated for an additional 22 h at 37 °C. Following incubation, presumptive colonies of *S.* Typhimurium with typical black colonies were enumerated. For enumerating injured cells of *E. coli* O157:H7, phenol red agar base with 1 % sorbitol (SPRAB; Difco) was used (Rhee et al., 2003). After incubation at 37 °C for 24 h, typical white colonies characteristic of *E. coli* O157:H7 were enumerated. Randomly selected isolates from SPRAB plates were subjected to serological confirmation as *E. coli* O157:H7 (RIM, *E. coli* O157:H7 latex agglutination test; Remel), because SPRAB is not typically used as a selective agar for enumerating *E. coli* O157:H7.

Temperature measurement. A fiber optic temperature sensor (FOT-L; FISO Technologies Inc., Quebec, Canada) connected to a signal conditioner (TMI-4; FISO Technologies Inc., Quebec, Canada) was used to measure real-time temperatures in the treatment chamber during combined NIR and UV treatment. The sensor was placed directly on the inner wall surface of the chamber, and the temperature was manually recorded every 5 s. Additionally, in order to measure the core temperature of treated samples precisely, a K-type thermocouple and a

data logger (34790A; Agilent Technologies, Palo Alto, CA, USA) were used. The thermocouple probe was directly inserted into the powder bed, and temperatures were recorded at selected treatment times. All experiments were replicated three times.

Transmission electron microscopy analysis. To investigate structural damages in the pathogen cells caused by NIR, UV, and NIR-UV treatments, transmission electron microscopy (TEM) analysis was utilized. Treated *S.* Typhimurium and *E. coli* O157:H7 cells in PBS were collected by centrifugation at 4,000 × g for 10 min. The pellet was fixed in modified Karnovsky's fixative (2 % paraformaldehyde and 2% glutaraldehyde in 0.05 M sodium cacodylate buffer) at 4 °C for 2 to 4 h. After primary fixation, cells were centrifuged and washed three times with 0.05 M sodium cacodylate buffer. The cells were then postfixed in 1 % osmium tetroxide in 0.05 M sodium cacodylate buffer (pH 7.2) at 4 °C for 2 h and briefly washed twice with distilled water. The washed cells were prestained in 0.5 % uranyl acetate for 30 min at 4 °C. The cells were then dehydrated using a graded ethanol series of 30, 50, 70, 80, 90 and three changes of 100 % for 10 min each. After dehydration, cells were processed in two changes of 100 % propylene oxide (transition material) at room temperature for 15 min each, infiltrated in a 1:1 solution of propylene oxide and Spurr's resin for 2 h, and then placed in Spurr's resin overnight. Infiltrated samples were

polymerized at 70 °C for 24 h. These specimens were sectioned (slices 70 nm thick) using an ultramicrotome (MT-X; RMC, Tucson, AZ, USA) and then stained with 2 % uranyl acetate for 7 min and Reynold's lead citrate for 7 min. The dried sections were examined by TEM (Libra 120; Carl Zeiss, Heidenheim, Germany) and digitally photographed.

Measurement of propidium iodine uptake. The fluorescent dye propidium iodine (PI; Sigma-Aldrich) was used to quantitatively assess membrane damage to pathogen cells induced by each treatment. Treated *S.* Typhimurium and *E. coli* O157:H7 cells were diluted in PBS to an optical density at 680 nm (OD_{680}) of approximately 0.4 and then mixed with PI solution to a final concentration of 2.9 μM. After incubation for 10 min, samples were centrifuged at 10,000 × g for 10 min and washed twice in PBS to remove excess dye. The cell pellet was resuspended in PBS, and fluorescence was measured with a spectrofluorophotometer (Spectramax M2e; Molecular Devices, Sunnyvale, CA, USA) at an excitation wavelength of 493 nm and an emission wavelength of 630 nm. Fluorescence values from untreated cells were subtracted from those of treated cells, and the data were normalized against the OD_{680} of the cell suspensions.

Color and capsaicinoid measurement. A Minolta colorimeter (model CR400; Minolta Co., Osaka, Japan) was used to measure the color changes of treated samples. The color attributes were quantified by the values of L*, a*, and b* and measured at random locations on red pepper powder. L*, a*, and b* values indicate color lightness, redness, and yellowness of the sample, respectively. All measurements were taken in triplicate.

Capsaicinoid measurement was conducted following the method of Attuquayefio and Buckle (Attuquayefio and Buckle, 1987). Each sample of treated red pepper powder (4 g) was mixed with 20 ml of acetonitrile and vortexed for 2 min. One ml of extract was diluted with 9 ml of distilled water and passed into conditioned C_{18} Sep-pak columns (Waters, MA, USA). A C_{18} Sep-pak column was conditioned with 5 ml of acetonitrile followed by 5 ml of double-distilled water. The capsaicinoids were then eluted with 4 ml of acetonitrile followed by 1 ml of acetonitrile containing 1 % acetic acid. To confirm the quantity of capsaicinoids (total amount of capsaicin and dihydrocapsaicin), high-performance liquid chromatography (HPLC) analysis was performed on a Waters Alliance 2695 separation module with a Waters 996 photodiode array detector (Waters, MA). The wavelength was set at 280 nm, and separation was performed using an INNO C_{18} column (4.6 mm by 250 mm; particle diameter of 5 μm; Innopia, South Korea) at 35 °C. The mobile phase consisted of MeOH-water (70:30, vol/vol) at a flow rate of 1.0 ml/min.

Statistical analysis. All experiments were repeated three times with duplicate samples. Data were analyzed by analysis of variance (ANOVA) and Duncan's multiple range test of a statistical analysis system (SAS Institute, Cary, NC, USA). A P value of < 0.05 was used to indicate significant differences.

IV-3. Results

Inactivation of pathogenic bacteria by NIR-UV simultaneous treatment. Viable-count reductions of *S.* Typhimurium and *E. coli* O157:H7 in red pepper powder during NIR radiant heating, UV-C irradiation, and simultaneous application of both technologies are shown in Table IV-1 and 2, respectively. The simultaneous NIR-UV combined treatment for 5 min achieved 3.34- and 2.78-log reductions in *S.* Typhimurium and *E. coli* O157:H7, respectively. For both pathogens, the sum of NIR and UV inactivation was lower than that obtained by the simultaneous application of both technologies, and the existence of a synergistic effect could be deduced. Furthermore, statistically significant ($P < 0.05$) differences between the sum of NIR and UV inactivation and inactivation achieved with combination treatment were observed in both *S.* Typhimurium and *E. coli* O157:H7 after treatment times of 3 min or more (Table IV-1 and 2). In *S.* Typhimurium, inactivation resulting from the synergistic effect occurred after 3 min of treatment, calculated by subtracting the sum of NIR and UV reductions from those obtained during NIR-UV simultaneous treatment, were 0.48, 1.17, and 1.86 logs at 3, 4, and 5 min of treatment, respectively. In the case of *E. coli* O157:H7, 0.38-, 0.91-, and 1.31-log reductions of synergism at 3, 4, and 5 min, respectively, were observed.

Table IV-1. Viable-count reductions of *S.* Typhimurium in red pepper powder treated with UV-C irradiation (UV), NIR radiant heating (NIR), and both technologies simultaneously (NIR-UV).

Treatment time (min)	Log reduction [$\log_{10}(N_0/N)$] by treatment type and selection medium[a]							
	UV		NIR		NIR-UV			
	XLD[b]		XLD		XLD		OV-XLD	
0	0.00±0.00	A	0.00±0.00	A	0.00±0.00	Aa	0.00±0.00	Aa
1	0.02±0.00	A	0.04±0.03	A	0.10±0.08	Aa	0.08±0.02	Aa
2	0.03±0.02	A	0.14±0.05	AB	0.34±0.12	Ba	0.21±0.08	Aa
3	0.03±0.03	A	0.33±0.11	B	0.83±0.18	Ca	0.60±0.04	Ba
4	0.04±0.03	A	0.77±0.10	C	1.98±0.23	Da	1.84±0.08	Ca
5	0.03±0.04	A	1.45±0.28	D	3.34±0.08	Ea	3.02±0.35	Da

[a] Values are means ± standard deviations from three replications. Means with the same capital letter in the same column are not significantly different ($P > 0.05$). Within the NIR-UV columns, means with the same lowercase letter in the same row are not significantly different ($P > 0.05$). XLD, xylose lysine desoxycholate; OV-XLD, overlay XLD agar on TSA.

Table IV-2. Viable-count reductions of *E. coli* O157:H7 in red pepper powder treated with UV-C irradiation (UV), NIR radiant heating (NIR), and both technologies simultaneously (NIR-UV).

Treatment time (min)	Log reduction [$\log_{10}(N_0/N)$] by treatment type and selection medium							
	UV		NIR		NIR-UV			
	SMAC [b]		SMAC		SMAC		SPRAB	
0	0.00±0.00	A	0.00±0.00	A	0.00±0.00	Aa	0.00±0.00	Aa
1	0.03±0.02	A	0.08±0.07	A	0.05±0.05	Aa	0.11±0.13	Aa
2	0.03±0.04	A	0.14±0.10	A	0.31±0.18	Ba	0.14±0.12	Aa
3	0.05±0.03	A	0.52±0.21	B	0.95±0.05	Ca	0.46±0.12	Bb
4	0.05±0.03	A	0.98±0.15	C	1.94±0.04	Da	1.56±0.10	Cb
5	0.04±0.04	A	1.42±0.07	D	2.78±0.11	Ea	2.55±0.14	Da

[a] Values are means ± standard deviations from three replications. Means with the same capital letter in the same column are not significantly different ($P > 0.05$). Within the NIR-UV columns, means with the same lowercase letter in the same row are not significantly different ($P > 0.05$). SMAC, sorbitol MacConkey agar; SPRAB, phenol red agar base with 1% sorbitol.

Recovery of NIR-UV-injured cells. Table IV-1 and 2 show levels of sublethally injured *S.* Typhimurium and *E. coli* O157:H7 cells in red pepper powder following simultaneous NIR-UV treatment. Determining the difference between inactivation of samples subjected to injured-cell recovery methods and those plated directly on selective media revealed the presence of 0.23, 0.14, and 0.32 log units of injured *S.* Typhimurium cells after 3-, 4-, and 5-min treatments, respectively. In the case of *E. coli* O157:H7, 0.23 to 0.49 log CFU/g of injured cells was observed after 3 to 5 min of treatment, respectively. Overall, slightly lower reductions of both pathogens were observed by the agar OV method (SPRAB in the case of *E. coli* O157:H7) than on selective agar. However, statistically significant ($P > 0.05$) differences between the reduction levels enumerated on the appropriate selective agar (XLD and SMAC) versus the agar for resuscitation (OV-XLD and SPRAB) were not observed after the maximum treatment of 5 min.

Average temperature-time histories of red pepper powder. Average temperatures of the treatment chamber and red pepper powder core during simultaneous NIR and UV treatment are shown in Fig. IV-2. Differences in temperature (about 10 to 13 °C) were detected between the inside of the chamber and the red pepper powder core during 1 to 5 min of treatment. After 3 min of treatment, the treatment chamber and sample core reached ca. 62 and 50 °C, respectively. At maximum treatment time (5 min), those temperatures increased

to 75 and 62 ℃, respectively (Fig. IV-2). Additionally, the heating rate of single NIR treatment was not different from that of the NIR-UV simultaneous treatment (data not shown).

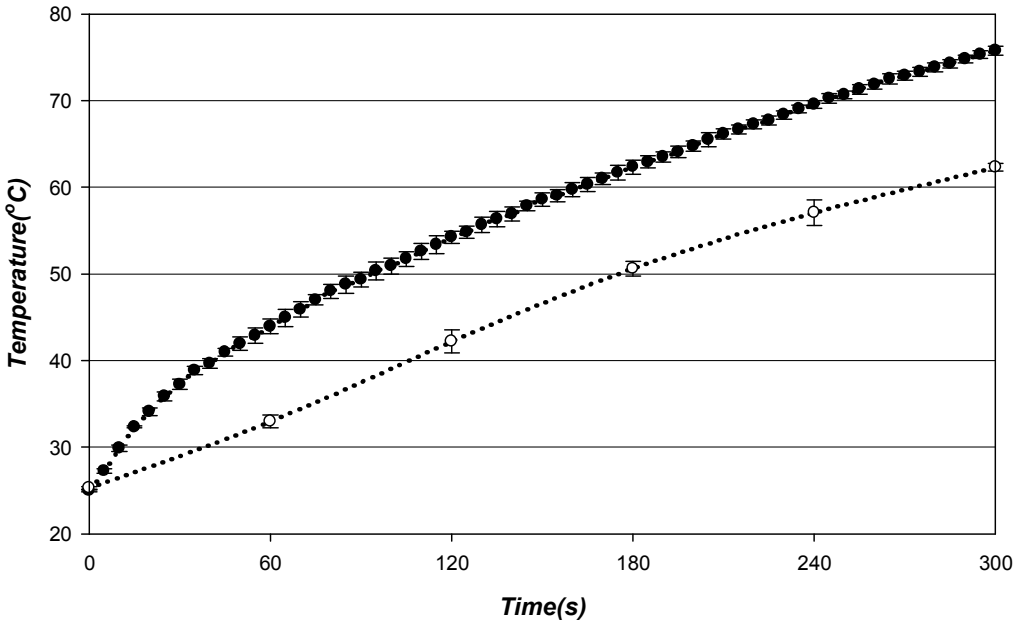

FIG. IV-2. Average temperature-time histories of the treatment chamber and red pepper powder cores during simultaneous NIR heating and UV-C irradiation. Error bars indicate standard deviations calculated from triplicates. ○, red pepper powder core; ●, inside of treatment chamber.

Microscopic evaluation of damages. Selected TEM images of ultrastructural changes in *S.* Typhimurium and *E. coli* O157:H7 cells induced by NIR, UV, and NIR-UV treatments are shown in Fig. IV-3 and 4, respectively. Microscopic analyses at the cellular level verified that there was cytoplasmic and membrane structural damage during NIR heating (Fig. IV-3C and 4C) and simultaneous NIR-UV treatment (Fig. IV-3D and 4D). More specifically, for both pathogens, cytoplasmic shrinkage and aggregation were observed in both NIR- and NIR-UV-treated cells, in contrast to untreated and UV-treated cells. Furthermore, NIR-UV-treated cells experienced significant cell wall damage, leading to a leakage of cellular contents from the cytoplasm. In the case of UV-treated cells, morphological changes as well as collapse of internal cellular structures were not observed compared to control cells (Fig. IV-3B and 4B).

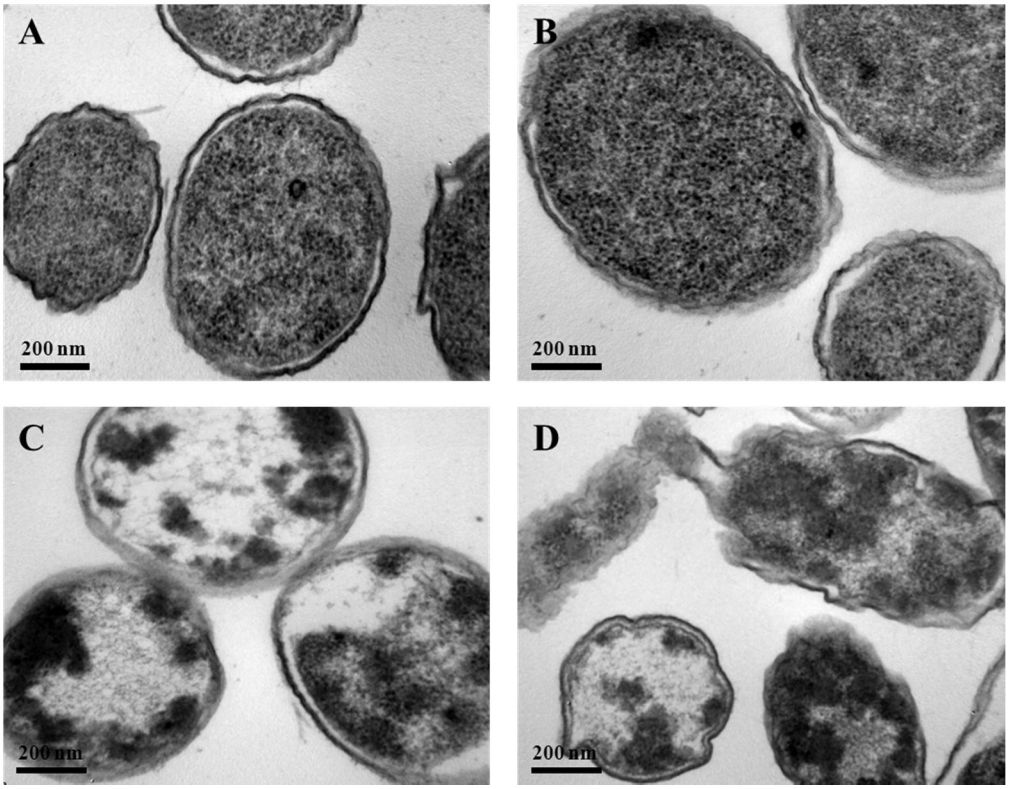

FIG. IV-3. Comparison of damage induced by UV-C irradiation, NIR heating, and their combination (for 3 min) in *S.* Typhimurium cells, observed by TEM. (A) Control sample; (B) UV-treated sample; (C) NIR-treated sample; (D) NIR-UV-treated sample.

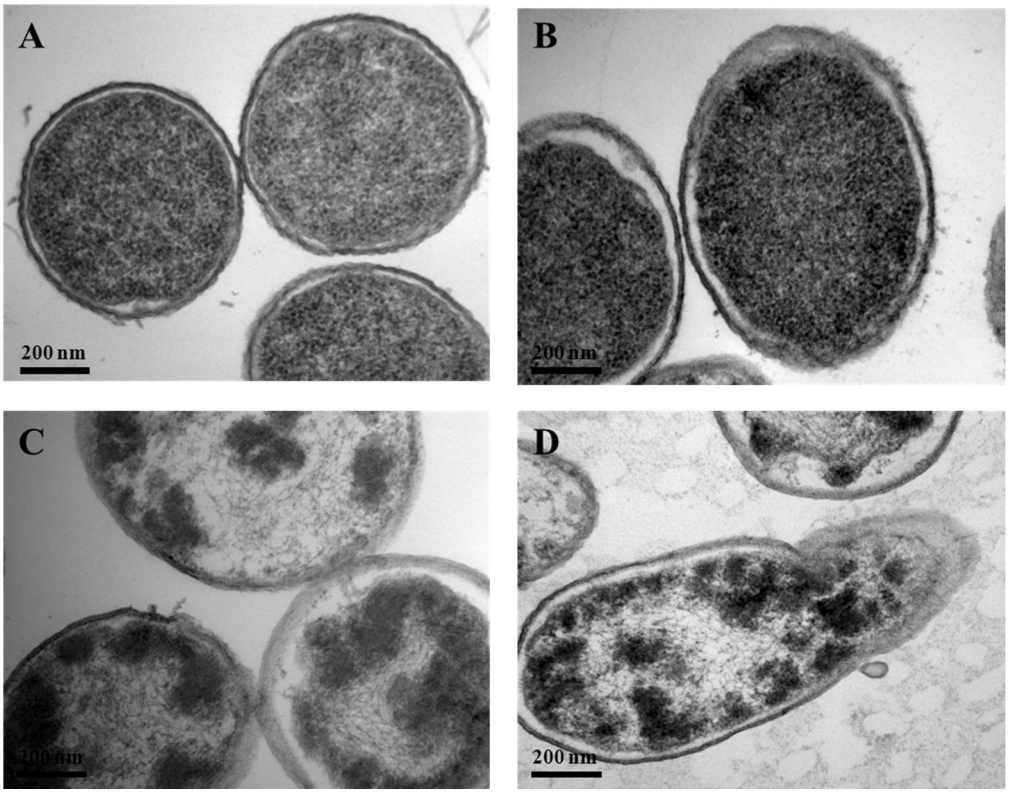

FIG. IV-4. Comparison of damage induced by UV-C irradiation, NIR heating, and their combination (for 3 min) in *Escherichia coli* O157:H7 cells, observed by TEM. (A) Control sample; (B) UV-treated sample; (C) NIR-treated sample; (D) NIR-UV-treated sample.

Determination of membrane damage by PI uptake. As a further quantitative test of membrane damage, NIR-, UV-, and NIR-UV-treated cells were stained with the fluorescent dye PI, which is excluded from cells with intact membranes. Table IV-3 shows the PI uptake values of *S.* Typhimurium and *E. coli* O157:H7 after each treatment. The overall pattern of results for *E. coli* O157:H7 was similar to that of *S.* Typhimurium. Based on PI uptake values, there was no significant ($P > 0.05$) damage to cellular membranes of either pathogen following UV treatment. The degree of PI uptake in NIR- and NIR-UV treated cells was much greater than that in UV-treated cells. Among them, the cells subjected to NIR-UV treatments showed significantly ($P < 0.05$) higher PI uptake values than did cells subjected to the other treatments.

Table IV-3. Levels of membrane damage of NIR-, UV-, and NIR-UV treated cells obtained from the propidium iodine (PI) uptake test.

Treatment type	PI uptake value[a]			
	S. Typhimurium		*E. coli* O157:H7	
Non-treated	0±0	a	0±0	a
UV	0.91±0.15	a	1.30±0.20	a
NIR	16.11±0.29	b	18.46±1.10	b
NIR-UV	20.14±2.61	c	22.23±1.74	c

[a] Values are means of three replications ± standard deviations. Values followed by the same letter within the column per microorganism are not significantly different ($P > 0.05$). The data were normalized by subtracting fluorescence values obtained from untreated cells and against OD_{680} (PI value = [fluorescence value after treatment - fluorescence value of untreated cells]/OD_{680}).

Effect of NIR-UV simultaneous treatment on product quality. Color values of red pepper powder after NIR-UV combined treatment are presented in Table IV-4. L*, a*, and b* values of NIR-UV treated (5 min) red pepper powder were not significantly ($P > 0.05$) different from those of untreated samples. Natural red color is a major attribute for determining the commercial quality of red pepper powder. A red color parameter was expressed as the product of L* (lightness) and a* (redness); values of > 500, 500 to 300, and 300 were rated as red, medium red, and dark red, respectively (Ramakrishnan and Francis, 1973). The red color parameters for all treatments stayed within acceptable levels (L* × a* ~ 700). Since the capsaicinoids, primarily capsaicin and dihydrocapsaicin, present in red pepper are responsible for its typical pungency and flavor, retention of these constituents during a given process is very important for ensuring acceptability of the commodity. Table IV-5 shows that NIR-UV simultaneous treatment for 5 min did not change the content of capsaicin and dihydrocapsaicin of red pepper powder significantly ($P > 0.05$). Thus, simultaneous application of NIR and UV treatment for 5 min did not affect the quality of red pepper powder product.

Table IV-4. Color values of NIR-UV simultaneously treated red pepper powder.

Treatment time (min)	Parameter[a]		
	L*	a*	b*
0	34.76±0.29 a	20.06±0.27 a	18.24±0.30 a
1	34.71±0.25 a	20.31±0.27 a	18.68±0.38 a
2	34.53±0.08 a	20.09±0.48 a	18.22±0.49 a
3	34.89±0.62 a	20.12±0.53 a	17.95±0.68 a
4	34.94±0.30 a	20.29±0.52 a	18.74±0.45 a
5	35.09±0.35 a	20.18±0.23 a	18.50±0.44 a

[a] Values are means from three replications ± standard deviations. No values are significantly different within a column per parameter ($P > 0.05$). L*, lightness; a*, redness; b*, yellowness.

Table IV-5. Capsaicinoid content of NIR-UV-treated red pepper powder.

Treatment time(min)	Capsaicinoid content (mg/100 g)[a]		
	CAP	DHC	total
0	31.86±1.81 a	26.03±1.77 a	57.88±3.24 a
1	32.96±1.91 a	25.57±1.74 a	58.53±3.65 a
2	33.30±1.02 a	26.32±0.90 a	59.62±0.55 a
3	31.66±2.65 a	26.69±0.99 a	58.35±1.88 a
4	31.68±2.76 a	24.25±0.99 a	55.93±3.44 a
5	31.72±2.40 a	25.83±1.69 a	57.55±4.07 a

[a] Values are means ± standard deviations from three replications. No values are significantly different within a column per parameter ($P > 0.05$). CAP, capsaicin; DHC, dihydrocapsaicin; total, capsaicin and dihydrocapsaicin.

IV-4. Discussion

After single treatment with NIR heating for 5 min, there was inactivation of 1.45 and 1.42 log in *S.* Typhimurium and *E. coli* O157:H7, respectively. To achieve > 3-log reductions, based on the calculated parameters of the Weibull model (R^2 = 0.96), 6.5 min and 7.2 min were needed for *S.* Typhimurium and *E. coli* O157:H7, respectively. However, darkening was visually observed on red pepper powder treated with NIR for a slightly excessive time (over 6.5 min). Moreover, treatment of red pepper powder with UV-C, where approximately 0.04-log reductions were observed in each pathogen after 5 min of exposure, was less effective than NIR treatment. A review of the literature shows that there have been only a few studies relevant to the effect of UV-C irradiation on spices. Erdogdu and Ekiz (2011) reported that the use of UV-C irradiation alone on cumin seeds for 60 min reduced total aerobic bacteria by about 0.6 log unit, and extending the UV-C application up to 120 min did not offer any additional reduction. As these results indicate, the effects of UV-C and NIR treatments alone were not effective in reducing the number of pathogens found in agricultural spices while maintaining product quality.

Hamanaka et al. (2011) investigated sequential UV-C and NIR treatment for surface decontamination of fresh fig fruit and reported that IR heating accelerated the cell-inactivating efficacy of UV-C irradiation. However, separate

30-s treatments of IR heating and UV irradiation reduced fungal counts by about 1 and 2.5 logs, respectively, in comparison with the control, while sequential treatment of IR heating and UV irradiation reduced fungal populations by 3 logs. Thus, sequential application of IR heating followed by UV treatment showed an additive effect that was not significantly different from the sum of IR and UV inactivation. This result was consistent with another report describing *Salmonella* inactivation by the combination of UV-C light with mild heat (Gayán et al., 2012). Gayán et al. (2012) reported that the sequential combination of heat (55 °C) followed by UV treatment showed an additive effect and also noted that a synergistic effect was observed when both technologies were applied simultaneously. Therefore, a simultaneous combination of NIR heating and UV-C irradiation was included in my study, and the required levels of protection ($\geq$ 3 log reduction) could be obtained based on synergism while retaining organoleptic attributes of red pepper powder, such as color and pungency.

Even though NIR-UV treatment was highly effective, the significance of sublethally injured pathogens in food samples should not be ignored. Injured cells are potentially as dangerous as their normal counterparts because they can resuscitate and become functionally normal under suitable conditions (Wu, 2008). In this study, the occurrence of sublethally injured pathogens in powdered red pepper was assessed by plating on selective agars with and without a

resuscitation step. There were no significant ($P > 0.05$) differences in levels of cells enumerated on XLD and OV-XLD and those on SMAC and SPRAB after the maximum treatment of 5 min (Table IV-1 and 2). This suggests that simultaneous NIR-UV treatment effectively inactivated *S.* Typhimurium and *E. coli* O157:H7 in powered red pepper without causing appreciable injury to bacterial cells.

The underlying inactivation mechanisms of the combination of UV-C irradiation and NIR heating are not well understood. In previous studies, Sawai et al. (1995) investigated the inactivation mechanism of *E. coli* treated with IR radiation in phosphate-buffered saline. They reported that IR irradiation damaged RNA polymerase and ribosomes before damaging DNA and cell membranes. Additionally, RNA, protein, and cell walls showed greater vulnerability to IR heating than conductive heating. Gayán et al. (2012) reported that the number of envelope-injured cells was higher after combined UV and heat processing than after heating alone, and this difference was more pronounced in outer membrane than in cytoplasmic membrane damage. Their results indicate that the mechanism of the synergistic effect of UV irradiation and heat is relevant to a sensitization of cell envelopes.

To clarify the mechanism of the synergistic lethal effect of NIR-UV combined treatment, membrane damage to *S.* Typhimurium and *E. coli* O157:H7 cells caused by NIR, UV, and NIR-UV simultaneous treatment was evaluated by

qualitative (TEM analysis) and quantitative (PI uptake test) methods. For this purpose, a 3-min treatment time was chosen, since the significant ($P < 0.05$) synergistic effects were detected at $\geq$ 3 min of treatment in both *S.* Typhimurium and *E. coli* O157:H7 (Table IV-1 and 2). The NIR-UV combined treatment significantly damaged cell envelopes of both pathogens, as detected in both sets of TEM images (Fig. IV-3 and 4) and PI uptake values (Table IV-3). Fluorescent stains that bind to intracellular components are useful in determining the viability or the physiological status of microorganisms. In particular, PI is a nucleotide-binding probe, which enters only cells with damaged membranes (Aeschbacher et al., 1986). Quantitative results of cell membrane damage measured by PI uptake were consistent with qualitative observations obtained by TEM analysis (Fig. IV-3 and 4) and logarithmic inactivation results obtained from each selective medium (Table IV-1 and 2). The synergism of NIR-UV simultaneous treatment evident in PI uptake values was also observed in log reduction data of each pathogen. The PI uptake values of simultaneous NIR-UV application were higher than total values reached by separate NIR and UV treatments for both *S.* Typhimurium and *E. coli* O157:H7 (Table IV-3). As a result, I confirmed that damage to the cell envelope was the main factor related to the synergistic lethal effect of combined NIR and UV treatment. Although it is well established that UV irradiation inactivates bacteria by damaging their nucleic acids, it has also been suggested that photons can interact with

components of cell envelopes, including the cell wall and membrane (Sawai et al., 1995). However, in my mechanism study, TEM images and PI uptake values of UV-treated cells were not significantly different from those of untreated cells. These results are in agreement with other findings from sensitivity analysis in my recent study (Ha and Kang, 2015). Based on the effect of metabolic inhibitors on resuscitation of UV-, NIR-, and NIR-UV-injured cells, disruption of the bacterial cell membrane and the inability of cells to repair these structures due to ribosomal damage were identified as the primary factors contributing to the synergistic lethal effect.

In studying the effect of excessive thermal treatment on the quality properties of spices, Almela et al. (2002) noted that high temperature promotes color degradation of spices, as paprika became darker and the red color became less intense. Rico et al. (2010) also reported that steaming treatment of red pepper powder led to quality degradation, with significant loss of color and flavor. Thus, it is important that spices be heated no longer than required, in order to prevent losses in flavor and color components. As shown in my study, simultaneous NIR-UV treatments did not change color values or capsaicin and dihydrocapsaicin content of red pepper powder significantly ($P > 0.05$), due to the shorter NIR processing time (Table IV-4 and 5). Also, in the present study, because a rotational mixer was used simultaneously with combined NIR-UV treatment, excessive heating on one side of the powder mass was prevented.

Furthermore, since UV-C radiation as well as NIR thermal energy is primarily absorbed on solid food surfaces and has very limited penetration capability, simultaneous mixing could increase the contact area of radiation on powder particles. For these reasons, rotational mixing should be incorporated on an industrial scale when powdered spices are being decontaminated.

In conclusion, performing simultaneous UV-C irradiation with NIR heating to temperatures lower than those used for inactivation was found to be suitable for reducing microbial contamination of red pepper powder without affecting product quality. The NIR-UV combination has some advantages not only regarding the germicidal effect but also in terms of simplified handling, environmental preservation, and reduced costs through lower inputs of energy. These factors suggest that this decontaminating procedure can be applied as an alternative to other interventions, such as fumigation and superheated steam. In addition, data obtained from this novel system will be useful in designing apparatus for NIR and UV-C combined bactericidal processing for various kinds of powdered/granulated food ingredients.

Chapter V.

Synergistic Bactericidal Effect of Simultaneous NIR Radiant Heating and UV Radiation against *Cronobacter sakazakii* in Powdered Infant Formula

This chapter was published in *Applied and Environmental Microbiology* (2014) 80(6): 1858-1863.

V-1. Introduction

Cronobacter sakazakii was first identified as yellow-pigmented *Enterobacter cloacae* in 1980 and then was reclassified into several genomospecies (Iversen et al., 2007; Joseph et al., 2012). While *C. sakazakii* has been a causal agent of diseases among all age groups, the great majority of cases are seen in infants less than 2 months old. *C. sakazakii* has been associated with food-borne outbreaks of a rare form of infant meningitis, necrotizing enterocolitis, bacteremia, and neonate deaths, with a fatality rate of 40 % to 80 % (Iversen and Forsythe, 2003). Although *C. sakazakii* has been isolated from a diverse range of environments and foods, dried infant formula, which is a main source of nutrition for neonates and infants, has been recognized as the major vehicle of transmission in *C. sakazakii* infections (Iversen and Forsythe, 2003; CDC, 2002; Kandhai et al., 2004). An international survey of powdered infant formulas from 36 countries found that approximately 14 % of the 141 canned products examined had detectable levels of *C. sakazakii* (Muytjens et al., 1988). A smaller survey by Nazarowec-White and Farber (1997) involved 5 factories (each supplying 24 samples) and reported that the prevalence of the bacterium ranged between 0 % and 12 % of the samples per factory. Iversen and Forsythe (2004) also found that 2.4 % of powdered infant formula products (in 82 brands) were positive for *C. sakazakii*.

Most studies involving inactivation of *C. sakazakii* in infant formula have focused on the reconstituted/rehydrated state, not the end product in powdered form (Nair et al., 2004; Edelson-Mammel and Buchanan,2004; González et al., 2006; Pina Pérez et al., 2007; Chen et al., 2009). Drying is an extreme form of osmotic stress and is important for the survival and persistence of *C. sakazakii* in the powder bed. *C. sakazakii* has been known to be more resilient in low-water-activity environments (Lehner and Stephan, 2004; Edelson-Mammel et al., 2005). Due to its ability to survive in dry food matrices, as in powdered infant formula, controlling *C. sakazakii* in the final dehydrated product is of great concern to the dairy industry.

Recently, some authors have proposed several decontamination methods in an effort to reduce levels of *C. sakazakii* in powdered infant formula, including gamma radiation (Lee et al., 2006; Osaili et al., 2007), electron beam irradiation (Hong et al., 2008), supercritical carbon dioxide and heat treatment (Kim et al., 2010), and gaseous ozone treatment (Torlak and Sert, 2013). However, all of these methods have limitations for industrial application because of high capital costs for installation and treatment. Therefore, it is necessary to develop a more efficient method for inactivation of *C. sakazakii* that can be applied to the final dehydrated product. This new intervention should be cost-effective, and its impact on product quality should enable its application in postpasteurization processing of powdered infant formula.

Infrared (IR) energy is a form of electromagnetic energy that, if absorbed, can cause heating on the surfaces of objects and is distinguished as near IR (NIR) (0.76 to 2 μm), medium IR (MIR) (2 to 4 μm), and far IR (FIR) (4 to 1,000 μm). IR heating has advantages over convection and conduction heating, as it heats the product directly without being influenced by air around the powdered infant formula and is a fast and effective thermal process (Ranjan et al., 2002). This rapid surface heating by IR can help improve the sealing of moisture, flavor, and aroma compounds, leading to products with better sensory characteristics (Sakai and Hanzawa, 1994). On the other hand, 253.7-nm UV irradiation (UV-C) holds considerable promise in food processing as an emerging nonthermal method for microbial inactivation on food surfaces. UV-C radiation has been recommended for use in combination with other antimicrobial techniques, since cumulative damage based on microbial DNA appears to be effective in inducing the synergistic inactivation (Rame et al., 1997). In my recent study, the simultaneous combination of NIR heating and UV-C irradiation was found to be suitable for reducing *Salmonella enterica* serovar Typhimurium and *Escherichia coli* O157:H7 in red pepper powder without affecting product quality (Ha and Kang, 2013). However, the feasibility of combined NIR-UV treatment for controlling *C. sakazakii* in dehydrated infant formula has not yet been evaluated, which is one of the purposes of the current study.

In this study, the efficacy of simultaneous near-infrared heating and UV-C irradiation for reducing populations of *C. sakazakii* in powdered infant formula was investigated. The mechanism of inactivation was evaluated by propidium iodide (PI) uptake values. Also, the effect of the combination treatment on the quality of powdered infant formula was determined by measuring the color change and by sensory evaluation.

V-2. Materials and Methods

Bacterial strains. Three strains of *C. sakazakii* (ATCC 12868, ATCC 29544, and ATCC 51329) were obtained from the Bacterial Culture Collection of Seoul National University (Seoul, South Korea) and were used in the experiments. Stock cultures were kept frozen at -80 °C in 0.7 ml of tryptic soy broth (TSB; Difco Becton, Dickinson, Sparks, MD, USA) and 0.3 ml of 50 % (vol/vol) glycerol. Working cultures were streaked onto tryptic soy agar (TSA; Difco), incubated at 37 °C for 24 h, and stored at 4 °C.

Preparation of pathogen inocula. All strains of *C. sakazakii* were cultured individually in 5 ml of TSB at 37 °C for 24 h, harvested by centrifugation (4,000 × g for 20 min at 4 °C), and washed three times with buffered peptone water (BPW; Difco). The final pellets were resuspended in BPW, corresponding to approximately 10^6 to 10^7 CFU/ml. Subsequently, the suspended pellets of each strain of the *Cronobacter* spp. were combined to produce mixed culture cocktails (three strains in total). These cell suspensions, consisting of a final concentration of ca. 10^7 CFU/ml, were used in the inactivation study. To analyze the mechanism of inactivation, a final pellet of *C. sakazakii* was resuspended in 5 ml of phosphate-buffered saline (PBS; 0.1 M) and inoculated into a sterile glass petri dish (16 mm [height] by 90 mm [inside diameter]).

Sample preparation and inoculation. Commercial powdered infant formula (Namyang Co., Gongju, South Korea) was purchased at a local grocery store (Seoul, South Korea). For inoculation, 6 ml of culture cocktail was added dropwise to 250-g samples inside sterile high-density polyethylene (HDPE) bags (300 mm by 450 mm). The inoculated samples were thoroughly mixed by hand massaging for 10 min to produce a homogeneous dispersal of inoculum throughout the powered infant formula and dried for 2 h inside a biosafety hood (22 ± 2 °C) with the fan running until the water activity (a_w) of the sample equaled that of an uninoculated sample (ca. 0.42). The water activities of uninoculated and inoculated samples were measured using the AquaLab model 4TE water activity meter (Decagon Devices, Pullman, WA, USA). The final cell concentration was 10^5 to 10^6 CFU/25 g. The inoculated infant formula powder samples were then immediately used in each experimental trial.

Near-infrared heating and UV irradiation. NIR and UV-C treatments were carried out in a previously described apparatus (Ha and Kang, 2013). A stainless steel chamber (concave-upwards base, 380 by 205 by 158 mm) with a rotational mixer was used for combined NIR and UV-C treatment (Fig. V-1). A UV germicidal lamp (G10T5/4P; 357 mm; Sankyo, Japan) with a nominal output power of 16 W (radiation intensity, 1.85 mW/cm^2 at the sample location) was

used as a UV-C-emitting source. A quartz halogen infrared heating lamp (NS-104; 350 mm; NSTECH, Gyunggido, South Korea) with a maximum power of 500 W (radiation intensity, 141.75 μW/cm^2/nm at the sample location) at a 230-V input was used as a NIR-emitting source. The maximum wavelength (λm) generated from the infrared heater used in this study was about 1,300 nm, which is in the near-infrared wavelength range. Since both lamps radiate in all directions, two aluminum reflectors were installed behind the emitters to redirect the radiation waves and enhance the efficiency of NIR and UV radiation (Fig. V-1). After the outputs of the NIR and UV lamps had been stabilized (following 2 min of run time), inoculated samples (250 g) were placed in the treatment chamber for the subsequent inactivation experiments (NIR radiant heating, UV-C irradiation, and simultaneous application of both technologies). All treatments were accompanied by stirring (23 rpm) by means of a rotational mixer in the chamber (Fig. V-1). For the inactivation mechanism study, 5-ml cell suspensions kept in glass petri dishes were treated with NIR, UV, and NIR-UV for 3 min under identical conditions. The volume of the cell suspension (5 ml) and the treatment time (3 min) were selected on the basis of the temperatures of powdered infant formula observed during NIR treatment.

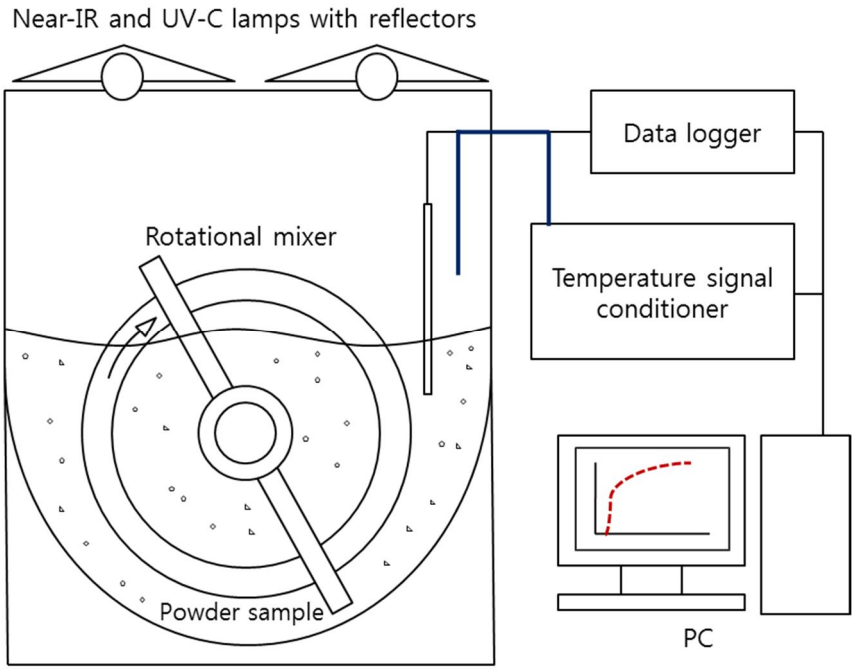

FIG. V-1. Schematic diagram of the combined NIR-UV treatment system used in this study.

Temperature measurement. A fiber optic temperature sensor (FOT-L; FISO Technologies Inc., Quebec, Canada) connected to a signal conditioner (TMI-4; FISO Technologies Inc., Quebec, Canada) was used to measure real-time temperatures in the treatment chamber during NIR-UV combined treatment. The sensor was placed directly on the inner wall surface of the chamber, and the temperature was manually recorded every 10 s. Additionally, in order to measure the core temperature of treated samples precisely, a K-type thermocouple and a data logger (34790A; Agilent Technologies, Palo Alto, CA, USA) were used (Fig. V-1). The thermocouple probe was directly inserted into the infant formula powder bed, and temperatures were recorded at selected treatment times. All experiments were replicated three times.

Bacterial enumeration. At selected time intervals, 25-g treated samples were removed and immediately transferred into sterile stomacher bags (Labplas Inc., Sainte-Julie, Quebec, Canada) containing 225 ml of BPW (detection limit, 10 CFU/g) and homogenized for 2 min with a stomacher (620 rpm, Easy Mix; AES Chemunex, Rennes, France). After homogenization, 1-ml aliquots of sample were 10-fold serially diluted in 9 ml blanks of BPW, and 0.1 ml of sample or diluent was spread-plated onto selective medium, chromogenic *Enterobacter sakazakii* agar (ESA) (Brilliance, DFI formulation; Oxoid, NY, USA), for the

enumeration of *C. sakazakii* cells. The agar plates were incubated at 37 °C for 24 h, and then the cells were enumerated by counting blue-green colonies.

Enumeration of injured cells. The liquid repair method was used to enumerate injured cells of *C. sakazakii*. One-milliliter aliquots of treated sample were 10-fold serially diluted in 9 ml of *Enterobacteriaceae* enrichment broth (Mossel formula; LAB, United Kingdom), and the diluted medium was incubated at 37 °C for 2 h to allow injured cells to be resuscitated. After the recovery step, 0.1 ml of diluent was spread-plated onto chromogenic selective medium. All agar plates were incubated for 22 h at 37 °C, and the typical blue-green colonies were counted. It has been reported that the optimal temperature range for growth of *Cronobacter* strains is 37 °C (Iversen et al., 2004). Injured cells are easily resuscitated on nonselective broth or liquid medium in less than 2 h, and the liquid medium resuscitation method is simpler and faster than solid agar repair methods, such as the overlay (OV) method (Cole et al., 1993). By performing preliminary experiments, I confirmed that the 2-h incubation period in liquid broth did not cause multiplication of uninjured cells in control samples and that the recovery level of injured *C. sakazakii* cells in liquid broth was not significantly different from that in the agar OV method (TSA-ESA).

Assessment of propidium iodide uptake. Cell membrane damage induced by each treatment was quantitatively assessed by using the fluorescent dye PI (Sigma-Aldrich). Untreated, UV-treated, NIR-treated, and NIR-UV-treated C. sakazakii cells were centrifuged (10,000 × g for 10 min), and the cell pellets were resuspended and diluted in PBS to an optical density at 680 nm (OD_{680}) of approximately 0.2 and then mixed with PI solution to a final concentration of 2.9 μM. After incubation for 10 min, the samples were centrifuged at 10,000 × g for 10 min and washed twice in PBS to remove excess dye. The final cell pellets were resuspended in PBS, and fluorescence was measured with a spectrofluorophotometer (Spectramax M2e; Molecular Devices, Sunnyvale, CA, USA) at an excitation wavelength of 493 nm and an emission wavelength of 630 nm. Fluorescence values for each sample were normalized with the OD_{680} of the cell suspensions, and data obtained for untreated cells were subtracted from those for treated cells.

Color measurement and sensory evaluation. To determine the effect of NIR-UV treatment on the color of infant formula powder, a Minolta colorimeter (model CR400; Minolta Co., Osaka, Japan) was used to measure the color changes of treated samples. The color attributes were quantified by the values of L*, a*, and b* and measured at random locations on powdered infant formula.

L*, a*, and b* values indicate color lightness, redness, and yellowness of the sample, respectively. All measurements were taken in triplicate.

Sensory evaluation was performed to determine how specific attributes (color, odor, and overall acceptability) varied over NIR-UV-treated powder samples (1-, 3-, 5-, and 7-min exposures) compared to those of a nontreated control. In all sensory tests, the panelists consisted of 12 members (5 men and 7 women; age range, 25 to 30 years) from the Department of Food and Animal Biotechnology, Seoul National University, Seoul, South Korea, and scores were obtained by rating the sensory attributes using the following 7-point hedonic scales: color intensity (7, brown; 1, white) and odor and overall acceptability (7, very good; 6, good; 5, below good/above fair; 4, fair; 3, below fair/above poor; 2, poor; 1, very poor). Powder samples, labeled with three-digit random numbers, were placed on white paper plates and presented after being cooled to room temperature. The presentation order was randomized, and the panelists were asked to use water to clean their palates between samples.

Statistical analysis. All experiments were repeated three times with duplicate samples. Triplicate data were analyzed by analysis of variance (ANOVA) with Duncan's multiple-range test of a statistical analysis system (SAS Institute, Cary, NC, USA). A P value of < 0.05 was used to indicate significant differences.

V-3. Results

Synergistic bactericidal effect of simultaneous NIR-UV treatment. The reduction in numbers of *C. sakazakii* cells in infant formula powder during NIR radiant heating, UV-C irradiation, and simultaneous application of both technologies is presented in Table V-1. Reductions of 1.55, 2.11, and 2.79 log units were observed in *C. sakazakii* after simultaneous NIR-UV combined treatment for 5, 6, and 7 min, respectively. The sums of results for NIR and UV inactivation were lower than values obtained by the simultaneous application of both technologies. In other words, synergistic effects were observed for all treatment times against *C. sakazakii* (Table V-1). However, statistically significant ($P < 0.05$) differences between the sums of NIR and UV inactivation and values for inactivation achieved with combination treatment were observed only after treatment times of 6 min or more. Log reductions resulting from the synergistic effect after 6 min of treatment, calculated by subtracting the sums of NIR and UV reductions from the values obtained during simultaneous NIR-UV treatment, were 0.73 and 0.95 log units at 6 and 7 min of treatment, respectively.

Table V-1. Reductions in numbers of viable *C. sakazakii* cells in powdered infant formula treated with UV-C irradiation, NIR radiant heating, and simultaneous application of both technologies.

Treatment time (min)	Log reduction [$\log_{10}(N_0/N)$] by treatment type and selective medium[a]							
	UV		NIR		NIR-UV			
	SA		SA		SA		SAR	
0	0.00±0.00	A	0.00±0.00	A	0.00±0.00	Aa	0.00±0.00	Aa
1	0.02±0.02	AB	0.07±0.09	A	0.10±0.10	ABa	0.22±0.20	Aa
2	0.01±0.01	AB	0.14±0.13	AB	0.33±0.11	BCa	0.29±0.22	Aa
3	0.01±0.01	AB	0.39±0.14	B	0.47±0.09	Ca	0.62±0.19	Ba
4	0.04±0.06	AB	0.67±0.16	C	0.81±0.07	Da	0.93±0.18	Ca
5	0.05±0.03	AB	1.20±0.18	D	1.55±0.12	Ea	1.32±0.25	Da
6	0.06±0.04	AB	1.32±0.29	D	2.11±0.19	Fa	1.82±0.17	Ea
7	0.07±0.06	B	1.77±0.01	E	2.79±0.22	Ga	2.43±0.08	Fa

[a] The values are means ± standard deviations from three replications. Values in the same column followed by the same uppercase letter are not significantly different ($P > 0.05$). Values in the same row followed by the same lowercase letter are not significantly different ($P > 0.05$). SA, plating directly on selective agar; SAR, plating on selective agar preceded by a resuscitation step. N_0, initial population; N, population after treatment.

Recovery of NIR-UV-injured cells. Levels of sublethally injured *C. sakazakii* cells in powdered infant formula following simultaneous NIR-UV treatment are shown in Table V-1. Determining the difference between inactivation of samples subjected to the injured-cell resuscitation method and that of samples plated directly on selective media revealed the presence of 0.23, 0.29, and 0.36 log units of injured *C. sakazakii* cells after 5-, 6-, and 7-min treatments, respectively. Slightly smaller reductions of *C. sakazakii* numbers were observed at the final stages of the treatment (5, 6, and 7 min) by the procedure involving the resuscitation step (liquid broth recovery method) than by direct plating on selective agar (ESA). However, no statistically significant ($P > 0.05$) differences between levels of surviving cells, including sublethally injured *C. sakazakii* cells, were observed during the entire treatment time (Table V-1).

Average temperature-time histories of powdered infant formula. Figure V-2 shows average temperatures of the treatment chamber and infant formula powder core during simultaneous NIR and UV treatment. About 6 and 3 °C temperature differences were observed between inside the chamber and the infant formula powder core at 1 and 2 min of treatment, respectively. This temperature disparity continued to decrease with treatment time, and from 3 min of treatment, the temperatures of the sample core and treatment chamber reached

equilibrium (ca. 50 °C). At maximum treatment time (7 min), the temperatures increased to ca. 73 °C (Fig. V-2). Additionally, the heating rate of NIR treatment alone was not different from that of simultaneous NIR-UV treatment of infant formula powder (data not shown).

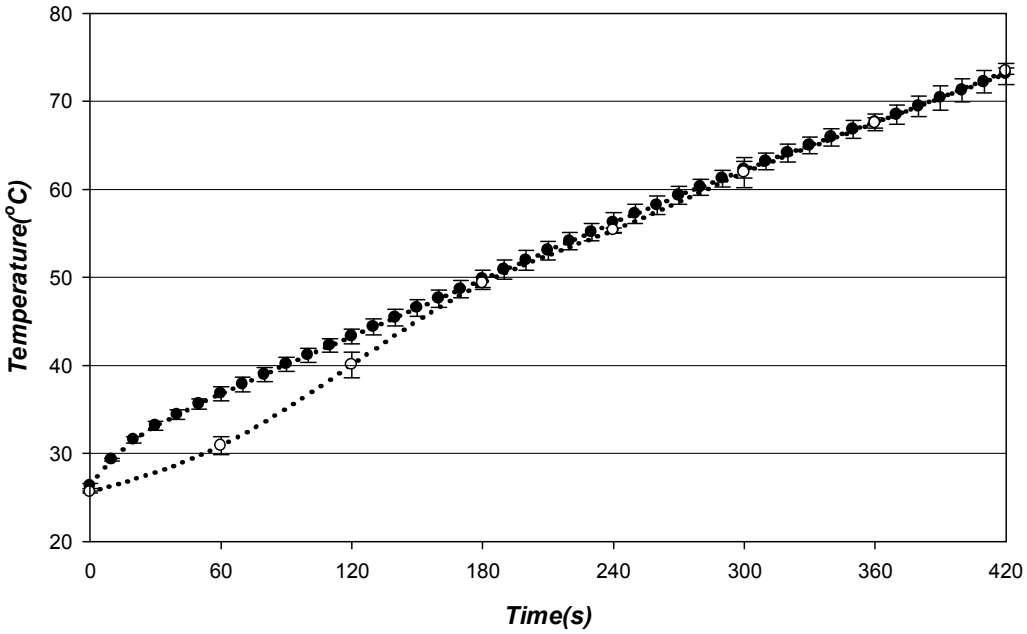

FIG. V-2. Average temperature-time histories for treatment chamber and infant formula powder cores during simultaneous NIR heating and UV-C irradiation. The error bars indicate standard deviations calculated from triplicates. ○, infant formula powder core; ●, inside treatment chamber.

Determination of cell membrane damage by PI uptake. As a quantitative analysis of membrane damage, NIR-, UV-, and NIR-UV-treated cells were stained with the fluorescent dye PI, which passes through only damaged cell membranes. The PI uptake values of *C. sakazakii* after each treatment are shown in Table V-2. The degree of PI uptake in NIR- and NIR-UV-treated cells was much higher than that in UV-treated cells, indicating there was no significant damage to cellular membranes of *C. sakazakii* following UV treatment. Cells subjected to simultaneous NIR-UV treatment showed significantly ($P < 0.05$) higher PI uptake values than did cells subjected to the other treatments (Table V-2).

Table V-2. Levels of membrane damage of UV-, NIR-, and simultaneously NIR-UV-treated cells obtained from the PI uptake test.

Treatment type	PI uptake value[a]	
	C. sakazakii	
Untreated Control	0±0	A
UV	2.18±0.13	B
NIR	13.21±2.21	C
NIR-UV	28.76±0.47	D

[a] The values are means of three replications ± standard deviations. Values followed by the same letters are not significantly different ($P > 0.05$). The data were normalized by subtracting fluorescence values obtained from untreated cells and against the OD_{680} as follows: PI value = (fluorescence value after treatment - fluorescence value of untreated cells)/OD_{680}.

Effect of simultaneous NIR-UV treatment on product quality. The color values of infant formula powder after combined NIR-UV treatment are summarized in Table V-3. The L*, a*, and b* values of NIR-UV-treated (7 min) powdered infant formula were not significantly ($P > 0.05$) different from those of nontreated samples. Although the b* value (yellowness) slightly decreased with prolonged treatment time, statistically significant differences were not detected during the entire treatment interval (Table V-3). Table V-4 shows the sensory attributes of powdered infant formula following NIR-UV treatment. There were no significant ($P > 0.05$) differences among all tested samples scored by the hedonic scale for color, odor, and overall acceptability, indicating that simultaneous application of NIR and UV treatment for 7 min does not alter the sensory quality of the infant formula powder product significantly.

Table V-3. Color values of simultaneously NIR-UV-treated infant formula powder.

Treatment time(min)	Color value for parameter[a]		
	L*	a*	b*
0	94.13±0.66 A	-4.42±0.08 A	21.80±0.35 A
1	94.27±0.75 A	-4.45±0.31 A	21.98±0.27 A
2	94.23±0.66 A	-4.31±0.03 A	21.90±0.26 A
3	94.22±0.64 A	-4.33±0.11 A	21.78±0.19 A
4	94.30±0.64 A	-4.37±0.09 A	21.66±0.34 A
5	94.17±0.59 A	-4.17±0.13 A	21.44±0.38 A
6	94.25±0.69 A	-4.11±0.16 A	21.26±0.63 A
7	94.29±0.76 A	-4.21±0.38 A	21.17±0.67 A

[a] The values are the means of three replications ± standard deviations. Values followed by the same letters within each column are not significantly different ($P > 0.05$).

Table V-4. Sensory attributes of powdered infant formula following simultaneous NIR-UV treatment (at day 0).

Treatment time(min)	Sensory attribute score[a]		
	Color	Odor	Overall
0	4.0±0.76 A	5.4±0.74 A	5.1±0.83 A
1	4.0±0.93 A	5.1±0.99 A	5.4±0.92 A
3	3.9±0.83 A	5.0±0.93 A	5.4±0.52 A
5	4.1±0.83 A	5.1±1.25 A	5.1±1.13 A
7	3.8±0.89 A	5.4±0.52 A	5.1±0.64 A

[a] Results are from panelist scorecard analysis on a 7-point hedonic scale. For color, 7, brown; 1, white. For odor and overall acceptability, 7, very good; 1, very poor. n = 12. The values are means. Values followed by the same letters within each column did not differ significantly ($P > 0.05$).

V-4. Discussion

The primary means of pasteurization in the manufacture of powdered foods is heating. However, *C. sakazakii* has been known to be more thermotolerant than any other member of the *Enterobacteriaceae* (Nazarowec-White and Farber, 1997), although thermal resistance among *C. sakazakii* strains varied as much as 20-fold (Edelson-Mammel and Buchanan. 2004). Moreover, thermal treatments cannot be efficiently applied to powdered matrices because of their low thermal conductivity. Kim et al. (2010) reported that heat treatment at 63, 68, and 73 °C for 30 min did not reduce populations of *C. sakazakii* in dehydrated infant formula. In my study, NIR treatment alone was also insufficient to inactivate *C. sakazakii* by the required amount (ca. 3-log-unit reduction) in infant formula powder (Table V-1). To obtain a 3-log-unit reduction, treatment for 9.6 min was needed for *C. sakazakii* based on the calculated parameters of the Weibull model (R^2 = 0.95).However, yellowing and darkening were visually observed on infant formula powder treated with NIR for a slightly excessive time (over 9 min).

Inactivation of *C. sakazakii* utilizing hurdle combinations has been performed in infant formula by several researchers. Pina-Pérez et al. (2009) obtained 2.2-log-unit reductions in numbers of *C. sakazakii* cells in reconstituted infant formula by the sequential combination of pulsed-electrical-field treatment and refrigerated storage (8 °C). They also reported that microwave heating followed

by refrigerated storage (5 °C) resulted in the progressive death of *C. sakazakii* in the rehydrated form (Pina-Pérez et al., 2013). UV radiation exposed infant formula powder reconstituted in 55, 60, and 65 °C hot water demonstrated either additive or synergistic effects for inactivation of *C. sakazakii* (Liu et al., 2012). The implementation of multiple-hurdle technology in food matrices is becoming more attractive in terms of product quality because individual treatments, especially heating, can be used at lower intensity. The use of excessive heat for inactivation of bacteria results in denaturation of whey proteins, as well as changes in physical, mechanical, and optical properties of powdered infant formula. In the present study, simultaneous NIR and UV treatments resulted in greater reductions in cell numbers of *Cronobacter* spp. than did either treatment alone as a result of synergism (Table V-1). Additionally, due to the shorter NIR processing time, combined NIR-UV treatments did not change the color values or sensory attributes of infant formula powder significantly ($P > 0.05$) (Table V-3 and 4).

Although UV radiation is well established for sanitization of air, water, and liquid food and for food surface decontamination, UV radiation as an intervention for powdered foods is still under investigation. Liu at al. (2012) treated powdered infant formula with UV-C radiation to inactivate *C. sakazakii*. Treatment with UV radiation for 25 min (60.7 kJ/m^2) reduced *C. sakazakii*'s presence by 1.38 log CFU/g; however, complete inactivation was not achieved

because UV radiation did not completely penetrate the dry infant formula. To overcome these limitations of the penetration capability of UV radiation, as well as NIR thermal energy in the powder bed, a rotational mixer was used simultaneously with combined NIR-UV treatment in this study. Simultaneous mixing could increase the contact area of radiation on powder particles and facilitate the use of NIR-UV radiant treatment for controlling *C. sakazakii* in dry infant formula.

To date, there are no published reports dealing with the effectiveness of NIR and UV-C combination treatment against pathogenic bacteria in powdered foodstuffs. For this reason, the results of this study can only be compared with the results obtained from my previous study (Ha and Kang, 2013), which dealt with a different powdered food matrix (red pepper powder) and different microorganisms (*S.* Typhimurium and *E. coli* O157:H7). The temperature increase rate of the infant formula powder core was similar to that of red pepper powder. However, a longer treatment time and higher core temperature (7 min and 73 °C) were required than for previously studied pathogens (5 min and 62 °C) to obtain the same (ca. 3-logunit) reduction in infant formula powder. These results might be attributed to the higher resistance of *C. sakazakii* than of other *Enterobacteriaceae* under dry conditions. *C. sakazakii* in the stationary phase can produce yellow pigments (carotenoids) known to stabilize cellular membranes, influence cellular membrane fluidity, and scavenge reactive oxygen

species and to be responsible for its survival and behavior in stressful environments (Gruszecki and Strzalka, 2005). Furthermore, the increased amount of fat, protein, and carbohydrate in infant formula powder may also protect *C. sakazakii* against NIR-UV treatment. Therefore, the optimized treatment conditions of a combined NIR-UV system could vary depending on the target pathogenic microorganisms and the model food being investigated.

In order to validate the application of this new bactericidal technology, it is essential to study the ongoing microbiological dynamics of the processed food. Sublethally injured cells could assume added significance, since they are able to be resuscitated and to regain their pathogenicity under suitable conditions (Wesche et al., 2009). Therefore, cell populations enumerated directly on selective media following treatment are likely not representative of the total surviving cells in infant formula powder. In this study, there were no significant ($P > 0.05$) differences in reduction levels determined by plating on selective agars with and without a resuscitation step at all treatment time intervals (Table V-1). This suggests that simultaneous NIR-UV treatment effectively inactivated *C. sakazakii* in powdered infant formula without generating many injured cells that potentially could recover.

In my previous study, the mechanism of the synergistic lethal effect of combined NIR-UV treatment was investigated, and I confirmed that damage to the bacterial cell envelope was the main factor related to the synergistic lethal

effect (Ha and Kang, 2013). In the present study, the PI uptake test was utilized to determine the inactivation mechanism of *C. sakazakii*. This method was evaluated in an investigation involving *S.* Typhimurium and *E. coli* O157:H7 (Ha and Kang, 2013). PI emits fluorescence when binding to nucleic acids and does not pass through intact cell membranes (Breeuwer and Abee, 2000). As shown in Table V-2, the value of PI uptake induced by the simultaneous application of NIR-UV was significantly higher than the sum of PI uptake values reached by separate NIR and UV treatments, and this tendency was consistent with the synergistic log reduction data obtained from selective media (Table V-1). These results were in accordance with my previous work and provide clear evidence for the inactivation mechanism underlying the synergistic effect of combined NIR-UV treatment for *C. sakazakii*.

According to the FDA's definition, an agent that provides a minimum 2-log-unit microbial reduction is accepted as an antimicrobial technology by the food industry (Torlak and Sert, 2013). My results revealed that about a 3-log-unit reduction in the number of *C. sakazakii* cells in powdered infant formula can be achieved by simultaneous NIR-UV treatment within 7 min of exposure. However, considering the very low observed level (0.36 to 0.66 CFU/100 g) of *C. sakazakii* contamination in powdered infant formula (Muytjens et al., 1988), NIR-UV treatment at a moderate intensity would virtually ensure that a serving would not contain this enteric pathogen and could be applied practically by the

dairy industry. Although the pilot instrument used in the current study was batch type and the capacity was comparatively small, this bactericidal system for powdered foods could easily be expanded to practical industrial scale by utilizing it in the form of continuous line processing.

Chapter VI.

Combining Organic Acid Spray with NIR Radiant Heating to Inactivate Food-Borne Pathogens on Dry Nut Kernels

This chapter was published in *Applied and Environmental Microbiology* (2015) 81(13): 4517-4524.

VI-1. Introduction

Consumption of edible nut kernels has shown an upward trend worldwide, as consumers have taken a profound interest in health and nutrition. Although nut-associated illness outbreaks are relatively uncommon, recent outbreaks of salmonellosis related to consumption of nut kernels including almonds and pine nuts have raised awareness of nuts as a potential vehicle for foodborne illness (CDC, 2004; 2011; Isaacs et al., 2005; Ledet-Muller et al., 2007). Two hundred five cases of salmonellosis associated with consumption of whole raw almonds in Canada and the United States have been attributed to *Salmonella enterica* serovar Enteritidis phage type 30 (PT 30) (Isaacs et al., 2005). More recently, the Centers for Disease Control and Prevention released a report stating that at least 53 people in 5 states of the US had become infected during a non-PT-30 *S.* Enteritidis outbreak that was linked to contaminated Turkish pine nuts (CDC, 2011). *Salmonella* spp. cannot multiply on nuts, but has the ability to survive on and in dry nut kernels for more than one year (Uesugi et al., 2006). In light of this, research interest in enhancing the microbial safety and quality of nuts potentially offers great health and economic benefits to the general public and to food processors (Lee et al., 2006).

Existing disinfection practices for all low-moisture foods including nuts are currently under evaluation. Several processes for eliminating *Salmonella* from

almond surfaces have been investigated, including propylene oxide fumigation (Danyluk et al., 2005), chlorine dioxide gas (Wihodo et al., 2005), and various heat processes involving steam (Lee et al., 2006; Chang et al., 2010). However, few treatments are available for the decontamination of almond kernels that are consumed raw due to limitations of these interventions. The major drawback of using fumigants, such as propylene oxide, is the potential presence of residues and their negative impact on export marketing (Brandl et al., 2008). Chlorine dioxide is an effective gaseous alternative to propylene oxide for inactivating *Salmonella* contamination on raw almonds, but it can lead to discoloration of the kernel surface at high concentrations (Wihodo et al., 2005). Steam is more effective than dry heat, but prolonged exposure causes quality loss and requires additional processing to remove condensed moisture before storage (Lee et al., 2006; Brandl et al., 2008). Furthermore, to date, there have been no published reports that focused on controlling foodborne pathogens on pine nut kernels despite the recent *S.* Enteritidis outbreak (CDC, 2011). Consequently, the development of new technologies that can effectively reduce *Salmonella* spp. on nut kernels without compromising product quality is needed.

Recently, infrared (IR) heating has been gaining wider acceptance because of its higher heat transfer capacity and high energy efficiency compared with conventional heating. Brandl et al (2008) employed catalytic IR heating for reducing *Salmonella* populations on almond kernels. In my previous studies,

near IR radiation (NIR; 0.76 to 2 μm) was shown to be more effective than conventional heating for inactivating pathogens on solid foods (Ha et al., 2012), and NIR heating combined with a non-thermal technology such as UV-C radiation showed significant synergistic lethal effects (Ha and Kang, 2013; 2014; 2015). On the other hand, a broad spectrum of chemical compounds and their usages has been developed by the food industry for minimizing microbial contamination on surfaces of raw agricultural commodities. Pao et al. (2006) reported on the potential use of acid sprays for eliminating *Salmonella* spp. on raw almonds. An estimated 5-log reduction can be achieved using combinations of spraying with 10 % citric acid, shelling, and storage. However, considering nut quality, acidic solutions should be applied at lower concentrations.

Since no published data exist on the behavior of *Salmonella* on the surface of nut kernels during simultaneous treatment with organic acid sprays and NIR heating, I chose to combine antimicrobial treatments to achieve maximal effectiveness against *S.* Enteritidis on nut kernels, using both chemical (spraying with organic acid solution) and physical (NIR heating) interventions. The essence of this approach is that nuts can remain microbiologically safe, and are acceptable organoleptically and nutritionally due to the mild heating applied. Among various organic acids of identical concentration and similar pH, the use of lactic acid offers the best antimicrobial potential based on our previous study (Park et al., 2011). Therefore, lactic acid was chosen for this investigation.

The objectives of this research were to evaluate the efficacy of lactic acid spray along with NIR heating for inactivating *Salmonella enterica* serovar Enteritidis on almond and pine nut kernels, and to determine the effect of the combination treatment on quality factors of the nut kernel product. Also, I explored the mechanism of inactivation.

VI-2. Materials and Methods

Bacterial strains. Three strains each of *S. enterica* serovar Enteritidis (NCCP 12236, NCCP 12243, and NCCP 14771) obtained from the National Culture Collection for Pathogens (NCCP; Osong, South Korea) and *S.* Enteritidis PT 30 (ATCC BAA-1045) obtained from the Bacterial Culture Collection of Seoul National University (Seoul, South Korea) were used in this experiment. Stock cultures were kept frozen at -80 °C in 0.7 ml of tryptic soy broth (TSB; Difco Becton Dickinson, Sparks, MD, USA) and 0.3 ml of 50 % glycerol (vol/vol). Working cultures were streaked onto tryptic soy agar (TSA; Difco), incubated at 37 °C for 24 h, and stored at 4 °C.

Preparation of pathogen inocula. All strains of *S.* Enteritidis were cultured individually in 5ml of TSB at 37 °C for 24 h, harvested by centrifugation (4,000 × g for 20 min at 4 °C) and washed three times with 0.2 % peptone water (PW; Difco). The final pellets were resuspended in PW, corresponding to approximately 10^7 to 10^8 CFU/ml. Subsequently, suspended pellets of *S.* Enteritidis NCCP 12236, NCCP 12243, and NCCP 14771 were combined to produce mixed culture cocktails while PT 30 was prepared as a single strain inoculum. These cell suspensions with a final concentration of approximately 10^8 CFU/ml were used in this study. To analyze the mechanism of inactivation, a

final pellet of non-PT-30 *S.* Enteritidis was resuspended in 3 ml of phosphate-buffered saline (PBS; 0.1 M) and inoculated onto a sterile glass petri dish (16 mm [height] by 90 mm [inside diameter]). The cell suspensions were thoroughly dried inside a biosafety hood prior to each treatment.

Sample preparation and inoculation. Raw shelled 'Nonpareil' almonds (California, USA) and pine nuts (Hongcheon, South Korea) were purchased at a local grocery store (Seoul, South Korea). For inoculation, 5 ml of prepared inoculum was added dropwise to 200-g samples (*S.* Enteritidis PT 30 to almonds / non-PT-30 *S.* Enteritidis cocktail to pine nuts) inside sterile high-density polyethylene (HDPE) bags (300 mm by 450 mm). The inoculated samples were thoroughly mixed by hand massaging for 3 min to produce a homogeneous dispersal of inoculum throughout the nut kernels and dried for 24 h inside a biosafety hood (21 ± 2°C) with the fan running until the moisture content (dry basis) of the samples equaled that of uninoculated samples (ca. 4.8 and 2.5 % for almonds and pine nuts, respectively). The final cell concentration was 10^5 to 10^6 CFU/25g. Inoculated nut kernel samples were then immediately used in each experimental batch.

Preparation of lactic acid solution. Lactic acid (LA, above 90.0 %; Daejung Chemical Co., Siheung-si, South Korea) was mixed with enough sterile distilled

water (DW) to make a 2 % (v/v) solution and the solution was prepared within 1 h before experiments. The pH for DW and 2 % LA solution was 6.86 and 2.03, respectively. The concentration and volume of LA applied to the sample were chosen after preliminary experiments were performed.

Spraying with LA and near-infrared heating. Near-infrared (NIR) heating and spraying with LA were carried out in a previously described apparatus (Ha and Kang, 2014). A stainless steel chamber (concave-upwards base, 380 by 205 by 158 mm) with a rotational mixer was used for combined NIR heating and LA spray treatment (Fig. VI-1). For spraying the 2 % LA solution or DW on nut kernel samples, a hand-operated sprayer (650 ml, Apollo, Siheung-si, South Korea) was used. The sprayer was held on the top of the treatment chamber (at a distance of 13 cm from the samples). An approximate volume of 10 ± 0.5 ml of 2 % LA or DW was sprayed evenly over inoculated almonds or pine nuts (200 g) during simultaneous operation of the rotational mixer (23 rpm). This was followed immediately with NIR heating applied for a maximum of 5 min. Two quartz halogen infrared heating lamps (NS-104, 350 mm; NSTECH, Gyunggido, South Korea), with a maximum power of 500 W (radiation intensity of 141.75 $\mu W/cm^2/nm$ at the sample location) at a 230-V input, was used as a NIR-emitting source. The maximum wavelength (λm) generated from the infrared heater used in this study was about 1,300 nm which is in the near-infrared wave

range. The radiation intensity generated from the NIR heater was measured and recorded with a NIR fiber optic spectrometer (AvaSpec-NIR256-1.7; Avantes, Eerbeek, Netherlands). Since both lamps radiate in all directions, two aluminum reflectors were installed behind the emitters to redirect the radiation waves and enhance the efficiency of NIR radiation (Fig. VI-1). After the outputs of the NIR lamps were stabilized (following 2 min of run time), the two lamps were placed on the treatment chamber for the inactivation experiments (NIR with 2 % LA spray, NIR with DW spray, NIR without supplemental spray, and 2 % LA spray without NIR). All treatments were accompanied by stirring (23 rpm) by means of the rotational mixer. For the inactivation mechanism study, 3-ml cell suspensions dried inside glass petri dishes were treated with LA, NIR, NIR-DW, and NIR-LA for 4 min under identical conditions. The treatment time (4 min) was selected based on the temperatures of nut samples observed during NIR treatment.

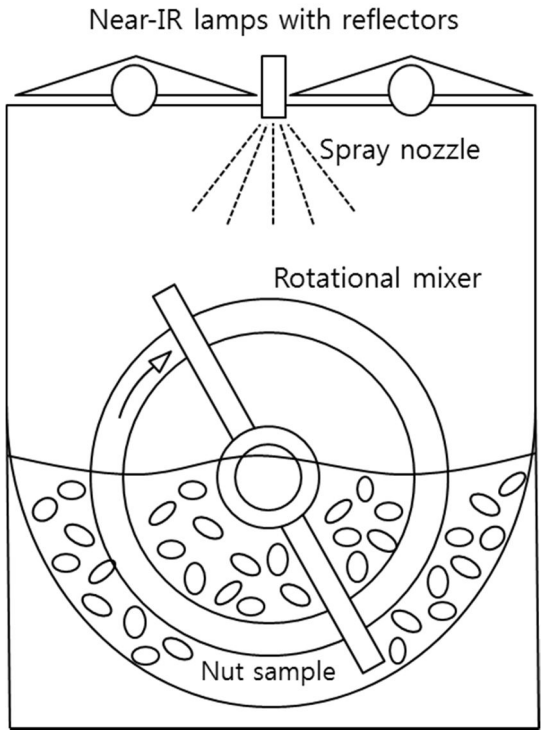

FIG. VI-1. Schematic diagram of the NIR-LA combined treatment system used in this study.

Bacterial enumeration. At selected time intervals, 25 g treated samples were removed and immediately transferred into sterile stomacher bags (Labplas Inc., Sainte-Julie, Quebec, Canada) containing 100 ml of 0.2 % PW (detection limit, 5 CFU/g) and homogenized for 2 min with a stomacher (620 rpm, Easy Mix; AES Chemunex, Rennes, France). After homogenization, 1-ml aliquots of sample were 10-fold serially diluted in 9-ml blanks of PW, and 0.1 ml of sample or diluent was spread-plated onto selective medium, Xylose lysine desoxycholate agar (XLD; Difco), for the enumeration of *S.* Enteritidis cells. None of the uninoculated control nuts yielded black colonies characteristic of *Salmonella* spp. on XLD agar (data not shown).Where low numbers of surviving cells were anticipated, 250 µl of sample was spread-plated onto each of four plates to lower the detection limit. All agar media were incubated at 37 °C for 24 h before counting. To confirm the identity of *S.* Enteritidis, random colonies were selected from the enumeration plates and subjected to the *Salmonella* latex agglutination assay (Oxoid, Ogdensberg, NY, USA), a serological test.

Enumeration of injured cells. The overlay (OV) method was used to enumerate injured cells of *S.* Enteritidis (Lee and Kang, 2001). TSA was used as a nonselective medium to repair injured cells. One hundred microliters of appropriate dilutions were spread-plated onto TSA medium in duplicate, and plates were incubated at 37 °C for 2 h to allow injured cells to resuscitate (Kang

and Siragusa, 1999). Plates were then overlaid with 7 to 8 ml of the selective medium XLD agar. After solidification, plates were further incubated for an additional 22 h at 37 °C. Following incubation, presumptive colonies of *S.* Enteritidis with typical black colonies were enumerated.

Temperature measurement. In order to measure the surface temperature of treated samples during single NIR heating and NIR heating combined with DW or 2 % LA sprays, a RAYTEK infrared precision thermometer (STProPlus, Raytek Co., Santa Cruz, CA, USA) was used. Temperatures were recorded at selected treatment times and all experiments were replicated three times.

Measurement of extracellular UV-absorbing substances. Cell membrane damage induced by each treatment was quantitatively assessed by determining the release of UV-absorbing materials from injured cells. Untreated and treated *S.* Enteritidis cells were resuspended using 10 ml of PBS and centrifuged at 10,000 × g for 10 min. UV-absorbance of sample supernatants at 260 and 280 nm was measured with a spectrophotometer (Spectramax M2e; Molecular Devices, Sunnyvale, CA, USA). The absorbance was presented as the mean of triplicated measurements.

Acid value, peroxide value, and total phenolic content measurement. To evaluate the effect of NIR-LA treatment for a maximum of 5 min on nutritional quality of nut kernels, the acid value, peroxide value, and total phenolic concentration was monitored under accelerated conditions during storage. Thirty g treated samples in 50 ml vial tubes were sealed with paper to facilitate gas exchange before being placed in an air-convection oven at 60 °C in the dark. After storage for 0, 9, and 18 days, about 5 g each of almond or pine nut sample was chopped and extracted with absolute ether (for acid value and peroxide value) or acetone (for total phenolic content) in a solvent recovery extractor (Soxhlet method, 4002842; JP Selecta S.A., Barcelona, Spain). The acid value and peroxide value in the oil extracted from the nut samples were determined by AOCS official methods Cd 3a-63 and Cd 8-53, respectively (AOCS, 2000). Total phenolic contents in the extracts were estimated by a colorimetric assay based on the procedure described by Singleton et al. (1999) with some modifications. Briefly, a 1 ml aliquot of the extract was mixed with 1 ml of Folin & Ciocalteu's phenol reagent (Sigma-Aldrich, St. Louis, MO, USA). After 3 min, 1 ml of saturated sodium carbonate solution was added to the mixture and adjusted to 10 ml with distilled water. The reaction was kept in the dark for 90 min, after which the absorbance was read at 725 nm using a spectrophotometer (Spectramax M2e; Molecular Devices). A blank devoid of any extract was used for background subtraction. Gallic acid (Sigma-Aldrich) was used as the

reference standard, and the results were expressed as mg of gallic acid equivalents (GAEs) per g of extract.

Color / post-treatment moisture content measurement and sensory evaluation. To determine the effect of NIR-LA treatment for 5 min on the color of nut kernel skin, a Minolta colorimeter (model CR400; Minolta Co., Osaka, Japan) was used to measure color changes of treated samples. The color attributes were quantified from the values of L^*, a^*, and b^*, which indicate the color lightness, redness, and yellowness of the sample, respectively, and which were measured at identical locations on surfaces of each almond and pine nut kernel. After 5 min of NIR-LA treatment, the post-treatment moisture content (dry basis, db) was measured immediately with a halogen moisture analyzer (HB43-S; Mettler Toledo, Columbus, OH, USA). All measurements were taken in triplicate.

Sensory evaluation was performed to determine how specific attributes (texture and flavor) varied over NIR-LA-treated nut samples (5-min exposure) compared to those of a non-treated control. In all sensory tests, the panelists consisted of 13 members (6 men and 7 women; age range, 25 to 31 years) from the Department of Food and Animal Biotechnology, Seoul National University, and scores were obtained by rating the sensory attributes using the following 7-point hedonic scales: 7, very good; 6, good; 5, below good/above fair; 4, fair; 3,

below fair/above poor; 2, poor; 1, very poor. Samples, labeled with three-digit random numbers, were placed on white paper plates and presented after being cooled to room temperature. The presentation order was randomized, and the panelists were asked to use water to clean their palates between samples.

Statistical analysis. All experiments were repeated three times with duplicate samples. Data were analyzed by the analysis of variance (ANOVA) procedure of the Statistical Analysis System (SAS Institute, Cary, NC, USA). Means were separated using Tukey-Kramer's multiple-range test, and $P < 0.05$ was used to indicate significant differences.

VI-3. Results

Survival curves of food-borne pathogens. Viable-count reductions of *S.* Enteritidis PT 30 on almond kernels and *S.* Enteritidis cocktail on pine nut kernels during single NIR or 2 % lactic acid (LA) spray treatment and NIR heating combined with distilled water (DW) or 2 % LA sprays are depicted in Fig. VI-2 and 3, respectively. The overall reduction patterns of *S.* Enteritidis PT 30 on almonds were similar to those of the *S.* Enteritidis cocktail on pine nuts. Significant ($P < 0.05$) log reductions of *S.* Enteritidis on almonds and pine nuts were observed after 1 min of NIR-LA combined treatment, whereas with NIR-DW combined treatment, the time to initiation of a significant ($P < 0.05$) reduction was delayed by an additional 1 to 2 min (Fig. VI-2 and 3). NIR-LA combined treatment for 5 min achieved 3.92- and 4.12- log reductions in *S.* Enteritidis PT 30 and cocktail, respectively. Reductions of 3.93 and 3.96 log CFU/g were observed in *S.* Enteritidis PT 30 and cocktail after NIR-DW treatment for 5 min, respectively. Especially for the NIR-DW combination, *S.* Enteritidis populations on both samples sharply declined after 3 min of treatment, and the reduction levels at 3, 4, and 5 min intervals were not significantly ($P > 0.05$) different from those of NIR-LA treatment (Fig. VI-2 and 3). NIR heating alone for 5 min reduced cell numbers of *S.* Enteritidis PT 30 and cocktail by 1.14 and 2.35 log CFU/g, respectively. After 5 min of LA spray treatment alone,

levels of *S*. Enteritidis PT 30 and cocktail were reduced by 0.67 and 0.17 log CFU/g, respectively.

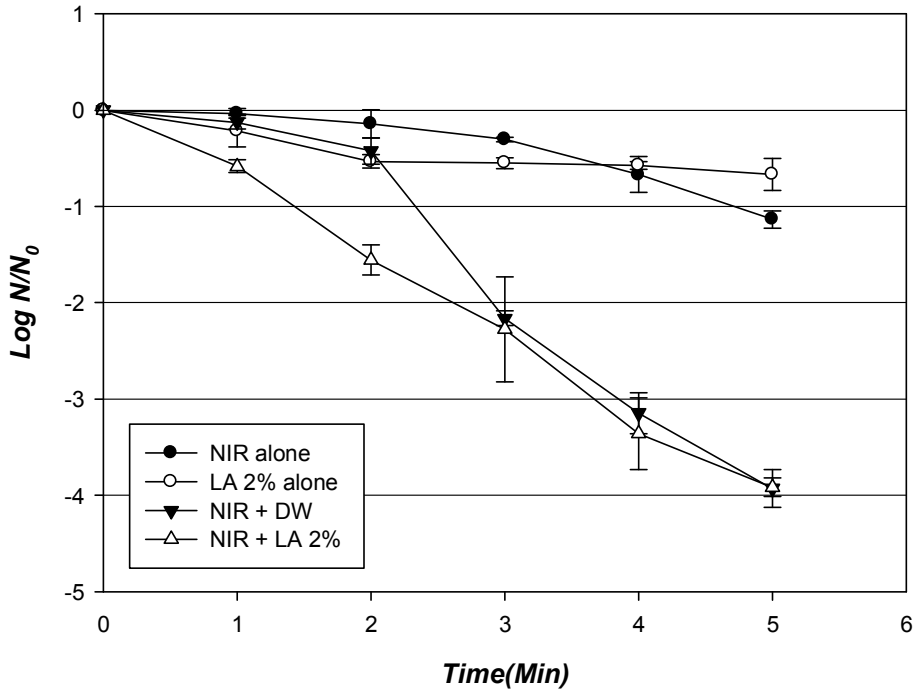

FIG. VI-2. Survival curves of *Salmonella* Enteritidis PT 30 on almond kernels treated with single NIR or 2 % lactic acid sprays and NIR heating combined with distilled water or 2 % lactic acid sprays. The error bars indicate standard deviations calculated from triplicates.

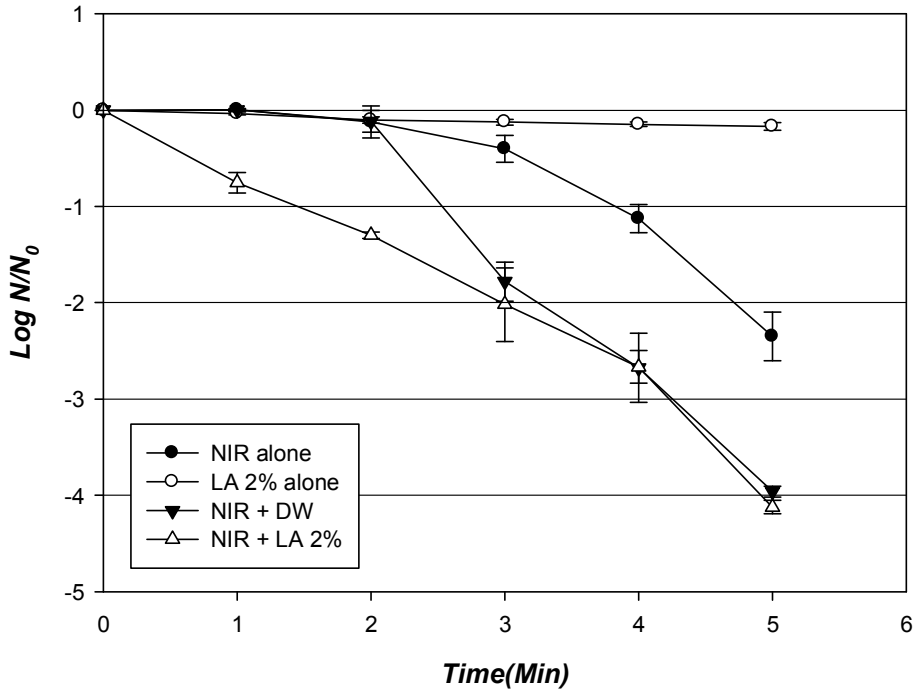

FIG. VI-3. Survival curves of *Salmonella enterica* serovar Enteritidis on pine nut kernels treated with single NIR or 2 % lactic acid sprays and NIR heating combined with distilled water or 2 % lactic acid sprays. The error bars indicate standard deviations calculated from triplicates.

Resuscitation of injured cells. Levels of sublethally injured *S.* Enteritidis PT 30 on almonds and *S.* Enteritidis cocktail on pine nuts following NIR-DW or NIR-LA treatment are presented in Table VI-1 and 2, respectively. When surface-inoculated nut kernels were subjected to NIR-DW combined treatment, smaller reductions of *S.* Enteritidis were observed by the agar OV method than by direct plating on selective agar, and statistically significant ($P < 0.05$) differences between levels of surviving cells (non-injured vs. total cells, including those sublethally injured) were observed after the maximum treatment time of 5 min (Table VI-1 and 2). For NIR-LA combined treatment, however, there were no significant ($P > 0.05$) differences between the reduction levels enumerated on the selective agar (XLD) versus the agar used for recovery (OV-XLD) during the entire treatment time.

Table VI-1. Levels of surviving cells and cells including injured *Salmonella* Enteritidis PT 30 on almond kernels following NIR heating combined with distilled water or 2 % lactic acid sprays.

Treatment time (min)	Log reduction [$\log_{10}$ (N_0/N)] by treatment type and selective medium[a]							
	NIR-DW				NIR-LA			
	XLD		OV-XLD		XLD		OV-XLD	
0	0.00±0.00	Aa	0.00±0.00	Aa	0.00±0.00	Aa	0.00±0.00	Aa
1	0.13±0.07	ABa	0.04±0.03	Aa	0.58±0.07	Aa	0.68±0.11	Aa
2	0.43±0.13	Ba	0.33±0.07	Aa	1.56±0.16	Ba	1.51±0.18	Ba
3	2.16±0.08	Ca	1.83±0.30	Ba	2.28±0.54	Ba	2.14±0.48	Ba
4	3.15±0.21	Da	2.60±0.32	Ca	3.36±0.37	Ca	3.16±0.37	Ca
5	3.93±0.20	Ea	3.06±0.26	Cb	3.92±0.10	Ca	3.90±0.11	Da

[a] The values are means ± standard deviations from three replications. Values in the same column followed by the same uppercase letter are not significantly different ($P > 0.05$). Means with the same lowercase letter in the same row are not significantly different ($P > 0.05$). XLD, xylose lysine desoxycholate; OV-XLD, overlay XLD agar on TSA.

Table VI-2. Levels of surviving cells and cells including injured *Salmonella enterica* serovar Enteritidis on pine nut kernels following NIR heating combined with distilled water or 2 % lactic acid sprays.

Treatment time (min)	Log reduction [$\log_{10}(N_0/N)$] by treatment type and selective medium[a]							
	NIR-DW				NIR-LA			
	XLD		OV-XLD		XLD		OV-XLD	
0	0.00±0.00	Aa	0.00±0.00	Aa	0.00±0.00	Aa	0.00±0.00	Aa
1	0.00±0.02	Aa	-0.08±0.04	Aa	0.75±0.11	Ba	0.88±0.06	Ba
2	0.12±0.11	Aa	0.16±0.12	Aa	1.30±0.04	Ca	1.27±0.04	Ba
3	1.78±0.20	Ba	1.35±0.12	Bb	2.02±0.38	Da	1.94±0.51	Ca
4	2.68±0.36	Ca	2.00±0.07	Cb	2.67±0.17	Ea	2.56±0.14	Da
5	3.96±0.06	Da	3.28±0.13	Db	4.12±0.07	Fa	4.02±0.04	Ea

[a] The values are means ± standard deviations from three replications. Values in the same column followed by the same uppercase letter are not significantly different ($P > 0.05$). Means with the same lowercase letter in the same row are not significantly different ($P > 0.05$). XLD, xylose lysine desoxycholate; OV-XLD, overlay XLD agar on TSA.

Average temperature-time histories of nut kernels. Fig. VI-4 shows average surface temperatures of almonds and pine nuts, respectively, during single NIR heating and NIR heating combined with DW or 2 % LA sprays. The surface temperature rose immediately in response to infrared waves when nut kernel samples were exposed to NIR radiation. The initial heating rates of all treatment combinations were similar on almonds and on pine nuts. However, after 3 min of treatment, the rate of temperature increase of nut kernels treated with NIR-DW or NIR-LA declined and these temperature disparities continued to increase with treatment time (Fig. VI-4). The heating rate of the NIR-LA treatment was not significantly ($P > 0.05$) different from that of the NIR-DW treatment at all treatment time intervals. At the maximum treatment time (5 min), surface temperatures of almonds and pine nuts increased to ca. 77 and 81 °C, respectively. Whereas, during 5 min of single NIR treatment, surface temperatures of almond and pine nut kernels reached ca. 93 and 101 °C, respectively.

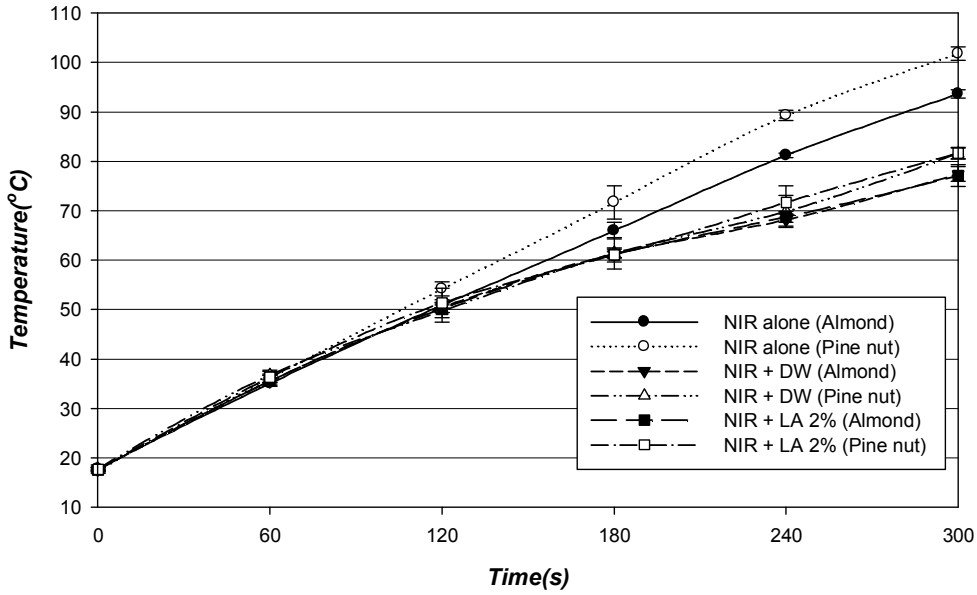

FIG. VI-4. Average temperature-time histories of almond and pine nut surfaces during single NIR heating and NIR heating combined with distilled water or 2 % lactic acid sprays. The error bars indicate standard deviations calculated from triplicates.

Leakage of bacterial intracellular substances. A disruption of the cell membrane or a change in membrane permeability causes an increase in the amount of intracellular substances found outside of the cell. Spectrophotometric observation can detect these substances at 260 nm for nucleic acids (ex. purines and pyrimidines) and 280 nm for proteinaceous materials (ex. tyrosine and tryptophane) (Ukuku and Geveke, 2010). Table VI-3 shows absorbance values at 260 and 280 nm after each treatment (LA, NIR, NIR-DW, and NIR-LA). The overall pattern for the leakage of nucleic acids (260 nm) was similar to that of proteins (280 nm). Based on trends of leaked intracellular components, I infer there was no significant ($P > 0.05$) damage to cellular membranes of *S.* Enteritidis following LA spray treatment alone. Cells subjected to NIR-DW and NIR-LA treatments showed significantly ($P < 0.05$) higher leakage of UV-absorbing substances than did cells subjected to NIR heating alone. However, the degree of membrane damage between NIR-DW- and NIR-LA-treated cells was not significantly ($P > 0.05$) different (Table VI-3).

Table VI-3. Levels of membrane damage of LA-, NIR-, NIR-DW-, and NIR-LA-treated cells inferred from leakage of intracellular UV-absorbing substances[a].

	Absorbance	
Treatment type	260 nm	280 nm
Untreated control	0.545±0.030 A	0.314±0.017 A
LA	0.537±0.024 A	0.314±0.024 A
NIR	1.278±0.062 B	0.622±0.019 B
NIR-DW	1.486±0.035 C	0.723±0.024 C
NIR-LA	1.502±0.042 C	0.716±0.030 C

[a] The values are means ± standard deviations from three replications. Values in the same column followed by the same letter are not significantly different ($P > 0.05$).

Effect of NIR-LA combined treatment on product quality. Lipid peroxidation parameters (acid value and peroxide value), total phenolic content, color values, post-treatment moisture content, and sensory attributes of almond and pine nut kernels after 5 min of NIR-LA combined treatment are summarized in Table VI-4, 5, and 6, respectively. Although the lipid peroxidation parameters and total phenolic concentrations of almonds and pine nuts slightly varied with prolonged storage time, regardless of treatment, there were no significant ($P > 0.05$) differences in acid value, peroxide value, and total phenolic content between untreated and treated samples over the entire storage time (Table VI-4 and 5). As shown in Table VI-6, color (L^*, a^*, and b^*) values of NIR-LA treated (5 min) nut kernels were not significantly ($P > 0.05$) different from those of untreated samples. NIR-LA treatment for 5 min did not significantly ($P > 0.05$) change moisture content (db) of almonds and pine nuts. Also, there were no significant ($P > 0.05$) differences among all tested samples scored by the hedonic scale for texture (mouthfeel) and flavor, indicating that NIR heating combined with 2 % LA spray for 5 min did not significantly alter the sensory quality of nut kernel products.

Table VI-4. Acid value, peroxide value, and total phenolic content[a] of NIR-LA treated almond kernels during storage under accelerated conditions.

Parameter and treatment type		Storage time (days) at 60 °C in the dark		
		0	9	18
Acid value (mgKOH/$g_{extract}$)				
	Control	0.97±0.14 A	1.28±0.03 A	1.38±0.09 A
	NIR-LA	1.08±0.02 A	1.26±0.08 A	1.32±0.06 A
Peroxide value (meq/$kg_{extract}$)				
	Control	0.60±0.17 A	0.73±0.06 A	1.13±0.20 A
	NIR-LA	0.65±0.06 A	0.77±0.22 A	1.11±0.12 A
Total phenolics (mgGAE/$g_{extract}$)				
	Control	1.81±0.11 A	1.66±0.13 A	1.30±0.16 A
	NIR-LA	1.76±0.20 A	1.58±0.05 A	1.25±0.11 A

[a] The values are means ± standard deviations from three replications. Values in the same column followed by the same letter are not significantly different ($P > 0.05$). GAE, gallic acid equivalent.

Table VI-5. Acid value, peroxide value, and total phenolic content[a] of NIR-LA treated pine nut kernels during storage under accelerated conditions.

Parameter and treatment type		Storage time (days) at 60 °C in the dark		
		0	9	18
Acid value (mgKOH/$g_{extract}$)				
	Control	0.83±0.02 A	0.90±0.04 A	0.96±0.11 A
	NIR-LA	0.88±0.05 A	0.87±0.08 A	0.95±0.08 A
Peroxide value (meq/$kg_{extract}$)				
	Control	0.24±0.11 A	3.11±0.13 A	3.17±0.10 A
	NIR-LA	0.32±0.04 A	3.15±0.06 A	3.24±0.17 A
Total phenolics (mgGAE/$g_{extract}$)				
	Control	2.03±0.08 A	1.91±0.08 A	1.58±0.17 A
	NIR-LA	1.94±0.09 A	1.83±0.09 A	1.42±0.05 A

[a] The values are means ± standard deviations from three replications. Values in the same column followed by the same letter are not significantly different ($P > 0.05$). GAE, gallic acid equivalent.

Table VI-6. Color values, moisture content, and sensory attributes[a] of nut kernels following 5 min of NIR-LA treatment (at day 0).

Sample and treatment type	Color value for parameter			Moisture contents (%)	Sensory attribute score	
	L*	a*	b*		Texture	Flavor
Almonds						
Control	52.53±0.95 A	13.96±0.75 A	36.20±0.39 A	4.81±0.06 A	4.83±1.03 A	4.25±1.48 A
NIR-LA	53.76±0.91 A	13.87±0.38 A	37.05±0.66 A	5.01±0.15 A	4.58±1.24 A	4.00±1.13 A
Pine nuts						
Control	68.39±0.83 A	-0.29±0.08 A	27.60±1.00 A	2.53±0.05 A	5.33±1.07 A	4.42±1.51 A
NIR-LA	66.90±0.64 A	-0.47±0.16 A	27.34±0.52 A	2.82±0.21 A	5.08±1.00 A	4.17±1.11 A

[a] Values are means from three replications ± standard deviations. Values followed by the same letters within each column are not significantly different ($P > 0.05$). L*, lightness; a*, redness; b*, yellowness. All moisture contents are expressed on a dry basis. Sensory attributes are from panelist scorecard analysis on a 7-point hedonic scale. 7, very good; 1, very poor. n=13.

VI-4. Discussion

The Almond Board of California has initiated several research projects addressing the lethality of dry heat processes, which revealed that typical dry roasting processes did not deliver a minimum 4-log reduction of *S. enterica* on almonds, which is the target lethality based on a prior risk assessment study (Danyluk et al., 2006). In my study, NIR treatment alone was also insufficient to reduce *S.* Enteritidis by the required amount (ca. 4-log-unit reduction) on almond and pine nut kernels (Fig. VI-2 and 3, respectively). To achieve > 4-log reductions, based on the calculated parameters of the Weibull model (the scale parameter = 3.367; the shape parameter = 2.435; R^2 = 0.95; *MSE* = 0.01), treatment for 8.4 min would be needed for *S.* Enteritidis PT 30 on almonds. However, a roasting effect was visually observed on almond kernels treated with NIR for a slightly excessive time (over 8 min, data not shown).

Despite high temperature exposure, the ability of *Salmonella* cells to survive on kernels suggests that their physiological state may have imparted to them enhanced heat tolerance. An increase in heat tolerance of *Salmonella* spp. after exposure to low-a_w environments has been well documented (Mattick et al., 2000) and is thought to have contributed to large outbreaks of salmonellosis linked to various low-a_w foods (Gill et al., 1983; Shachar and Yaron, 2006). *Salmonella* cells on dry nut kernels have similarly high tolerance to heat because of their

dehydration. To overcome this limitation, hurdle combinations have been performed on nut kernels by several researchers. Pretreatment of almonds with water before dry roasting provides a means to increase antimicrobial efficacy (Kim and Harris, 2006). Jeong et al. (2009) used high-humidity hot air (moist-air impingement) to enhance the inactivation rate of *S.* Enteritidis on almonds. Brandl et al. (2008) reported that wetting almond kernels by brief immersion under water before 45 s of dry heating yielded an additional reduction of *S.* Enteritidis of 0.43 log. Differences in moisture content of nutmeats used in hot air and oil roasting studies may have affected the rate of inactivation of *Salmonella*, as heat resistance of *Salmonella* was less in wet nutmeats than in dry nutmeats (Kaur and Harris, 2010; Beuchat and Mann, 2011). These studies suggest that a pre-wetting of the nut kernels has the potential to increase the antimicrobial efficacy of NIR heat treatment, possibly by improving the heat transfer to microsites where *Salmonella* cells are located. Therefore, I employed the pre-wetting procedures by spraying with DW or LA solution on almonds and pine nuts for increasing the moisture content of nut kernels. Also, in the present study, because a rotational mixer was used simultaneously with combined NIR-DW or -LA treatment, excessive heating on one side of the nut samples was prevented and DW or LA sprays could evenly contact nut kernel surfaces. Even though surface temperatures of almonds and pine nuts during the single NIR treatment were higher than during the NIR and DW or LA spray combined

treatments (Fig. VI-4), NIR-DW or -LA treatments yielded greater reductions in cell numbers of *Salmonella* spp. than did NIR treatment alone (Fig. VI-2 and 3). This tendency was also observed in levels of membrane damage to each treated cell, inferred from leakage of intracellular UV-absorbing substances (Table VI-3).

Since sublethally injured food-borne pathogens, which are potentially as dangerous as their uninjured counterparts, are able to resuscitate and regain their pathogenicity under favorable conditions (Wu, 2008), it is essential to study the ongoing microbiological dynamics of the processed food after bactericidal treatments have been applied. In the present study, the extent to which sublethally injured pathogens survived after NIR-DW or -LA treatment was evaluated by plating on selective media with and without a resuscitation step. As treatment time increased, more sublethally injured cells were observed in the NIR-DW treatment than in the NIR-LA combination (Table VI-1 and 2). In other words, the NIR-DW spray combined treatment for 5 min was not sufficient to achieve the target inactivation of *S.* Enteritidis (ca. 4-log reduction) on almond or pine nut kernels due to the resuscitation of injured cells. Whereas the NIR-LA spray combined treatment effectively inactivated *S.* Enteritidis on nut samples without causing apparent sublethal injury to bacterial cells.

The difference in inactivation efficacy between NIR-DW and NIR-LA combination treatments may be attributed to the interaction of lactic acid with

NIR heat. Low pH has long been recognized as one of the factors responsible for decreasing the heat resistance of bacterial spores and vegetative cells. Many studies have been published on the pH dependence of the heat resistance of *Salmonella* spp. (Teo et al., 1996; Blackburn et al., 1997; Casadei et al., 2001). Low-pH exposure can cause sublethal injury to cell membranes, which in turn can cause disruption of the proton motive force across cell membranes, owing to loss of H^+-ATPase (Lin et al., 2004). This could make bacterial cell membranes more susceptible to heat treatment. However, in the present study, the level of membrane damage that can be inferred as a result of the leakage of intracellular substances of NIR-LA-treated cells was not significantly different from those of NIR-DW- treated cells (Table VI-3). Therefore, it is not a fully proven hypothesis, but NIR heat treatment of *S.* Enteritidis cells might induce a disturbance in the outer membrane, allowing the cells to become permeable to the lactic acid solution sprayed rather than damaging the cell membrane per se. In addition, temperature is a primary factor influencing organic acid activity, with increasing temperature enhancing the effectiveness of organic acids (Presser et al., 1998; Uljas et al., 2001). Thus, the use of lactic acid sprays as a sensitizing agent to heat could be exploited as a novel technique to reduce intensity of NIR heat and to increase the efficacy of existing thermal treatment. Due to the lower levels of NIR and applied LA, combined NIR-LA treatments

did not change quality attributes of nut kernels significantly ($P > 0.05$) (Table VI-4, 5, and 6).

In conclusion, although there were small differences in inactivation levels between almonds and pine nuts due to the kernel size or morphological characteristics, about a 4-log reduction of *S.* Enteritidis can be achieved on almond or pine nut kernels by incorporating a simple LA spraying step prior to NIR radiant heat treatment without causing any deterioration in product quality. While spraying with organic acids has been widely adapted and proven effective by the meat industry for decontaminating livestock carcasses (Berry and Cutter, 2000; Castillo et al., 2001), this is not currently used in nut processing. Given the results of the present study, the potential utilization of lactic acid sprays during NIR heating could be considered as an alternative to other interventions that are currently employed. This combination of approaches would have the benefit of increasing bacterial inactivation while removing the water pre-sprayed on the kernels during NIR heating (Table VI-6). Thus, it avoids the need for an additional drying step during post-processing. Furthermore, the effectiveness of this NIR-LA combined treatment could be further improved by refining the procedure, such as rearranging the radiation intensity of NIR emitters and spray volume or concentration of lactic acid (e.g., improving the effect of lactic acid through adjusting pH, taking into account pKa).

References

Adair C, Kilsby DC, Whittall PT. 1989. Comparison of the Schoolfield (non-linear Arrhenius) model and the square root model for predicting bacterial growth in foods. Food Microbiol. **6**: 7-18.

Aeschbacher M, Reinhardt CA, Zbinden G. 1986. A rapid cell membrane permeability test using fluorescent dyes and flow cytometry. Cell Biol. Toxicol. **2**: 247-255.

Almela L, Nieto-Sandoval JM, Fernandez-Lopez JA. 2002. Microbial inactivation of paprika by a high-temperature short-x time treatment Influence on color properties. J. Agri. Food Chem. **50**: 1435-1440.

American Oil Chemist's Society. 2000. Official Methods and Recommended Practices of the American Oil Chemists' Society. Champaign, IL, USA.

Baird-Parker AC. 1990. Foodborne salmonellosis. Lancet **336**: 1231-1235.

Baranyi J, Roberts TA. 1994. A dynamic approach to predicting bacterial growth in foods. Int. J. Food Microbiol. **23**: 277-294.

Belgin Erdoğdu S, Ibrahim H. 2011. Effect of ultraviolet and far infrared radiation on microbial decontamination and quality of cumin seeds. J. Food Sci. **76**: 284-292.

Belongia EA, MacDonald KL, Parham GL, Kasale KA, and Osterholm MT. 1991. An outbreak of *Escherichia coli* O157:H7 colitis associated with consumption of precooked meat patties. J. Infect. Dis. **164**: 339-343.

Benedito J, Cambero MI, Ortuno C, Cabeza MC, Ordonez JA, De la Hoz L. 2011. Modeling and optimization of sensory changes and shelf-life in vacuum-packaged cooked ham treated by E-beam irradiation. Radiat. Phys. Chem. **80**: 505-513.

Berry ED, Cutter CN. 2000. Effects of acid adaptation of *Escherichia coli* O157:H7 on efficacy of acetic acid spray washes to decontaminate beef carcass tissue. Appl Environ Microbiol. **66**: 1493-1498.

Berzins A, Hellström S, Silins I, Korkeala H. 2010. Contamination patterns of

Listeria monocytogenes in cold-smoked pork processing. Journal of Food Protection **73**: 2103-2109.

Beuchat LR, Mann DA. 2011. Inactivation of *Salmonella* on pecan nutmeats by hot air treatment and oil roasting. J Food Prot. **74**: 1441-1450.

Bhaduri S, Smith PW, Palumbo SA, Turner-Jones CO, Smith JL, Marmer BS, Buchanan RL, Zaika LL, Williams AC. 1991. Thermal destruction of *Listeria monocytogenes* in liver sausage slurry. Food Microbiol. **8**: 75-78.

Bialka K, Demirci A, Puri VM. 2008. Modeling the inactivation of *Escherichia coli* O157:H7 and *Salmonella enterica* on raspberries and strawberries resulting from exposure to ozone or pulsed UV-light. J. Food Eng. **85**: 444-449.

Blackburn CW, Curtis LM, Humpheson L, Billon C, McClure PJ. 1997. Development of thermal inactivation models for *Salmonella* enteritidis and *Escherichia coli* O157:H7 with temperature, pH and NaCl as controlling factors. Int J Food Microbiol. **38**: 31-44.

Bolshakov AS, Boreskov VG, Kasulin GN, Rogov FA, Skryabin UP, Zhukov NN. 1976. Effects of Infrared radiation rates and conditions of preliminary processing of quality index on baked products. Paper **15**, 22nd European meeting of meat research workers. Malmo, Sweden.

Bover-Cid S, Belletti N, Garriga M, Aymerich T. 2011. Model for *Listeria monocytogenes* inactivation on dry-cured ham by high hydrostatic pressure processing. Food Microbiol. **28**: 804-809.

Brandl M, Pan Z, Huynh S, Zhu Y, McHugh TH. 2008. Reduction of *Salmonella* Enteritidis population sizes on almond kernels with infrared heat. J Food Prot. **71**: 897-902.

Bravo D, de Alba M, Medina M. 2014. Combined treatments of high-pressure with the lactoperoxidase system or lactoferrin on the inactivation of *Listeria monocytogenes*, *Salmonella* Enteritidis and *Escherichia coli* O157:H7 in beef carpaccio. Food Microbiology **41**: 27-32.

Breeuwer P, Abee T. 2000. Assessment of viability of microorganisms employing fluorescence techniques. International Journal of Food Microbiology **55**: 193-200.

Casadei MA, Ingram R, Hitchings E, Archer J, Gaze JE. 2001. Heat resistance of *Bacillus cereus*, *Salmonella typhimurium* and *Lactobacillus delbrueckii* in relation to pH and ethanol. Int J Food Microbiol. **63**: 125-134.

Castillo A, Lucia LM, Roberson DB, Stevenson TH, Mercado I, Acuff GR. 2001. Lactic acid sprays reduce bacterial pathogens on cold beef carcass surfaces and in subsequently produced ground beef. J Food Prot. **64**: 58-62.

Centers for Disease Control and Prevention (CDC). 2001. *Enterobacter sakazakii* infections associated with the use of powdered infant formula-Tennessee, JAMA **287**: 2204-2205.

Centers for Disease Control and Prevention (CDC). 2004. Outbreak of *Salmonella* serotype Enteritidis infections associated with raw almonds – United States and Canada, 2003–2004. Morb Mortal Wkly Rep **53**: 484-487.

Centers for Disease Control and Prevention (CDC). 2005. Investigation update: multistate outbreak of listeriosis. Available at: http://wwwn.cdc.gov/foodborneoutbreaks/.

Centers for Disease Control and Prevention (CDC). 2006. Investigation update: multistate outbreak of listeriosis. Available at: http://wwwn.cdc.gov/foodborneoutbreaks/.

Centers for Disease Control and Prevention (CDC). 2006. Investigation update: multistate outbreak of human *Salmonella* Typhimurium infections. Available at: http://wwwn.cdc.gov/foodborneoutbreaks/.

Centers for Disease Control and Prevention (CDC). 2011. Foodborne outbreak online database. Investigation update: multistate outbreak of *Salmonella* infections. Available at: http://wwwn.cdc.gov/foodborneoutbreaks/.

Centers for Disease Control and Prevention (CDC). 2013. Foodborne outbreak online database. Investigation update: multistate outbreak of listeriosis, *E. coli*, and human *Salmonella* infections. 2005-2011. Available at: http://wwwn.cdc.gov/foodborneoutbreaks/.

Centers for Disease Control and Prevention (CDC). 2014. Foodborne

outbreak online database. Investigation update: multistate outbreak of listeriosis, *E. coli*, and human *Salmonella* infections. Available at: http://wwwn.cdc.gov/foodborneoutbreaks/.

Chaitiemwong N, Hazeleger WC, Beumer RR, Zwietering MH. 2014. Quantification of transfer of *Listeria monocytogenes* between cooked ham and slicing machine surfaces. Food Control **44**: 177-184.

Chang SS, Han AR, Reyes-De-Corcuera JI, Powers JR, Kang DH. 2010. Evaluation of steam pasteurization in controlling *Salmonella* serotype Enteritidis on raw almond surfaces. L Appl Microbiol. **50**: 393-398.

Char CD, Mitilinaki E, Guerrero SN, Alzamora SM. 2010. Use of high-intensity ultrasound and UV-C light to inactivate some microorganisms in fruit juices. Food Bioprocess Technol. **3**: 797-803.

Chen D, Zhao T, Doyle MP. 2014. Transfer of foodborne pathogens during mechanical slicing and their inactivation by levulinic acid-based sanitizer on slicers. Food Microbiology **38**: 263-269.

Chen H, Hoover DG. 2003a. Pressure inactivation kinetics of *Yersinia enterocolitica* ATCC 35669. Int. J. Food Microbiol. **87**:161-171.

Chen H, Hoover DG. 2003b. Modeling the combined effect of high hydrostatic pressure and mild heat on the inactivation kinetics of *Listeria monocytogenes* Scott A in whole milk. Innov. Food Sci. Emerg. Technol. **4**: 25-34.

Chen H, Hoover DG. 2004. Use of Weibull model to describe and predict pressure inactivation of *Listeria monocytogenes* Scott A in whole milk. Innov. Food Sci. Emerg. Technol. **5**: 269–276.

Chen PC, Zahoor T, Oh SW, Kang DH. 2009. Effect of heat treatment on *Cronobacter* spp. in reconstituted, dried infant formula: preparation guidelines for manufacturers. Letters in Applied Microbiology **49**: 730-737.

Chun HH, Kim JY, Chung KS, Won MS, Song KB. 2009. Inactivation kinetics of *Listeria monocytogenes*, *Salmonella enterica* serovar Typhimurium, and *Campylobacter jejuni* in ready to-eat sliced ham using UV-C irradiation. Meat Sci. **83**: 599-603.

Cole MB, Davies KW, Munro G, Holyoak CD, Kilsby DC. 1993. A vitalistic model to describe the thermal inactivation of *Listeria monocytogenes*. J. Ind. Microbiol. **12**: 232-239.

D'Aoust JY. 1991. Psychrotrophy and foodborne *Salmonella*. Int. J. Food Microbiol. **13**: 207-215.

Dagerskog M, Osterstrom L. 1979. Infra-red radiation for food processing: I. A study of the fundamental properties of infra-red energy. Lebsensmittel-Wissenschaft Und Technologie, **12**: 237-242.

Danyluk MD, Vesugi AR, Harris LJ. 2005. Survival of *Salmonella* Enteritidis PT30 on inoculated almonds after commercial fumigation with propylene oxide. J Food Prot. **68**: 1613-1622.

Danyluk MD, Harris LJ, Schaffner DW. 2006. Monte Carlo simulations assessing the risk of salmonellosis from consumption of almonds. J. Food Prot. **69**: 1594-1599.

Doyle MP. 1991. *Escherichia coli* O157:H7 and its significance in foods. International Journal of Food Microbiology. **12**: 289-302.

Edelson-Mammel SG, Buchanan RL. 2004. Thermal inactivation of *Enterobacter sakazakii* in rehydrated infant formula. Journal of Food Protection **67**: 60-63.

Edelson-Mammel SG, Porteous MK, Buchanan RL. 2005. Survival of *Enterobacter sakazakii* in a dehydrated powdered infant formula. Journal of Food Protection **68**: 1900-1902.

European Food Safety Authority (EFSA). 2007. The community summary report on trends and sources of zoonoses, zoonotic agents, antimicrobial resistance and foodborne outbreaks in the European Union in 2006. EFSA J. **130**: 1-352.

Fernández A, Collado J, Cunha LM, Ocio MJ, Martínez A. 2002. Empirical model building based on Weibull distribution to describe the joint effect of pH and temperature on the thermal resistance of *Bacillus cereus* in vegetable substrate. Int. J. Food Microbiol. **77**: 147-153.

Flowers RS, Adams DM. 1976. Spore membrane(s) as the site of damage within heated *Clostridium perfringens* spores. Journal of Bacteriology.

125: 429-434.

Fowels J, Mitchell J, McGrath H. 2001. Assessment of cancer risk from ethylene oxide residues in spices imported into New Zealand. Food Chem. Toxicol. **39**: 1055-1062.

Gande N, Muriana P. 2003. Prepackage surface pasteurization of ready-to-eat meats with a radiant heat oven for reduction of *Listeria monocytogenes*. J. Food Prot. **66**: 1623-30.

Gayán E, Serrano MJ, Raso J, Álvarez I, Condón S. 2012. Inactivation of *Salmonella enterica* by UV-C light and by its combinations with mild temperatures. Appl. Environ. Microbiol. **78**: 8353-8361.

Gill ON, Sockett PN, Bartlett CL, Vaile MS, Rowe B, Gilbert RJ, Dulake C, Murrell HC, Salmaso S. 1983. Outbreak of *Salmonella* napoli infection caused by contaminated chocolate bars. Lancet. **1**: 574-577.

Grau FH, Vanderlinde PB. 1993. Aerobic growth of *Listeria monocytogenes* on beef lean and fatty tissue: equations describing the effects of temperature and pH. J. Food Prot. **56**: 96-101.

Gruszecki WI, Strzalka K. 2005. Carotenoids as modulators of lipid membrane physical properties. Biochimica et Biophysica Acta (BBA) **1740**: 108-115.

Gómez N, García D, Álvarez I, Condón S, Raso J. 2005. Modelling inactivation of *Listeria monocytogenes* by pulsed electric fields in media of different pH. Int. J. Food Microbiol. **103**: 199-206.

Gomez RF, Blais KD, Herrero A, Sinskey AJ. 1976. Effects of inhibitors of protein, RNA and DNA synthesis on heat-injured *Salmonella* Typhimurium LT2. Journal of General Microbiology. **97**: 19-27.

González S, Flick GJ, Arritt FM, Holliman D, Meadows B. 2006. Effect of high-pressure processing on strains of *Enterobacter sakazakii*. Journal of Food Protection **69**: 935-937.

Ha JW, Ryu SR, Kang DH. 2012. Evaluation of nearinfrared pasteurization in controlling *Escherichia coli* O157:H7, *Salmonella enterica* serovar Typhimurium, and *Listeria monocytogenes* in ready-to-eat sliced ham. Appl. Environ. Microbiol. **78**: 6458-6465.

Ha JW, Kang DH. 2013. Simultaneous near-infrared radiant heating and UV radiation for inactivating *Escherichia coli* O157:H7 and *Salmonella enterica* serovar Typhimurium in powdered red pepper (*Capsicum annuum* L.). Appl. Environ. Microbiol. **79**: 6568-6575.

Ha JW, Kang DH. 2014. Synergistic bactericidal effect of simultaneous near-infrared radiant heating and UV radiation against *Cronobacter Sakazakii* in powdered infant formula. Appl. Environ. Microbiol. **80**: 1858-1863.

Ha JW, Kang DH. 2015. Enhanced inactivation of food-borne pathogens in ready-to-eat sliced ham by NIR heating combined with UV-C irradiation and mechanism of the synergistic bactericidal action. Appl. Environ. Microbiol. **81**: 2-8.

Hadjok C, Mittal GS, Warriner K. 2008. Inactivation of human pathogens and spoilage bacteria on the surface and internalized within fresh produce by using a combination of ultraviolet light and hydrogen peroxide. J. Appl. Microbiol. **104**: 1014-1024.

Hamanaka D, Norimura N, Baba N, Mano K, Kakiuchi M, Tanaka F, Uchino T. 2011. Surface decontamination of fig fruit by combination of infrared radiation heating with ultraviolet irradiation. Food Cont. **22**: 375-80.

Hassani M, Condon S, Pagan R. 2007. Predicting Microbial Heat Inactivation under Nonisothermal Treatments. J. Food Prot. **70**: 1457-1467.

Hong YH, Park JY, Park JH, Chung MS, Kwon KS, Chung KS, Won MS, Song KB. 2008. Inactivation of *Enterobacter sakazakii*, *Bacillus cereus*, and *Salmonella* Typhimurium in powdered weaning food by electron-beam irradiation. Radiation Physics and Chemistry **77**: 1097-1100.

Huang L, Sites J. 2004. Infrared surface pasteurization of turkey frankfurters. Innov. Food Sci. Emerg. Technol. **5**: 345-351.

Huang L, Sites J. 2008. Elimination of *Listeria monocytogenes* on hotdogs by infrared surface treatment. J. Food Sci. **73**: M27-M31.

Huang L, Sites J. 2009. Elimination of *Listeria monocytogenes* on cooked chicken breast meat surfaces by near-infrared surface pasteurization prior to final packaging. Journal of Food Process Engineering. **35**: 1-15.

Isaacs S, Aramini J, Ciebin B, Farrar JA, Ahmed R, Middleton D, Chandran AU, Harris LJ, Howes M, Chan E, Pichette AS, Campbell K, Gupta A, Lior LY, Pearce M, Clark C, Rodgers F, Jamieson F, Brophy I, Ellis A. 2005. An international outbreak of salmonellosis associated with raw almonds contaminated with a rare phage type of *Salmonella* Enteritidis. J Food Prot **68**: 191-198.

Iversen C, Forsythe S. 2003. Risk profile of *Enterobacter sakazakii*, an emergent pathogen associated with infant milk formula. Trends in Food Science & Technology **14**: 443-454.

Iversen C, Forsythe S. 2004. Isolation of *Enterobacter sakazakii* and other *Enterobacteriaceae* from powdered infant formula milk and related products. Food Microbiology **21**: 771-777.

Iversen C, Lane M, Forsythe SJ. 2004. The growth profile, thermotolerance and biofilm formation of *Enterobacter sakazakii* grown in infant formula milk. Letters in Applied Microbiology **38**: 378-382.

Iversen C, Lehner A, Mullane N, Bidlas E, Cleenwerck I, Muragg J, Fanning S, Stephan R, Joosten H. 2007. The taxonomy of *Enterobacter sakazakii*: proposal of a new genus *Cronobacter* gen. nov. and descriptions of *Cronobacter sakazakii* comb. nov., *Cronobacter sakazakii* spp. *sakazakii*, comb. nov., *Cronobacter sakazakii* spp. *malonaticus* spp. nov., *Cronobacter turicensis* sp. nov., *Cronobacter muytjensii* sp. nov., *Cronobacter dublinensis* sp. nov. and *Cronobacter genomospecies* 1. BMC Evolutionary Biology **7**: 64.

Jeong S, Marks BP, Orta-Ramirez A. 2009. Thermal inactivation kinetics for *Salmonella* Enteritidis PT30 on almonds subjected to moist-air convection heating. J Food Prot. **72**: 1602-1609.

Jones SL, Carr TR, McKeith FK. 1987. Palatability and storage characteristics of precooked pork roasts. J. Food Sci. **52**: 279-281, 285.

Joseph S, Sonbol H, Hariri S, Desai P, McClelland M, Forsythe SJ. 2012. Diversity of the *Cronobacter* genus as revealed by multi locus sequence typing. Journal of Clinical Microbiology **50**: 3031-3039.

Jung YJ, Oh BS, Kang JW. 2008. Synergic effect of sequential or combined use of ozone and UV radiation for the disinfection of *Bacillus subtilis* spores. Water Res. **42**: 1613-1621.

Kandhai MC, Reij MW, Gorris LG, Glullame Gentil O, Schothorst van M. 2004. Occurrence of *Enterobacter sakazakii* in food production environments and households. Lancet **363**: 39-40.

Kang DH, Siragusa GR. 1999. Agar underlay method for recovery of sublethally heat-injured bacteria. *Appl. Environ. Microbiol.* **65**: 5334-5337.

Kaur H, Harris LJ. 2010. The impact of almond moisture on the survival of *Salmonella* Enteritidis PT30 after exposure to hot oil. J Food Prot. **73**: 169.

Kim BU, Harris LJ. 2006. The effect of pre-treatments on the reduction of *Salmonella* Enteritidis PT30 on almonds during dry roasting, 93rd Annu. Meet. IAFP. International Association for Food Protection, Des Moines, IA.

Kim SA, Kim OY, Rhee MS. 2010. Direct application of supercritical carbon dioxide for the reduction of *Cronobacter* spp. (*Enterobacter sakazakii*) in end products of dehydrated powdered infant formula. Journal of Dairy Science **93**: 1854-1860.

Kim SY, Sagong HG, Choi SH, Ryu SR, Kang DH. 2012. Radio-frequency heating to inactivate *Salmonella* Typhimurium and *Escherichia coli* O157:H7 on black and red pepper spice. Int. J. Food Microbiol. **153**: 171-175.

Knudsen JG, Bell KJ, Holt AD, Hottel HC, Sarofim AF, Stanford FC, Stuhlbarg UVW. 1984. Heat transmission by radiation. In Perry's Chemical Engineers' Handbook, 16th, Ed. (Perry RH, Green S and Maloney JO, eds.) pp. 10-52–10-68. McGraw-Hill, New York, NY.

Kohanski MA, Dwyer DJ, Collins JJ. 2010. How antibiotics kill bacteria: from targets to networks. Nature Reviews. **8**: 423-435.

Kohanski MA, Dwyer DJ, Hayete B, Lawrence CA, Collins JJ. 2007. A common mechanism of cellular death induced by bactericidal antibiotics. Cell. **130**: 797-810.

Kotzekidou P, Bloukas JG. 1996. Effect of protective cultures and packaging film permeability on shelf-life of sliced vacuum-packed cooked ham. Meat Sci. **42**(3): 333-345.

Krishnamurthy K, Khurana HK, Jun SJ, Irudayaraj J, Demirci A. 2008. Infrared Heating in Food Processing: An Overview. Comprehensive reviews in food science and food safety. **7**: 2-12.

Krzymien ME, Carlsson DJ, Deschênes L, Mercier M. 2001. Analysis of volatile transformation products from additives in γ-irradiated polyethylene packaging. Food Addit. Contam. **18**: 739-749.

Lechevallier MW, Schiemann DA, McFeters GA. 1987. Factors contributing to the reduced invasiveness of chlorine-injured *Yersinia enterocolitica*. Appl. Environ. Microbiol. **53**: 1358-1364.

Ledet Muller L, Hjertqvist M, Payne L, Pettersson H, Olsson A, Plym Forshell L, Andersson Y. 2007. Cluster of *Salmonella* Enteritidis in Sweden 2005-2006 - suspected source: almonds. Euro Surveill. **12**: E9-E10.

Lee JH, Sung TH, Lee KT, Kim MR. 2004. Effect of gamma-irradiation on color, pungency, and volatiles of korean red pepper powder. J. Food Sci. **69**: 585-592.

Lee JW, Oh SH, Kim JH, Yook HS, Byun MW. 2006. Gamma radiation sensitivity of *Enterobacter sakazakii* in dehydrated powdered infant formula. Journal of Food Protection **69**: 1434-1437.

Lee SY, Kang DH. 2001. Suitability of overlay method for recovery of heat-injured *Listeria monocytogenes* and *Salmonella* Typhimurium. *Food Sci. Biotechnol.* **10**: 323-326.

Lee SY, Oh SW, Chung HJ, Reyes-de-corcuera JI, Powers JR, Kang DH. 2006. Reduction of *Salmonella enterica* serovar Enteritidis on the surface of raw shelled almonds by exposure to steam. J Food Prot. **69**: 591-595.

Lehner A, Stephan R. 2004. Microbiological, epidemiological, and food safety aspects of *Enterobacter sakazakii*. Journal of Food Protection **67**: 2850-2857.

Lilie M, Hein S, Wilhelm P, Mueller U. 2007. Decontamination of spices by combining mechanical and thermal effects – An alternative approach for quality retention. Int. J. Food Sci. Technol. **42**: 190-193.

Lin CM, Takeuchi K, Zhang L, Dohm CB, Meyer JD, Hall PA. 2006. Cross-contamination between processing equipment and deli meats by *Listeria monocytogenes*. Journal of Food Protection **69**: 71-79.

Lin YT, Labbe RG, Shetty K. 2004. Inhibition of *Listeria monocytogenes* in fish and meat systems by use of oregano and cranberry phytochemical synergies. Appl Environ Microbiol. **70**: 5672-5678.

Little CL, Omotoye R, Mitchell RT. 2003. The microbiological quality of ready-to-eat foods with added spices. Int. J. Environ. Health Res. **13**: 31-42.

Liu Q, Lu X, Swanson BG, Rasco BA, Kang DH. 2012. Monitoring ultraviolet (UV) radiation inactivation of *Cronobacter sakazakii* in dry infant formula using fourier transform infrared spectroscopy. Journal of Food Science **71**: 86-93.

Mattick KL, Jorgensen F, Legan JD, Lappin-Scott HM, Humphrey TJ. 2000. Habituation of *Salmonella* spp. at reduced water activity and its effect on heat tolerance. Appl Environ Microbiol. **66**: 4921-4925.

Mead PS, Slutsker L, Dietz V, McCraig LF, Bresee S, Shapiro C, Griffin P, Tauxe RV. 1999. Food-related illness and death in the United States. Emerg. Infect. Dis. **5(**60): 7-25.

McCleer DR, Rowe MT. 1995. Development of a selective plating technique for the recovery of *Escherichia coli* O157:H7 after heat stress. Lett. Appl. Microbiol. **21**: 252-256.

McMeekin TA, Ross T. 2002. Predictive microbiology: providing a knowledge-based framework for change management. Int. J. Food Microbiol. **78**: 133-153.

Mol JHH, Hietbrink JEA, Mollen HW, Van Tinteren J. 1971. Observations on the microflora of vacuum-packed sliced cooked cured meats. J. Appl. Bacterial. **34**: 377-9.

Murphy HM, Payne SJ, Gagnon GA. 2008. Sequential UV- and chlorine based disinfection to mitigate *Escherichia coli* in drinking water biofilms. Water Res. **42**: 2083-2092.

Muytjens HL, Roelofs-Willemse H, Jaspar GHJ. 1988. Quality of powdered

substitutes for breast milk with regard to members of the family *Enterobacteriaceae*. Journal of Clinical Microbiology **26**: 743-746.

Nair MKM, Joy J, **Venkitanarayanan KS**. 2004. Inactivation of *Enterobacter sakazakii* in reconstituted infant formula by monocaprylin. Journal of Food Protection **67**: 2815-2819.

Nazarowec-White M, Farber JM. 1997. Incidence, survival and growth of *Enterobacter sakazakii* in infant formula. Journal of Food Protection **60**: 226-230.

Osaili TM, Shaker RR, Abu Al-Hasan AS, Ayyash MM, Martin EM. 2007. Inactivation of *Enterobacter sakazakii* in infant milk formula by gamma irradiation: determination of D_{10}-value. Journal of Food Science **72**: 85-88.

Pagan R, Condo´n S, Sala FJ. 1997. Effect of several factors on the heat-shock–induced thermotolerance of *Listeria monocytogenes*. Appl. Environ. Microbiol. **63**: 3225-3232.

Pao S, Kalantari A, Huang G. 2006. Utilizing acidic sprays for eliminating *Salmonella enterica* on raw almonds. J Food Sci. **71**: M14-M19.

Park SH, Choi MR, Park JW, Park KH, Chung MS, Ryu S, Kang DH. 2011. Use of organic acids to inactivate *Escherichia coli* O157:H7, *Salmonella* Typhimurium, and *Listeria monocytogenes* on organic fresh apples and lettuce. J Food Sci. **76**: M293-M298.

Peleg M, Cole MB. 1998. Reinterpretation of microbial survival curves. Crit. Rev. Food Sci. Nutr. **38**: 353-380.

Peleg M, Cole MB. 2000. Estimating the survival of *Clostridium botulinum* spores during heat treatments. J. Food Prot. **63**: 190-195.

Pina Pérez MC, Rodrigo Aliaga D, Ferrer Bernat C, Rodrigo Enguidanos M, Martinez A. 2007. Inactivation of *Enterobacter sakazakii* by pulsed electric field in buffered peptone water and infant formula milk. International Dairy Journal **17**: 1441-1449.

Pina-Pérez MC, Rodrigo D, Martinez A. 2009. Sub-lethal damage in *Cronobacter sakazakii* subsp. *Sakazakii* cells after different pulsed electric field treatments in infant formula milk. Food Control, **20**: 1145-1150.

Pina Pérez MC, Benlloch-Tinoco M, Rodrigo D, Martinez A. 2014. *Cronobacter sakazakii* Inactivation by Microwave Processing. Food and Bioprocess Technology **7**: 821-828.

Presser KA, Ross T, Ratkowsky DA. 1998. Modeling the growth limits (growth/no-growth interface) of *Escherichia coli* as a function of temperature, pH, lactic acid concentration, and water activity. Appl Environ Microbiol. **64**: 1773-1779.

Ramakrishnan TV, Francis FJ. 1973. Color and carotenoid changes in heated paprika. J. Food Sci. **38**: 25-28.

Rame J, Chaloupecky V, Sojkova N, Bencko V. 1997. An attempt to demonstrate the increased resistance of selected bacterial strains during repeated exposure to UV radiation at 254 nm. Central Euro. J. Pub. Health. **4**: 30-31.

Rangel JM, Sparling PH, Crowe C, Griffin PM, Swerdlow DL. 2005. Epidemiology of *Escherichia coli* O157:H7 outbreaks, United States, 1982–2002. Emerging Infect. Dis. **11**: 603-609.

Ranjan R, Irudayaraj J, Jun SJ. 2002. Simulation of infrared drying process. Drying Technol. **20**: 363-379.

Restaino L, Jeter WS, Hill WM. 1980. Thermal injury of *Yersinia enterocolitica*. Appl. Environ. Microbiol. **40**: 939-949.

Rhee MS, Lee SY, Dougherty RH, Kang DH. 2003. Antimicrobial effects of mustard flour and acetic acid against *Escherichia coli* O157:H7, *Listeria monocytogenes*, and *Salmonella* enterica serovar Typhimurium. Applied and Environmental Microbiology **69**: 2959-2963.

Rhee MS, Lee SY, Hillers VN, McCurdy SM, Kang DH. 2003. Evaluation of consumer-style cooking methods for reduction of *Escherichia coli* O157:H7 in ground beef. J. Food Prot. **66**: 1030-1034.

Rhim JW, Gennadios A, Fu D, Weller CL, Hanna MA. 1999. Properties of ultraviolet irradiated protein films. Lebensm. Wiss. Technol. **32**: 129-133.

Rico CW, Kim GR, Ahn JJ, Kim HK, Furuta M, Kwon JH. 2010. The comparative effect of steaming and irradiation on the physicochemical and microbiological properties of dried red pepper (*Capsicum annum* L.).

Food Chem. **119**: 1012-1016.

Ross T. 1996. Indices for performance evaluation of predictive models in food microbiology. J. Applied Microbiol. **81**: 501-508.

Ross T. 1999. Predictive Food Microbiology Models in the Meat Industry. Meat and Livestock Australia, Sydney, Australia. p. 196.

Ruckman SA, Rocabayera X, Borzelleca JF, Sandusky CB. 2004. Toxicological and metabolic investigations of the safety of N-a-Lauroyl-larginine ethyl ester monohydrochloride (LAE). Food Chemistry and Toxicology **42**: 245-259.

Ryser ET, Marth ET. 1991. *Listeria*, listeriosis, and food safety. New York: Marcel Dekker Inc.

Sakai N, Fujii A, Hanzawa T. 1993. Heat transfer analysis in a food heated by far infrared radiation. Nippon Shokuhin Kogyo Gakkaishi. **40**(7): 469-477.

Sakai N, Hanzawa T. 1994. Review applications and advances in far-infrared heating in Japan. Trends Food Sci. Technol. **5**: 357-362.

Sawai J, Sagara K, Igarashi H, Hashimoto A, Kokugan T, Shimizu M. 1995. Injury of *Escherichia coli* in physiological phosphate-buffered saline induced by far-infrared irradiation. Journal of Chemical Engineering of Japan. **28**: 294-299.

Sawai J., Kojima H, Igarashi H, Hashimoto A, Shoji S, Sawaki T, Hakoda A, Kawada E, Kokugan T, Shimizu M. 2000. Antibacterial characteristics of magnesium oxide powder. World Journal of Microbiology and Biotechnology. **16**: 187-194.

Schwartz B, Broome CV, Brown GR, Hightower AW, Ciesielski CA, Geveneta S, Gellin B, Mascola L. 1988. Association of sporadic listeriosis with consumption of uncooked hot dogs and undercooked chicken. Lancet. **1**: 779.

Schweiggert U, Carle R, Schieber A. 2007. Conventional and alternative processes for spice production - a review. Trends Food Sci. Tec. **18**: 260-268.

Shachar D, Yaron S. 2006. Heat tolerance of *Salmonella enterica* serovars Agona, Enteritidis, and Typhimurium in peanut butter. J Food Prot. **69**: 2687-2691.

Singleton VL, Orthofer R, Lamuela-Raventós RM. 1999. Analysis of total phenols and other oxidation substrates and antioxidants by means of Folin-Ciocalteu reagent. Methods Enzymol. **299**: 152-178.

Sommers CH, Boyd G. 2006. Variations in the radiation sensitivity of foodborne pathogens associated with complex ready-to eat food products. Radiat. Phys. Chem. **75**: 773-778.

Staack N, Ahrne L, Borch E, Knorr D. 2008a. Effects of temperature, pH, and controlled water activity on inactivation of spores of *Bacillus cereus* in paprika powder by near-IR radiation. J. Food Eng. **89**: 319-324.

Staack N, Ahrne L, Borch E, Knorr D. 2008b. Effect of infrared heating on quality and microbial decontamination in paprika powder. J. Food Eng. **86**: 17-24.

Steele JE, Stiles ME. 1981. Microbial quality of vacuum-packaged sliced ham. J. Food Prot. **44**: 435-439.

Stites CR, Mckeith FK, Bechtel PJ, Carr TR. 1989. Palatability and Storage Characteristics of Precooked Beef Roasts, Journal of Food Science. **54**: 3-6.

Tainter DR, Grenis AT. 2001. Spices and seasonings: a food technology handbook. 2nd ed. New York: Wiley. 249.

Te-Griffel MC, Zwietering MH. 1999. Validation of predictive models describing the growth of *Listeria monocytogenes*. Int. J. Food Microbiol. **46**: 135-149.

Teo YL, Raynor TJ, Ellajosyula KR, Knabel SJ. 1996. Synergistic effect of high temperature and high pH on the destruction of *Salmonella* enteritidis and *Escherichia coli* O157:H7. J Food Prot. **59**: 1023-1030.

Threlfall EJ, Frost JA, Ward LR, Rowe B, 1996. Increasing spectrum of resistance in multiresistant *Salmonella* Typhimurium. Lancet. **347**: 1053-1054.

Tomlins RI, Ordal ZJ. 1971. Requirements of *Salmonella* Typhimurium for recovery from thermal injury. Journal of Bacteriology. **105**: 512-518.

Torlak E, Sert D. 2013. Inactivation of *Cronobacter* by gaseous ozone in milk powders with different fat contents. International Dairy Journal **32**: 121-125.

Tsuchido T, Aoki I, Takano M. 1989. Interaction of the fluorescent dye 1-*N*-Phenylnaphthylamine with *Escherichia coli* cells during heat stress and recovery from heat stress. Journal of General Microbiology. **135**: 1941-1947.

Tuttle J, Gomez T, Doyle MP, Wells JG, Zhao T, Tauxe RV, Griffin PM. 1999. Lessons from a large outbreak of *Escherichia coli* O157:H7 infections : insights into the infectious dose and method of widespread contamination of hamburger patties. Epidemiol. Infect. **122**: 185-192.

Uesugi AR, Danyluk MD, Harris LJ. 2006. Survival of *Salmonella* Enteritidis phage type 30 on inoculated almonds stored at -20, 4, 23 and 35 °C. J Food Prot. **69**: 1851-1857.

Ukuku DO, Geveke DJ. 2010. A combined treatment of UV-light and radio frequency electric field for the inactivation of *Escherichia coli* K-12 in apple juice. Int. J. Food Microbiol. **138**: 50-55.

Uljas HE, Schaffner DW, Duffy S, Zhao L, Ingham SC. 2001. Modeling of combined processing steps for reducing *Escherichia coli* O157:H7 populations in apple cider. Appl Environ Microbiol. **67**: 133-141.

United States Department of Agriculture (USDA). 1989. Food Safety and Inspection Service (FSIS). Revised policy for controlling Listeria monocytogenes. Fed. Reg. **54**(98): 22345-22346.

United States Department of Agriculture (USDA). 2010. Food Safety and Inspection Service (FSIS). FSIS comparative risk assessment for *Listeria monocytogenes* in ready-to-eat meat and poultry deli meats. Available at: http://www.fsis.usda.gov/.

United States Department of Agriculture (USDA). 2011. Food Safety and Inspection Service (FSIS). Recall case archive. Available at: http://www.fsis.usda.gov/fsis_recalls/Recall_Case_Archive.

United States Department of Agriculture (USDA). 2014. Food Safety and Inspection Service (FSIS). Recall case archive. Available at: http://www.fsis.usda.gov/fsis_recalls/Recall_Case_Archive.

van Boekel MAJS. 2002. On the use of the Weibull model to describe thermal inactivation of microbial vegetative cells. Int. J. Food Microbiol. **74**: 139-159.

Vincent KA, Ken AB. 1987. Rapid sample preparation method for HPLC analysis of capsaicinoids in Capsicum fruits and oleoresins. J. Agric. Food Chem. **35**: 777-779.

Virto R, Sanz D, Alvarez I, Condon S, Raso J. 2006. Application of the Weibull model to describe inactivation of *Listeria monocytogenes* and *Escherichia coli* by citric and lactic acid at different temperatures. J. Sci. Food Agric. **86**: 865-870.

Walkling-Ribeiro M, Noci F, Cronin DA, Riener J, Lyng JG, Morgan DJ. 2008. Reduction of *Staphylococcus aureus* and quality changes in apple juice processed by ultraviolet irradiation, preheating and pulsed electric fields. J. Food Eng. **89**: 267-273.

Wang G, Zhao T, Doyle MP. 1996. Fate of enterohemorrhagic *Escherichia coli* O157: H7 in bovine feces. Applied and Environmental Microbiology. **62**: 2567-2570.

Wang Y, Wig TD, Tang J, Hallberg LM. 2003. Sterilization of foodstuffs using radio frequency heating. Journal of Food Science. **68**: 539-543.

Wesche AM, Gurtler JB, Marks BP, Ryser ET. 2009. Stress, sublethal injury, resuscitation, and virulence of bacterial foodborne pathogens. Journal of Food Protection **72**: 1121-1138.

Wihodo M, Han Y, Selby TL, Lorcheim P, Czarneski M, Huang G, Linton RH. 2005. Decontamination of raw almonds using chlorine dioxide gas. Int Food Technol Conference, Wuxi, China.

Wu VCH. 2008. A review of microbial injury and recovery methods in food. Food Microbiol. **25**: 735-744.

Yura T, Nagai H, Mori H. 1993. Regulation of the heat-shock response in bacteria. Annual Reviews in Microbiology. **47**: 321-350.

Zaika L, Palumbo SA, Smith JL, Corral FD, Bhaduri S, Jones CO, Kim AH. 1990. Destruction of *Listeria monocytogenes* during frankfurter processing. Journal of Food Protection, **53**: 18-21.

Zhang L, Moosekian SR, Todd EC, Ryser ET. 2012. Growth of *Listeria monocytogenes* in different retail delicatessen meats during simulated home storage. J. Food Prot. **75**: 896-905.

Zhu M, Du M, Cordray J, Ahn DU. 2005. Control of Listeria monocytogenes Contamination in Ready-to-Eat Meat Products. Comprehensive Reviews in Food Science and Food Safety. **4**(2): 34-42.

국문 초록

식품 가공 공정에서 적외선(infrared) 조사 가열의 적용은 기존 가열 시스템을 뛰어 넘는 장점들로 인해 최근 산학 전반에서 큰 관심을 받고 있다. 특히 적외선 조사 가열이 가진 대표적인 복사 및 투과능은 산업 적용 부분에 유리한 특성이라고 할 수 있다. 적외선은 전자기파의 형태로 열 에너지를 전달하며 그 파장에 따라 근적외선(0.76−2 μm), 중적외선(2−4 μm), 원적외선(4−1,000 μm)으로 구분된다. 본 연구에서는 적외선 영역 중 가열 및 투과 효율이 높은 근적외선(near−infrared, NIR) 가열원을 통해 대체 가능한 신 살균 공정 시스템을 개발하고자 다음과 같은 순서로 연구를 진행하였다. 1) 대표적인 즉석편이 식품 중 하나인 육가공 제품에 존재하는 주요 병원균 제어를 위한 NIR 가열 시스템의 효율 검증(기존 대류 가열 방식 대비) 및 품질 영향 평가, 2) NIR 가열 시스템의 핵심적인 공정 요소인 조사 강도(radiation intensity)의 변화에 따른 주요 병원균 저감화 예측 모델식 개발 및 검증, 3) 비가열 살균 시스템인 자외선(ultraviolot, UV) 조사와의 조합을 통한 시너지 효과 관찰, 4) 도출된 시너지 효과의 기작 규명, 5) 기존 살균 기술들의 적용이 어려운 건조 분말 식품 류의 효율적인 살균을 위한

NIR-UV 조합 시스템의 확장 적용, 6) 추가적인 허들 기술로써 NIR 가열과 유기산 처리(organic acid spray)와의 조합을 통한 건조 견과류의 살균 가능성 검토.

주요 병원균인 *S.* Typhimurium, *E. coli* O157:H7, *L. monocytogenes* 를 육가공품인 슬라이스 햄의 표면과 내부에 나누어 접종 한 후 NIR 가열과 기존 대류 가열을 동일한 크기의 챔버에서 동일한 전력량(1.8 kW)으로 각각 처리한 결과, NIR 가열 처리는 샘플의 품질변화 없이 표면에 접종된 각 병원균을 50 초 만에 3.38~4.19 log CFU/g 저감시키는 반면, 기존 대류 가열은 상응하는 저감 효과를 거두기 위해서 180 초의 처리시간이 소요되었다. 특히, 50 초간 NIR 가열로 처리한 샘플 군에서는 표면과 내부에 접종된 병원균의 저감 효율이 서로 유의적인 차이($P > 0.05$)를 보이지 않았으나, 기존 대류 가열 방식은 처리 후반의 샘플 군(150, 180 초)에서 내부 접종 병원균의 저감 효율이 유의적으로 떨어졌다. 이처럼, NIR 가열 시스템은 육가공 식품 내, 외부에 존재하는 병원균을 신속하고 효율적으로 제어 할 수 있어 기존 가열 방식을 대체할 수 있음을 확인하였다. 또한 조사 강도(radiation intensity)에 따른 세 병원균의 저감화 예측 모델을 개발하기 위해서, 약 100, 150, 200 $\mu W/cm^2/nm$ 단위를 기반으로 각각의 저감화 결과를 확보하였다.

모든 저감화 곡선은 shoulder 와 tailing 의 형태적 특성을 보였으며 비직선형 모델들 중 Weibull 모델의 scale 과 shape parameter(α와 β값)가 변수인 radiation intensity 와 상응하여 변화하였으며 그 관계가 직선에 수렴하는 것을 확인하였다. 이렇게 도출된 1 차식을 Weibull 모델의 두 parameter 에 치환하여 줌으로써 공정 요소인 radiation intensity 및 처리 시간만을 변수로 가지는 최종적인 제 3 의 저감화 모델식을 얻을 수 있었다. 마지막으로 실험에 사용된 NIR 조사 강도 범위내의 또 다른 intensity 를 선정하여 개발된 예측 모델식의 검증을 진행하였고 실측치와의 R^2, $RMSE$, B_f, A_f 의 결과 모두 수용 가능한 범위 내에 있음을 확인하였다. 이러한 결과들을 토대로 실제 육가공 산업에서 목표치의 살균력을 충족시키는 최적의 NIR 가열 살균 시스템을 구축하기 위한 방안을 제시할 수 있었다.

NIR 가열 시스템의 살균효율 증진을 위해 비가열 살균 시스템인 자외선(ultraviolot, UV) 조사와의 동시 처리를 진행한 결과 약 절반의 전력 사용량으로 슬라이스 햄의 품질변화 없이 70 초 만에 주요 병원균을 3.43~4.17 log CFU/g 줄일 수 있었다. 또한 모든 병원균에서 NIR 과 UV 의 개별 처리로 인한 저감효과의 합보다 동시 처리시 저감 정도가 큰 것으로 그 시너지 효과를 유의적으로 관찰 할 수 있었다. 이러한 NIR-UV 시너지 효과의 기작을 식품상에서

확인하기 위해 합성 저해가 잘 알려진 4 가지 대사 저해재들을 선정하여 배지 오버레이(agar over-lay) 방법과 접목해보았다. 그 결과 세포막 파괴 및 리보좀 손상으로 인한 세포 자체의 막 구조 회복 저해가 NIR-UV 시너지 효과의 주 기작임을 확인할 수 있었다. 추가적으로, NIR-UV 조합 시스템은 병원균 제어가 어려웠던 건조 분말 식품 중 대표적인 고춧가루(주요 병원균: *S.* Typhimurium, *E. coli* O157:H7)와 조제분유(주요 병원균: *C. sakazakii*)의 효율적인 살균을 위해 적용되었다. NIR-UV 동시처리는 상대적으로 낮은 가열 강도로 각 식품의 품질변화 없이 고춧가루에서 타겟 병원균을 2.78~3.34 log CFU/g(5 분처리), 조제분유에서는 2.79 log CFU/g(7 분처리) 만큼 저감 시켰다. 이 결과 역시 동시 처리로 인한 시너지 효과에 의한 영향임을 확인할 수 있었다. 전자 현미경의 관찰(정성적 분석)과 propidium iodide 흡착 정도 측정(정량적 분석)을 통해서 세포막의 손상이 NIR-UV 시너지 효과의 주 요인임을 다시 한번 규명할 수 있었다. 본 확장 연구를 통해 NIR-UV 조합 시스템이 다양한 분말형 식품군의 살균을 위한 대체 기술로써 활용 가능성이 높음을 알 수 있었다.

적용 가능한 또 다른 허들 기술로써, 대표적인 유기산인 젖산(lactic acid, LA)을 선정하여 2%의 수용액 형태로 식품에 분무

처리하고 NIR 조사 가열을 적용하는 조합 시스템을 구축하였고 건조 견과류(알몬드 및 잣)의 살균 가능성을 검토해보았다. 견과류에 적용하는 살균 기술은 최소 4 log CFU/g 의 저감 기준을 권고하고 있으나 기존 NIR-UV 조합을 통해서는 이를 품질변화 없이 달성하기 어려웠다. 비록 NIR 단독 처리에서 견과류 표면의 온도가 NIR-증류수(distilled water, DW) 또는 NIR-LA 분무 조합 처리군 보다 급격히 올라갔으나, NIR 단독 처리에서 많은 수준의 *S.* Enteritidis 가 생존하는 것을 확인하였다. 살균 효율은 NIR-DW 와 NIR-LA 가 비슷했으나, NIR-DW 에서는 유의적인 수준으로 병원균이 회복되어 목표한 제어 수준(4 log CFU/g)을 달성하기 어려웠다. 이러한 NIR-LA 의 살균 증진 효과가 세포막 손상 자체에 기인하지 않음을 실험적으로 확인함으로써, NIR 가열로 인한 세포막의 일부 손상 및 투과도 변화가 분무된 LA 수용액의 세포 내 침투를 촉진 시켰음을 추정할 수 있었다. 또한 두 기술이 낮은 강도 및 농도로 적용되어 견과류 품질에 유의적인 변화를 주지 않았다. 이로써, 개발된 NIR-LA 조합 시스템은 다양한 견과류의 미생물적 안전성을 확보할 수 있는 기술로 활용될 수 있을 것이다.

본 연구를 통해 도출된 NIR 가열의 조합 살균 시스템은 살균효과의 증진뿐만 아니라 처리가 간편하고 식품에 위해 잔여물질이 남지 않아

환경 친화적이며 단독처리 대비 투입되는 에너지 수준을 낮출 수 있어 공정비용 절감이 가능하다는 장점이 있다. 또한 연속식 공정을 기반으로 쉽게 대형화 및 산업화가 가능하다. 결론적으로 NIR 가열의 활용 기술들은 식품 산업에서 저비용으로 고품질의 식품을 안전하게 생산하기 위한 새로운 차세대 살균 공정으로 활용될 수 있을 것이다.

주제어 : 근적외선 가열, 자외선 조사, 유기산, 젖산, 분무, 살균, 식품유래 병원균, 조사 강도, 저감화 예측 모델, 육가공품, 건조 분말 식품, 견과류

학 번 : 2011-21325